CENTRE FOR ECONOMIC POLICY RESEARCH

CEPR PRESS

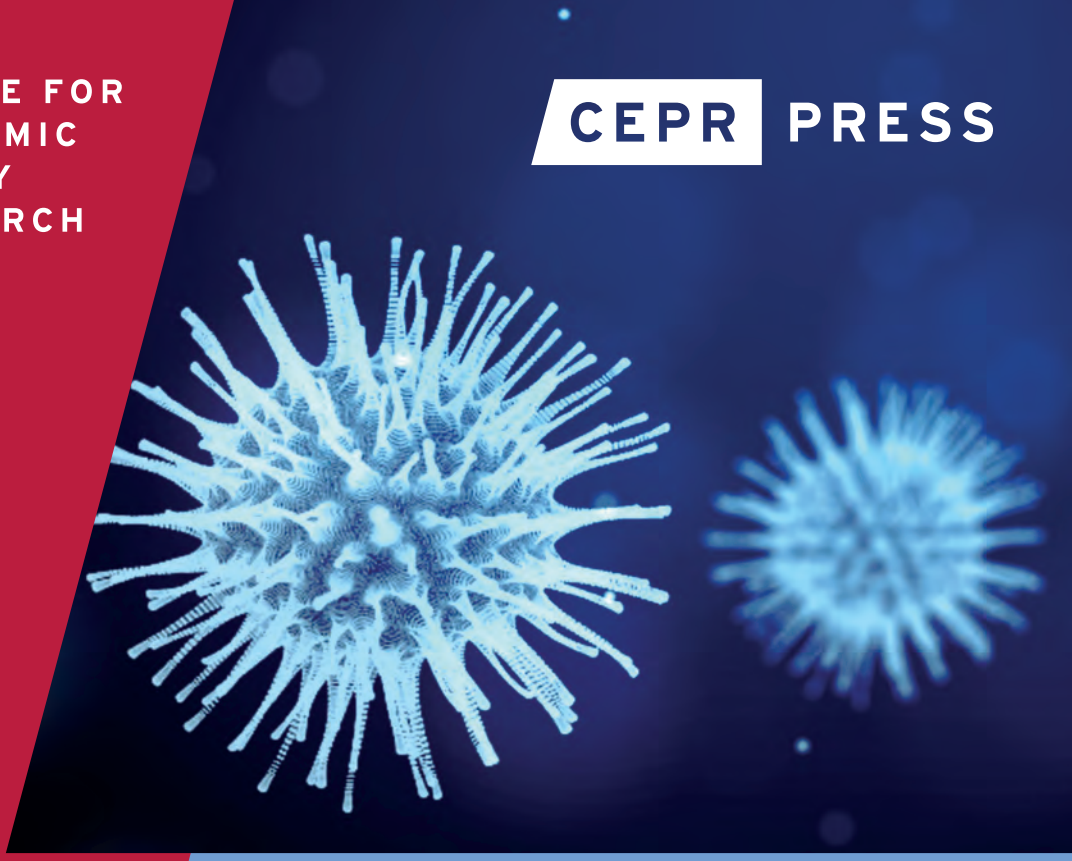

COVID ECONOMICS

VETTED AND REAL-TIME PAPERS

ISSUE 4
14 APRIL 2020

Covid Economics
Vetted and Real-Time Papers

Covid Economics, Vetted and Real-Time Papers, from CEPR, brings together formal investigations on the economic issues emanating from the Covid outbreak, based on explicit theory and/or empirical evidence, to improve the knowledge base.

Founder: Beatrice Weder di Mauro, President of CEPR
Editor: Charles Wyplosz, Graduate Institute Geneva and CEPR

Contact: Submissions should be made at https://portal.cepr.org/call-papers-covid-economics-real-time-journal-cej. Other queries should be sent to covidecon@cepr.org.

Ethics

Covid Economics will publish high quality analyses of economic aspects of the health crisis. However, the pandemic also raises a number of complex ethical issues. Economists tend to think about trade-offs, in this case lives vs. costs, patient selection at a time of scarcity, and more. In the spirit of academic freedom, neither the Editors of *Covid Economics* nor CEPR take a stand on these issues and therefore do not bear any responsibility for views expressed in the journal's articles.

Editorial Board

Covid Economics
Vetted and Real-Time Papers

Issue 4, 14 April 2020

Contents

Editor's note

We started to work on *Covid Economics* on 23 March. The first submissions arrived on 26 March. Since then we have received 101 papers, an average of 5.6 submissions per day.

The Editorial Board includes 33 reviewers. They are asked to evaluate papers in less than 48 hours. Many react within 2 hours and, with very few exceptions, I send the editorial decision to the submitting author well within the 48 hours period, often in one day or less.

So far, 39 papers have been accepted and 47 have been rejected.

It has taken some time between the day when a paper is accepted and when it is published. In order to reduce this lag and the accompanying backlog, starting with the third issue, we have stopped typesetting the papers, a time-consuming process. The papers now appear as submitted. We should be able to publish at least two issues per week and thus quickly eliminate the backlog so that papers will be published within days of their acceptance.

The response of the economics profession to the Covid-19 pandemic is impressive. I thank the members of the Editorial Board, whom I relentlessly solicit (on average once every six days), for the quality of their reviews, their speed of reaction, and their dedication toward this original venture. The staff of CEPR, who were instantaneously mobilized, should be warmly congratulated as well.

Charles Wyplosz
Editor

Covid Economics **Issue 4, 14 April 2020**

Aggregate and firm-level stock returns during pandemics, in real time[1]

Laura Alfaro,[2] Anusha Chari,[3] Andrew Greenland[4] and Peter K. Schott[5]

Date submitted: 3 April 2020; **Date accepted:** 4 April 2020

We exploit unexpected changes in the trajectory of pandemics to quantify their effects on aggregate and firm-level stock returns. We find that an unanticipated doubling of predicted infections during the Covid-19 and SARS outbreaks forecasts aggregate equity market value declines of 4% to 11%. Firm returns are sensitive to this information even after accounting for their co-movement with the market, and vary widely both within and across sectors. Our results imply a decline in returns' reaction to new infections as the trajectory of the pandemic becomes clearer.

Covid Economics 4, 14 April 2020: 2-24

1 This paper is preliminary and incomplete. Missing citations and discussions of related research will be be added in future drafts. We thank Nick Barberis, Lorenzo Caliendo, Teresa Fort, Mihai Ion, and Ed Kaplan for comments and suggestions. We thank Alex Schott and Mengru Wang for excellent research assistance.

2 Warren Alpert Professor of Business Administration, Harvard Business School.
3 Professor of Economics and Finance, University of North Carolina at Chapel Hill.
4 Assistant Professor of Economics, Elon University.
5 Professor of Economics, Yale School of Management.

Covid Economics 4, 14 April 2020: 2-24

1 Introduction

We show that unanticipated changes in predicted infections based on daily re-estimation of simple epidemiological models of infectious disease forecast stock returns during the SARS and COVID-19 pandemics. This relationship is consistent with investors using such models to update their beliefs about the economic severity of the outbreak, in real time, as they attempt to gauge risk in the face of uncertainty (Knight, 1921; Keynes, 1937).

We emphasize that we are *not* epidemiologists and are *not* outlining a method to characterize the true path of pandemics. We also are not trying to infer the efficacy of various intervention strategies.[1] Such efforts, while of immense value, require data which may not be available until after the outbreak is substantially underway. Rather, we view real-time changes in the predicted severity of an outbreak as potentially useful summary statistics of its ultimate consequences, especially before the true model is revealed.

We model cumulative infections as either exponential or logistic. We re-estimate the parameters of these models each day of the outbreak using information on reported cases up to that day (which arrives after trading closes on that day). We then use these parameters to compute the predicted number of cases for the next trading day t using the cumulative counts reported after closing on days $t-1$ and $t-2$. The difference in these forecasts reflect unanticipated changes in the trajectory of the pandemic due to newly available information. We examine how these differences in projections covary with aggregate market returns on day t.

Applying this procedure to the United States during the current COVID-19 pandemic and to Hong Kong during the 2003 SARS outbreak, we find that sharper increases in predictions are associated with larger declines in market returns.[2] In the United States thus far, coefficient estimates imply declines of 4 to 10 percent in the Wilshire 5000 index in response to a doubling of predicted COVID-19 infections. We find a similar relationship during SARS, where a doubling of projected cases implies declines of 8 to 11 percent in the Hong Kong stock market's Hang Seng index. These findings suggest equity markets become less responsive to new cases the more they adhere to *previously* estimated parameters.

We find that changes in forecasts retain their aggregate-market explanatory power even after controlling for a simpler summary of the severity of the outbreak, the most recent increase in reported cases. In contrast to this simple measure, estimated model parameters explicitly predict the eventual number of people that may be infected (e.g., the "carrying capacity" under the logistic model), and the speed with which that number may be reached. For example, a jump in estimated share of the population that ultimately will be infected suggests a larger labor supply shock, while an increase in the estimated growth rate of infections has implications for healthcare capacity constraints. We show that our results for the United States are robust to the inclusion of coarse controls for changes in federal and local policy.

Using disaggregate data, we find that individual firms' returns are sensitive to unanticipated increases in predicted infections, and that this sensitivity persists even after accounting for their co-movement with the market (Sharpe, 1964a). While there is substantial heterogeneity in firm returns within sectors, average returns by sector vary in an intuitive way. Firms operating in industries more heavily affected by social distancing – Accommodations, Entertainment and Transportation – exhibit the greatest exposure to the pandemic and the largest declines in market value. Firms in Education, Professional Services and Finance, by contrast, are less sensitive, likely due to their

[1] Piguillem and Shi (2020) and Berger et al. (2020), by contrast, use estimates of micro-founded SEIR models to argue that expanded testing generates substantial welfare gains relative to quarantines.

[2] While our results at present focus on SARS in Hong Kong and COVID-19 in the United States, we are expanding the set of countries we analyze during the latter, and have begun a similar analysis for the 2009 H1N1 outbreak.

Covid Economics 4, 14 April 2020: 2-24

greater ability to continue operations online.

Our analysis contributes to several literatures. First, we add to the very large body of research on asset pricing that examines the predictability of stock returns. Seminal papers by Campbell and Shiller (1988), Fama and French (1988) and others show that factors ranging from valuation ratios to corporate payout and financing policies forecast stock returns. In this paper we draw upon standard epidemiological models to infer how investors might update their beliefs about disease progression.

Second, our examination of firm returns in response to changes in model predictions contributes to numerous studies in corporate finance, pioneered by Ball and Brown (1968) and Fama et al. (1969), which use plausible changes in investors' information sets to understand market dynamics. In a typical event study, researchers examine specific events, such as an earnings announcements, that may release information relevant to investors' beliefs about firm market value. Firms' "abnormal" returns relative to a benchmark asset pricing model during such events summarize these changes expectations.[3] Here, we demonstrate that plausibly exogenous changes in the daily information set regarding the epidemic's trajectory are correlated with firms' stock returns.[4]

Third, our paper contributes to the very large literature in public health which attempts to explain the trajectory of infections during a pandemic.[5] In contrast to that research, we link changes in the estimated parameters and predictions of these models in real time to economic outcomes. To reiterate, we do not claim that the evolution of a pandemic must follow a purely exponential or logistic growth path. Rather, we explore whether the predictions of these models are informative of economic conditions, as manifest in their correlation with the market.[6] An interesting question for further research is the extent to which feedback from the predicted health and economic consequences of the outbreak affects future infections. For example, dire enough anticipated economic consequences might influence the set of policies used to combat the outbreak, thereby altering its trajectory (Lucas, 1976).

Finally, this paper relates to a rapidly emerging literature studying the economic consequences of COVID-19, and a more established literature investigating earlier pandemics. Barro et al. (2020), for example, argue that the decline in output during the 1918 to 1920 "Spanish Flu" epidemic provide a plausible mode of the economic consequences of COVID-19. Our analysis complements (Ramelli and Wagner, 2020), who focus on debt and international supply chains as key channels of exposure to the COVID-19 epidemic, and Gormsen and Koijen (2020), who use the performance of US futures' markets during the outbreak to infer bounds on future GDP growth. Analyzing newspaper articles since 1900, Baker et al. (2020) find that the COVID-19 pandemic is the first infectious disease outbreak whose mention in the press is associated with a large daily market movement.

This paper proceeds as follows. Section 2 provides a brief description of infectious disease models and how investors might link the predictions of these models and to asset prices. Sections 3 and 4 apply our framework to COVID-19 and SARS. Section 5 concludes.

[3] Wang et al. (2013), for example, examines how the stocks of Taiwanese biotechnology companies respond to a series of infectious disease outbreaks.

[4] Greenland et al. (2019) exploit a change in US trade policy to identify firms' exposure to greater import competition from China.

[5] Early contributions to this literature include Ross (1911), Kermack and McKendrick (1927), Kermack and McKendrick (1937) and Richards (1959).

[6] For an interesting discussion on the complexities associated with modeling an outbreak in real time, see https://fivethirtyeight.com/features/why-its-so-freaking-hard-to-make-a-good-covid-19-model/.

CEPR PRESS

Covid Economics 4, 14 April 2020: 2-24

2 Modeling

In this section we outline how infectious disease outbreaks can be modeled in real time, and how investors might make use of the model's estimated parameters.

2.1 Simple Models of Infectious Diseases

Exponential and logistic growth models are frequently used in biology and epidemiology to model infection and mortality. An exponential model,

$$C_t = ae^{(rt)} \tag{1}$$

predicts the cumulative number of cases on day t, C_t, as a function of the growth rate of infections in that country, r, the initial number of infected persons a, and time. In an exponential model, the number of infections per day continues to climb indefinitely. While clearly unrealistic ex-post, the exponential growth model is consistent with early stage pandemic growth rates.

In a logistic model (Richards, 1959), by contrast, the growth in infections grows exponentially initially, but then declines as the stock of infections approaches the population's "carrying-capacity," i.e., the cumulative number of people that ultimately will be infected. Carrying capacity is generally less than the full population. The cumulative number of infections on day t is given by

$$C_t = \frac{k}{1 + ce^{(-rt)}}, \tag{2}$$

where k is the carrying, c is a shift parameter (characterizing the number of initially infected persons) and r is the growth rate. Figure 1 provides an example of logistic infections for three different growth rates (2.5, 5 and and 7.5 percent) assuming $k = 250$ and $c = 50$. For each growth rate, we plot both the number of new cases each day (right axis) and the cumulative number of cases up to each day (left axis). As indicated in the figure, higher growth rates both shorten the time required to reach carrying capacity and increase the peak number of infections.

Figure 1: New and Cumulative New Cases Under the Logistic Model

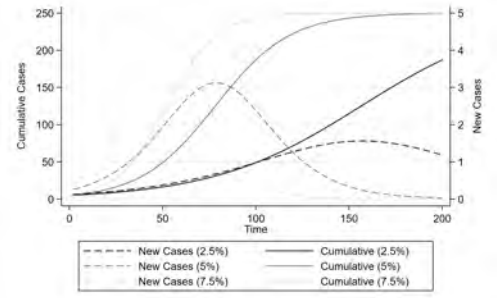

Source: Authors' calculations. Figure compares new and cumulative infections from days 1 to 200 assuming a logistic model with $k = 250$ and $c = 50$ and noted growth rates (r).

Given data on the actual evolution of infections, the two parameters in equation 1 and the three parameters in equation 2 can be updated each day using the sequence of infections up to that

Covid Economics 4, 14 April 2020: 2-24

date. We estimate these sequences using STATA's nonlinear least squares command (`nl`).[7] This command requires a vector of starting values, one for each parameter to be estimated.

We encounter two problems during our estimation of logistic functions in our applications below. First, estimates for each day t are sensitive to the choice of starting values for that day, particularly in the initial days of the pandemic. This feature of the estimation is not surprising: when the number of cases is relatively small, the data are consistent with a wide range of logistic curves, and the objective function across them may be relatively flat.

To increase the likelihood that our parameter estimates represent the *global* solution, we estimate 500 epidemiological models for each day, 250 for the logistic case, and 250 for the exponential case. In each iteration we use a different vector of starting values. For each day t, our first starting values are the estimated coefficients from the prior day, if available.[8] In the case of the logistic model, we then conduct a grid search defined by all triples $\{r, c, k\}$ such that

$$r \in \{0.01, 0.21, 0.41, 0.61, 0.81\}$$
$$c \in \{\widehat{c^{t-1}}, 2 * \widehat{c^{t-1}}, 4 * \widehat{c^{t-1}}, \ldots, 10 * \widehat{c^{t-1}}\}$$
$$k \in \{\widehat{k^{t-1}}, 2 * \widehat{k^{t-1}}, 3 * \widehat{k^{t-1}}, \ldots, 10 * \widehat{k^{t-1}}$$

where hats over variables indicate prior estimates, and superscripts indicate the day on which they are estimated. If more than one of these initial starting values produces estimates, we choose the parameters from the model with the highest adjusted R^2. We estimate the exponential model similarly.

The second, more interesting, problem that we encounter during estimation of the logistic outbreak curves is that STATA's `nl` routine may fail to converge. This failure generally occurs in the transition from relatively slow initial growth to subsequent, more obviously exponential growth as the pandemic proceeds. During this phase of the outbreak, the growth in the number of new cases each day is too large to fit a logistic function, i.e., the drop in the growth of new cases necessary to estimate a carrying capacity has not yet occurred.[9]

In our application below, we re-estimate both exponential and logistic parameters each day of an outbreak. To fix ideas, we simulate a 200-day cumulative logistic disease outbreak by generating a sequence of $C_t = \frac{k}{1+ce^{(-rt)}} + |\epsilon_t|$ for $t \in (1:200)$, assuming $k = 250$, $r = .025$, $c = 50$ and $|\epsilon_t|$ is the absolute value of a draw from a standard normal distribution. For each day t, we estimate logistic and exponential parameters using the sequence of simulated infections up to that day.

Figure 2 displays the results. Both sets of parameter estimates are volatile in the early stage of the outbreak. Logistic parameters are not available from days 47 through 78 due to lack on convergence, but settle down shortly thereafter, as the data increasingly conform to underlying logistic path. Exponential parameters are available for each day, but do not settle down as time goes on. The intuition for the unending increase in $\widehat{a_t}$ and decline in $\widehat{r_t}$ is as follows: because the simulated data are logistic, the only way to reconcile them with an exponential function is to have the estimate of initial exposure ($\widehat{a_t}$) rise as the estimate of the growth rate, $\widehat{r_t}$, drops.

[7] We are exploring other estimation procedures for use in a future draft, including use of SIR and SEIR models, e.g., Li et al. (2020) and Atkeson (2020).

[8] If the prior day did not converge, we use the most recent prior day for which we have estimates.

[9] In a future draft we will consider an estimation strategy that nests these functions.

Covid Economics 4, 14 April 2020: 2-24

Figure 2: Parameter Estimates Using Simulated Logistic Pandemic

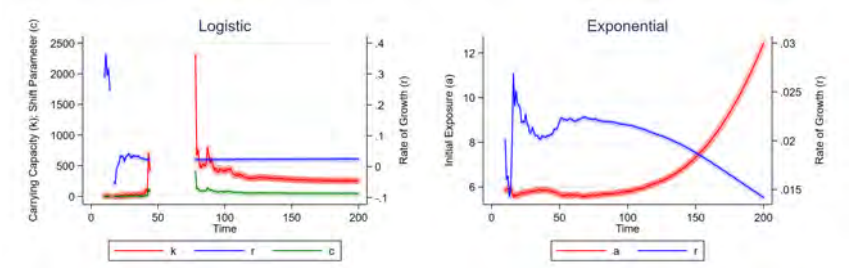

Source: authors' calculations. The left panel plots the sequence of logistic parameters, $\widehat{k_t}$, $\widehat{c_t}$ and $\widehat{r_t}$, estimated using the information up to each day t on simulated data (see text). Right panel of Figure plots the analogous sequence of exponential parameters, $\widehat{a_t}$ and $\widehat{r_t}$, using the same data. Missing estimates indicate lack of convergence (see text). Circles represent estimates. Solid lines connect estimates.

Figure 3 compares predicted cumulative cases for each model for each day t using the parameter estimates from day $t-1$. We denote these predictions $\widehat{C_t^{t-1}}$, where the superscript $t-1$ refers to the timing of the information used to make the prediction, and the subscript refers to the day being predicted. As illustrated in the figure, predictions for the two models line up reasonably well during the initial phase of the pandemic. Their 95 percent confidence intervals (not shown) cease overlapping on $t = 104$. After this point, the exponential model continues to project an ever-increasing number of infections, while the logistic model's predictions head towards the "true" carrying capacity of 250.

Figure 3: Simulated Pandemic Daily Predictions $(\widehat{C_t^{t-1}})$

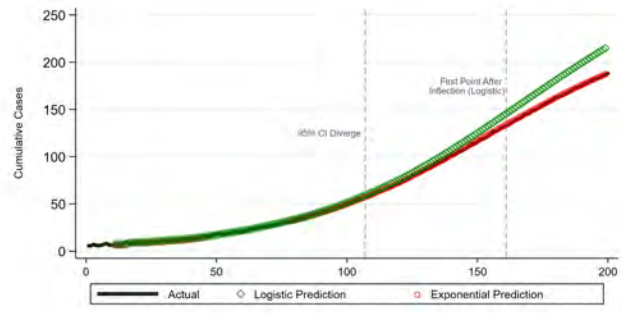

Source: authors' calculations. Figure compares simulated "actual" cumulative infections to predicted infections $(\widehat{C_t^{t-1}})$ under the logistic and exponential models. The prediction for each day t is based on the information available up to day $t-1$. The two vertical lines in the figure note when the 95 percent confidence intervals of the two models' predictions (not shown) initially diverge, and when the logistic model's estimates first indicate that its inflection point has passed.

2.2 Modeling Economic Impact

Predicted cumulative cases for day t based on day $t-1$ information, $\widehat{C_t^{t-1}}$, can be compared to the day t forecast made with day $t-2$ information, $\widehat{C_t^{t-2}}$. The log difference in these predictions,

$$\Delta ln\left(\widehat{C_t^{-2,-1}}\right) = ln\left(\widehat{C_t^{t-1}}\right) - ln\left(\widehat{C_t^{t-2}}\right), \tag{3}$$

captures *unexpected* changes in severity of the outbreak between these two days.[10] This potentially noisy "news" may be an important input into investors' assessment of the economic impact of a pandemic. For example, a jump in estimated carrying capacity suggests a larger ultimate supply shock in terms of lost labor supply, while an uptick in the estimated growth rate has implications for healthcare capacity constraints.[11]

In our application below, we compare aggregate equity returns on day t to the difference in forecasts for that day using an OLS regression,

$$\Delta ln\left(Index_t\right) = \alpha + \gamma_1 * \Delta ln\left(\widehat{C_t^{-2,-1}}\right) + \gamma_2 X_t + \epsilon_t. \tag{4}$$

where $\Delta ln\left(Index_t\right)$ is the daily log change in either opening-to-opening or closing-to-closing prices in the aggregate market index of country i, and X_t represents a vector of country controls, e.g., changes in policy.[12]

We assess *firm* j's sensitivity to the pandemic via an analogous specification,

$$R_{jt} = \delta + \beta_j^{C^{-2-1}} * \Delta ln\left(\widehat{C_t^{-2,-1}}\right) + \beta_j^{MKT} * \Delta ln\left(Index_t\right) + \epsilon_t, \tag{5}$$

where the dependent variable is the daily return of firm j on day t. The second term on the right hand side accounts for the possibility that COVID-19 is no different than any other aggregate shock, and that a firm's return during the pandemic merely reflects its more general co-movement with the market (Sharpe, 1964b). In our baseline assessment of firms' exposure to the pandemic, we do not include this second covariate. When it is included, $\beta_j^{C^{-2-1}}$ represents the firm's return in excess of its covariance with the market.

3 Application to COVID-19

In this section we provide real-time estimates of the outbreak parameters and infection predictions for COVID-19 in the United States. We then examine the relationship between changes in these predictions and both aggregate and firm-level returns in the United States.

[10] Timing is as follows. The number of infections on day $t-1$ is observed after the market closes on that day but before the market opens on day t. This day $t-1$ information is used to predict the number of cases for day t, $\widehat{C_t^{t-1}}$, which is compared to $\widehat{C_t^{t-2}}$.

[11] As noted in the introduction, the evolution of these parameters may also trigger policy "events" either directly or as a result of their economic consequences, which may alter the underlying parameters of the outbreak. We do not currently account for such feedback, but plan to do so in a future draft.

[12] We are currently exploring more flexible specifications, e.g., those which might capture the switch between exponential and logistic models, as well as those which reveal any over- or undershooting of reactions.

Covid Economics 4, 14 April 2020: 2-24

3.1 Epidemiological Model Paremeters

Data on the cumulative number of COVID-19 cases in the United States as of each day are from the Johns Hopkins Coronavirus Resource Center.[13] The first COVID-19 case appeared in China in November of 2019, while the first cases in the United States and Italy appeared on January 20, 2020. Our analysis begins on January 22, 2020, the first day that the World Health Organization began issuing situation reports detailing new case emergence internationally. Appendix Figure A.1 displays the cumulative reported infections in the United States from January 22 through April 3, 2020.

We estimate logistic and exponential parameters (equations 1 and 2) for the United States by day as discussed in Section 2.1. The daily parameter estimates for the logistic estimation, $\widehat{k_t}$, $\widehat{c_t}$ and $\widehat{r_t}$ are displayed the left panel of Figure 4, while those for the exponential model, $\widehat{a_t}$ and $\widehat{r_t}$, are reported in the right panel. Gaps in the time series in either figure represent lack of convergence.

Figure 4: Parameter Estimates for COVID-19

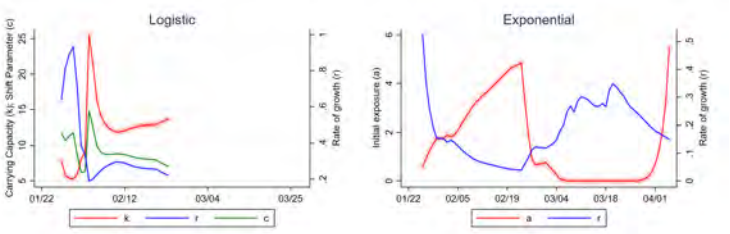

Source: Johns Hopkins Coronavirus Resource Center and authors' calculations. The left panel plots the sequence of logistic parameters, $\widehat{k_{it}}$, $\widehat{c_{it}}$ and $\widehat{r_{it}}$, estimated using the cumulative infections in the US up to each day t. Right panel plots the analogous sequence of exponential parameters, $\widehat{a_{it}}$ and $\widehat{r_{it}}$, using the same data. Missing estimates indicate lack of convergence (see text). Circles represent estimates. Solid lines connect estimates. Data currently extend to Friday March 27, 2020.

Logistic parameter estimates for the United States fail to converge after February 23, when the number of cases jumps abruptly from 15 to 51. That no parameter estimates are available after this date suggests that growth in new cases observed thus far is inconsistent with a leveling off, or carrying capacity, at least according to our estimation method. The exponential model, by contrast, converges for all days. As a result, we focus on the exponential model for the remainder of our analysis.

As the sharp changes in US exponential model parameters suggest, predicted cumulative infections vary substantially depending upon the day in which the underlying parameters are estimated. Figure 5 highlights this variability by comparing predicted cumulative infections based on the information available as of February 29 and March 7, 13, 21 and 28. The left panel displays these projections in levels, while the right panel uses a log scale. The five colored lines in the figure trace out each set of predictions. Dashed lines highlight 95 percent confidence intervals around these predictions. Finally, the confidence intervals are shaded for all days following the day upon which the prediction is based. To promote readability, we restrict the figure to the period after February 29. The black, solid line in the figure represents actual reported cases.

Predicted cumulative infections based on information as of February 29 are strikingly lower than predictions based on information as of March 21 due to the jump in reported cases between

[13] These data can be downloaded from https://github.com/CSSEGISandData/COVID-19 and visualized at https://coronavirus.jhu.edu/map.html.

Figure 5: Predicted Cumulative Cases Using Different Days' Estimates (COVID-19)

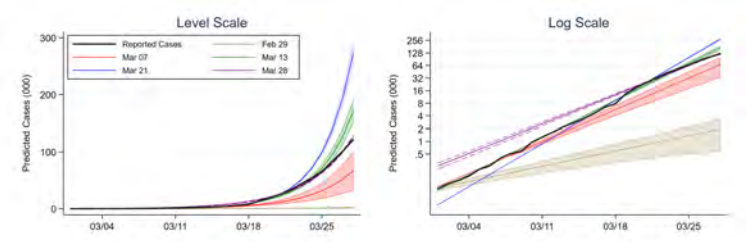

Source: Johns Hopkins Coronavirus Resource Center and authors' calculations. Figure displays predicted cases for the United States from March 18 onwards using the cumulative reported cases as of five dates: February 29, March 7, March 13, March 21 and March 28. Dashed lines represent 95 percent confidence intervals. Confidence intervals are shaded for all days after the information upon which the predictions are based.

those days. Indeed, according to the parameter estimates from March 21, US cases would number close to 300 thousand by the end of March. Equally striking is the downward shift in predicted cumulative cases that occurs between March 21 and March 28. It is precisely these kinds of changes in predicted cumulative cases that our analysis seeks to exploit.

Figure 6 uses the logistic parameter estimates in Figure 4 to plot $\widehat{C_t^{t-1}}$ and $\widehat{C_t^{t-2}}$ for the exponential model, i.e., the predicted number of cases on day t using the information up to day $t-1$ and day $t-2$. Magnitudes for these cumulative cases are reported on the left axis. The right axis reports $\Delta(\widehat{C_t^{-2,-1}})$, the log difference in these two predictions. Intuitively, $\widehat{C_t^{t-1}}$ and $\widehat{C_t^{t-2}}$ for the most part track each other closely. The former rises above the latter on days when reported cases jump, while the reverse happens when new cases are relatively flat.

Figure 6: Daily Logistic Predictions ($\widehat{C_t^{t-1}}$ and $\Delta ln(\widehat{C_t^{-2,-1}})$) for COVID-19

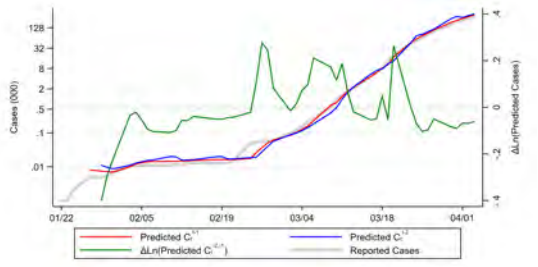

Source: Source: Johns Hopkins Coronavirus Resource Center and authors' calculations. Left axis reports the predicted cumulative cases for day t using information as of day $t-1$, $\widehat{C_t^{t-1}}$, and day $t-2$, $\widehat{C_t^{t-2}}$, under the exponential model. Right axis reports the log change in these two predictions, $\Delta ln(\widehat{C_t^{-2,-1}})$. Data currently extend to Friday April 3, 2020.

Covid Economics 4, 14 April 2020: 2-24

Covid Economics 4, 14 April 2020: 2-24

3.2 Aggregate US Returns During COVID-19

We examine the link between changes in model predictions and aggregate US stock via the Wilshire 5000 index.[14] We choose this index for its breadth, but note that results are qualitatively similar for other US market indexes.

Figure 7 plots the daily log change in the Wilshire 5000 index against unanticipated increases in cases, $\Delta ln(\widehat{C_t^{-2,-1}})$. Their negative relationship indicates that returns are higher when the difference in predictions is lower, and *vice versa*. In particular, the approximate 20 percent decline in predicted cases that occurs on March 24 coincides with a greater than 9 percent growth in the market index.

Figure 7: Change in Predicted COVID-19 Cases ($\Delta\widehat{C_t^{-2,-1}}$) vs Aggregate Market Returns

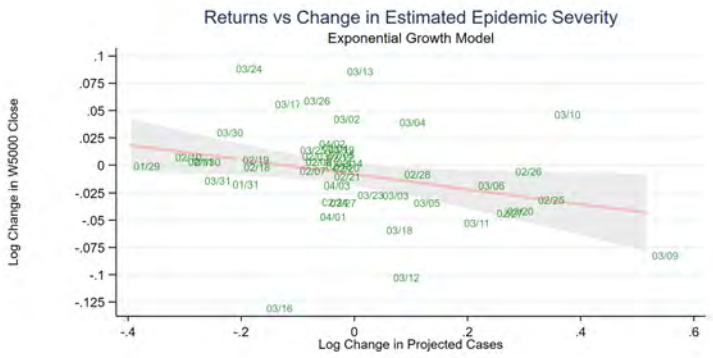

Source: Johns Hopkins Coronavirus Resource Center, Yahoo Finance and authors' calculations. Figure displays the daily log change in the Wilshire 5000 index against the log change in predicted cases under the exponential model for day t based on day $t-1$ and day $t-2$ information. Sample period is January 22 to April 3, 2020.

We investigate the relationship displayed in Figure 7 formally by estimating equation 4 via OLS. For each day, we compute $\Delta ln\left(Index_t\right)$ as the daily log change in either the closing or opening values of the Wilshire 5000. The estimation period consists of 47 trading days from January 22 to April 3.[15] The unit of observation is one day.

Coefficient estimates as well as robust standard errors are reported in Tables 1 and 2, where the former focuses on the daily opening-to-opening return and the latter on the daily closing-to-closing return. Coefficient estimates in the first column of each table indicate that a doubling of predicted cases using information from day $t-1$ versus day $t-2$ leads to average declines of -7.0 and -3.8 percent for closing and opening prices respectively. These effects are statistically significant at conventional levels.

In the second and subsequent columns of each table, we adjust the dependent and independent variables by the number of days since the last trading day. This adjustment insures that changes which transpire across weekends and holidays, when markets are closed, are not spuriously large compared to those that take place across successive calendar days. As indicated in the second column of each table, relationships remain statistically significant at conventional levels and now

[14] Data for the Wilshire 5000 are downloaded from Yahoo Finance.

[15] The actual number of trading days between these two dates is 50. We lose 3 days due to lack of estimates in the initial days of the outbreak.

Table 1: Changes in Predicted COVID-19 Cases ($\Delta\widehat{C_t^{-1,-2}}$) vs Market Open Returns

	(1) ΔLn(Open)	(2) ΔLn(Open)	(3) ΔLn(Open)	(4) ΔLn(Open)	(5) ΔLn(Open)	(6) ΔLn(Open)
$\Delta Ln(\widehat{C^{-2,-1}})$	-0.040***	-0.049**	-0.061**	-0.063**	-0.085**	-0.055**
	(0.013)	(0.024)	(0.024)	(0.025)	(0.033)	(0.025)
$\Delta Ln(C^{-2,-1})$			0.019	0.026	0.028	0.006
			(0.028)	(0.026)	(0.026)	(0.033)
$I(\Delta SIndex)$				-0.014		
				(0.014)		
$\Delta Ln(SIndex)$					-0.055	
					(0.061)	
Fiscal Stimulus						0.017
						(0.013)
Constant	-0.007*	-0.005	-0.008**	-0.007*	-0.006	-0.008*
	(0.004)	(0.004)	(0.004)	(0.004)	(0.004)	(0.004)
Observations	47	47	47	47	43	47
R^2	0.084	0.069	0.078	0.121	0.144	0.118
Daily Adjustment	N	Y	Y	Y	Y	Y

Source: Johns Hopkins Coronavirus Resource Center and authors' calculations. $\Delta Ln(Open_t)$ and $\Delta Ln(Close_t)$ are the daily log changes in the opening (i.e., day $t-1$ to day t open) and closing values of the Wilshire 5000. $\Delta ln(\widehat{C_t^{-2,-1}})$ is the change in predicted cases. $\Delta ln(C_t^{-2,-1})$ is the change in actual observed cases between days $t-2$ and $t-1$. $\Delta ln(C_t^{-1,0})$ is the change in actual observed cases between days $t-1$ and t. Robust standard errors in parenthesis. Columns 2-6 divide all variables by the number of days since the last observation (i.e. over weekends). Sample period is January 22 to April 3, 2020.

have the interpretation of daily growth rates. Here, a doubling of predicted cases per day leads to average declines of 8.6 percent for closing and 4.8 percent for opening prices.

In column 3 of each table, we examine whether the explanatory power of $\Delta\widehat{C_t^{-2,-1}}$ remains after controlling for a simple, local proxy of outbreak severity, the most recent change in reported cases. We use a slightly different variable in each table to account for the timing of the opening and closing returns. For the opening price regressions, we use $\Delta Ln(C^{-2,-1})$ under the assumption that the only information available to predict the opening price on day t is the difference in reported cases from days $t-2$ and $t-1$. For the closing price regressions, however, we use $\Delta Ln(C^{-1,0})$ to informally allow for the possibility that, although day t cases are not officially available until after closing, some information might "leak out" during day t trading.

In both cases, these measures are positive but not statistically significant at conventional levels. Moreover, they have little impact on our coefficients of interest. These results suggest that the primary role local increases in reported cases play in determining market value is through their contribution to the overall sequence of reported infections, manifest in the estimated model parameters.

In the final three columns of Tables 1 and 2 we examine the robustness of our results to including coarse controls for policy. As the COVID-19 pandemic has unfolded in the United States, state and local governments as well as the federal government have undertaken various measures to control its spread and limit the economic burden the disease itself imposes. Enactment of such policies is by definition correlated with the severity of the outbreak, and some of them may be designed to stabilize equity markets, confounding our results.

Covid Economics 4, 14 April 2020: 2-24

Table 2: Change in Predicted COVID-19 Cases ($\Delta\widehat{C_t^{-2,-1}}$) vs Market Close Returns

	(1) ΔLn(Close)	(2) ΔLn(Close)	(3) ΔLn(Close)	(4) ΔLn(Close)	(5) ΔLn(Close)	(6) ΔLn(Close)
$\Delta Ln(\widehat{C^{-2,-1}})$	-0.067**	-0.080**	-0.089***	-0.093***	-0.146***	-0.089***
	(0.030)	(0.030)	(0.031)	(0.034)	(0.041)	(0.032)
$\Delta Ln(C^{-1,-0})$			0.033	0.055	0.065*	0.034
			(0.031)	(0.037)	(0.035)	(0.032)
$I(\Delta SIndex)$				-0.021		
				(0.018)		
$\Delta Ln(SIndex)$					-0.091	
					(0.076)	
Fiscal Stimulus						-0.005
						(0.018)
Constant	-0.009	-0.005	-0.010**	-0.010**	-0.010**	-0.010**
	(0.006)	(0.005)	(0.004)	(0.004)	(0.004)	(0.004)
Observations	47	47	47	47	43	47
R^2	0.092	0.086	0.103	0.145	0.224	0.104
Daily Adjustment	N	Y	Y	Y	Y	Y

Source: Johns Hopkins Coronavirus Resource Center and authors' calculations. $\Delta Ln(Open_t)$ and $\Delta Ln(Close_t)$ are the daily log changes in the opening (i.e., day $t-1$ to day t open) and closing values of the Wilshire 5000. $\Delta ln(\widehat{C_t^{-2,-1}})$ is the change in predicted cases for day t using information from days $t-1$ anfd $t-2$. $\Delta ln(C_t^{-2,-1})$ is the change in actual observed cases between days $t-2$ and $t-1$. $\Delta ln(C_t^{-1,0})$ is the change in actual observed cases between days $t-1$ and t. Robust standard errors in parenthesis. Columns 2-6 divide all variables by the number of days since the last observation (i.e. over weekends). Sample period is January 22 to April 3, 2020.

We consider two controls for policy. The first is a country-level index developed at Oxford University, the Government Response Stringency Index (SIndex), which tracks travel restrictions, trade patterns, school openings, social distancing and other such measures, by country and day.[16] We make use of this index in two ways in columns 4 and 5 of Tables 1 and 2. First, we include an indicator function $I\{\Delta SIndex\}$ which takes a value equal to one if the index changes on day t. Second, we use log changes in the index itself, $\Delta Ln(SIndex)$. As indicated in the tables, neither covariate is statistically significant at conventional levels, and their inclusion has little impact on the coefficient of interest.

Our second control for policy is a coarse measure of fiscal stimulus. This dummy variable is set to one for four days (chosen by the authors) upon which major fiscal policies were enacted. The "Coronavirus Preparedness and Response Supplemental Appropriations Act, 2020", which appropriated 8.3 billion dollars for preparations for the COVID-19 outbreak, was signed into law on March 6. Then, from March 25 to March 27, Congress voted for and the President signed into law the 2 trillion dollar "Coronavirus Aid, Relief, and Economic Security Act." As reported in the table, this dummy variable, too, is statistically insignificant at conventional levels, and exerts no influence on the coefficient of interest.

Policy variables' lack of statistical significance is somewhat puzzling. One explanation for this outcome is that these measures are a function of the information contained in the cumulative reported cases, and therefore retain no independent explanatory power. On the other hand, the various government policies included in the SIndex may have offsetting effects. For example, while

[16] This index can be downloaded from https://www.bsg.ox.ac.uk/research/research-projects/oxford-covid-19-government-response-tracker.

Covid Economics 4, 14 April 2020: 2-24

social distancing measures might be interpreted by the market as a force that reduces the economic severity of the crisis, they may also be taken as a signal that the crisis is worse than publicly available data suggest. At present, we do not have the degrees of freedom to explore the impact of individual elements of the this index, but plan to do so in a future draft when inclusion of additional countries in the analysis allows for panel estimation.

3.3 Firm-Level US Returns During COVID-19

In this section we examine the relationship between unanticipated changes in predictions and returns at the firm level. The sample period is January 22 to April 3, 2020. Data are taken from Bloomberg and Yahoo finance.[17] We link firms to balance sheet information in Compustat via their CUSIP numbers. In the analysis that follows, we focus on the sample of 4070 firms incorporated in the United States for which we observe returns. These firms span 505 six-digit NAICS classifications and 249 4-digit NAICS classifications.

As a baseline, we assess firms' exposure to COVID-19 by estimating equation 5 *omitting* the market term $\Delta ln\left(Index_t\right)$. We estimate this regression separately for each firm j, yielding 4070 $\widehat{\beta_j^{C^{-2-1}}}$. The distribution of these exposures is summarized by the kernal density reported in Figure 8. Intuitively, given the behavior of the overall market discussed in the above, we find that the overwhelming majority of firm-level sensitivities are below zero, indicating that the firms' returns generally have a negative relationship with predicted increases in cumulative infections, $\Delta ln(\widehat{C_t^{-2,-1}})$.

Figure 8: Distribution of US Firms' Sensitivity to COVID-19: $\widehat{\beta_j^{C^{-2-1}}}$

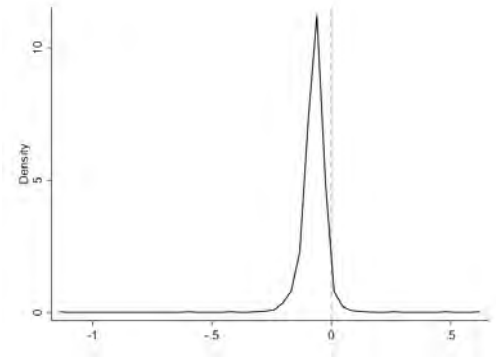

Source: Johns Hopkins Coronavirus Resource Center, Bloomberg, Yahoo Finance and authors' calculations. Figure reports the distribution of firm sensitivities ($\widehat{\beta_j^{C^{-2-1}}}$) to unanticipated changes in exponential model predictions, $\Delta\widehat{C_t^{-2,-1}}$, estimated using equation 5. Sample period is January 22 to April 3, 2020.

[17] We use Yahoo for stock prices after March 18, the last day for which we had access to Bloomberg terminals. We use the Bloomberg data to filter our Yahoo sample as follows. We match firms by ticker from January, 22 to March 18. If returns from the two sources differ by 0.01 on more than one day, or if they differ by more than 1 on any day, we deem that firm's returns unreliable and drop them from the analysis. The remaining returns have an in-sample correlation of 99.6 percent during the overlap period.

Covid Economics 4, 14 April 2020: 2-24

The right panel of Figure 9 summarizes firms' exposure to COVID-19 by two-digit NAICS sector. While sectors clearly vary in (and are sorted by) their median level of exposure, there is substantial variation across firms within sectors. The left panel of the figure plots firms' average exposure by sector against their average daily returns between January 17, the last trading day prior to the United States' first case, and April 3. We compute a firm's mean daily return over this period, $\overline{r_j}$, where the bar denotes an average, as the geometric mean of its daily returns, R_{jt}, during the holding period.

The position of sectors in the figure is intuitive. First, all sectors exhibit a negative average return in response to the COVID-19 shock. Second, firms operating in sectors more heavily affected by the imposition of social distancing – Accommodations, Entertainment, and Transportation – exhibit more negative values for $\widehat{\beta_j^{C^{-2-1}}}$ and relatively larger declines in daily average returns. The position of Mining, in the extreme lower left position of the figure, is also unsurprising given the sharp contraction in economic activity.[18] Agriculture, Utilities, Education, Professional Services and FIRE (Finance, Insurance and Real Estate) are towards the upper right of the figure. These sectors are less exposed to COVID-19 due to their necessity or their ability to conduct business online, and experience relatively less negative average returns.

Figure 9: US Firms' Sensitivity to COVID-19 ($\widehat{\beta_j^C}$), by NAICS Sector

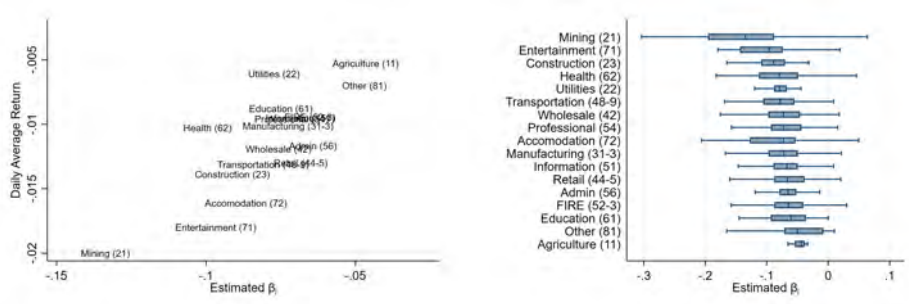

Source: Johns Hopkins Coronavirus Resource Center, Bloomberg, Yahoo Finance and authors' calculations. Figure reports the distribution of firm sensitivities ($\widehat{\beta_j^C}$) to unanticipated changes in exponential model projections, $\Delta C_t^{-2,-1}$, estimated using equation 5. Geometric average of daily returns calculated from January 17 - April 3, 2020.

We examine the extent to which exposure to COVID-19 affects firms' *cumulative* change in firm value (thus far) using a cross-sectional OLS regression,

$$\overline{r}_j = \nu_1 \widehat{\beta_j^C} + \nu_2 \widehat{\beta_j^{MKT}} + \xi_j, \tag{6}$$

where $\overline{r_j}$ is firm j's average daily return from January 22 to April 3, and $\widehat{\beta_j^C}$ and $\widehat{\beta_j^{MKT}}$ are its sensitivities to the log changes in predicted cumulative infections and the US market index (Wilshire 5000) estimated from equation 5. To the extent that exposure to COVID-19 influences firm returns beyond their co-movement with the market, both terms in equation 6 will have explanatory power.[19]

[18] Returns in mining, which include oil and gas extraction, are also affected by recent disagreements within OPEC, which are potentially endogenous to the pandemic.

[19] This regression similar in spirit to those proposed by Fama and MacBeth (1973), though here we use a single cross section rather than repeated cross sections, i.e., one for each day as the crisis unfolds. We plan to exploit the panel nature of our data in a future drafts.

CEPR PRESS

Covid Economics 4, 14 April 2020: 2-24

Table 3: Attributing Holding Period Returns to US COVID-19 Cases

	$\overline{r_j}$	$\overline{r_j}$
$\widehat{\beta_j^{C-2,-1}}$	0.050***	0.023***
	(0.008)	(0.007)
$\widehat{\beta_j^{MKT}}$		-0.007***
		(0.001)
Constant	-0.006***	-0.003***
	(0.001)	(0.001)
Observations	4070	4070
R^2	0.114	0.198

Source: Johns Hopkins Coronavirus Resource Center, Bloomberg, Yahoo Finance and authors' calculations. Table reports results of cross-sectional OLS regression of firms' average return between January 22 and April 3, $\overline{r_j}$, on $\widehat{\beta_j^C}$ and $\widehat{\beta_j^{MKT}}$, the coefficient estimates from equation 5. Robust standard errors reported in parenthesis below coefficients. The standard deviations of $\overline{r_j}$, $\widehat{\beta_j^C}$ and $\widehat{\beta_j^{MKT}}$ are 0.008, 0.051 and 0.043.

Results are reported in Table 3, where the first column focuses on firms' sensitivity to COVID-19, and the second column includes both exposures. The coefficient estimate in column 1, 0.050, implies that a one standard deviation increase in $\widehat{\beta_j^{C-2,-1}}$ is associated with a 0.33 standard deviation reduction in average daily returns, a sizable influence.[20] The estimates in column 2 indicate that this influence remains even after accounting for firms' sensitivity to the market. Here, the magnitude of the coefficient, 0.023, implies that a one standard deviation increase in exposure to COVID-19 is associated with a 0.11 standard deviation decrease in daily returns, or roughly one quarter of the magnitude of the implied impact of a standard deviation change in market exposure.

4 Application to SARS

In this section we demonstrate historical precedent for the link between US stock market returns and COVID-19 discussed above by reporting a similar link during the Severe Acute Respiratory Syndrome (SARS) outbreak in Honk Kong nearly 20 year years earlier.

The first SARS case was identified in Foshan, China in November 2002, but was not recognized as such until much later. According to WHO (2006), on February 10, 2003 a member of the WHO in China received an email asking:

> "Am wondering if you would have information on the strange contagious disease (similar to pneumonia with invalidating effect on lung) which has already left more than 100 people dead in ... Guangdong Province, in the space of 1 week. The outbreak is not allowed to be made known to the public via the media, but people are already aware of it (through hospital workers) and there is a 'panic' attitude."

[20] The standard deviations of $\overline{r_j}$, $\widehat{\beta_j^C}$ and $\widehat{\beta_j^{MKT}}$ are 0.008, 0.051 and 0.043.

CEPR PRESS

Covid Economics 4, 14 April 2020: 2-24

The WHO immediately began an investigation into SARS, and started releasing regular reports of suspected and confirmed cases beginning March 17, 2003.[21] The World Health Organization (WHO) declared SARS contained in July 2003, though cases continued to be reported until May 2004. Figure 10 plots the cumulative number of confirmed SARS infections worldwide (left scale) and in Hong Kong (right scale). The two vertical lines in the figure note the days on which the WHO officially received the aforementioned email, and the first day on which the WHO began reporting the number of infections on each weekday.

Figure 10: SARS Infections in Hong Kong and Worldwide During 2003

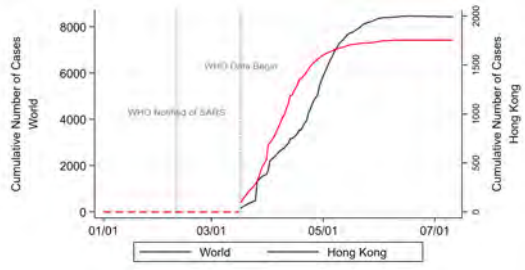

Source: World Health Organization and authors' calculations. Figure displays the cumulative reported SARS infections in Hong Kong and the rest of the world from January 1, 2003 to July 11, 2003. The two vertical lines in the figure note the days on which the WHO officially received the aforementioned email, and the first day on which the WHO began reporting the number of infections on each weekday.

Hong Kong and China accounted for the vast majority of cases worldwide.[22] We focus our analysis on Hong Kong for two reasons related to data reliability. First, while China acknowledged having over 300 cases of "atypical pneumonia" in February, the Ministry of Health did not provide day-by-day counts until March 26. In fact, on March 17, the day before WHO began releasing daily situation reports, Chinese authorities informed the WHO that "[t]he outbreak in Guangdong is said to have tapered off." The next day, cases were reported in 8 locations other than China – including Hong Kong. When China did begin reporting daily counts, on March 26, the first count was 800 cases. This large initial level of infections accounts for the sharp jump in world counts displayed for that day in Figure 10. Lack of real-time infection updates in mainland China prior to this jump undermines reliable estimation of model parameters, thereby impeding accurate assessment of unanticipated changes in infections. Second, it is unclear how China's restrictions on foreign ownership of companies' "A shares" during this period affects the extent to which such unanticipated changes will be reflected in Mainland firms' equity value.

We estimate equations 1 and 2 by day for each country as discussed in Section 2. The daily parameter estimates for the logistic estimation, $\widehat{k}_t$, $\widehat{c}_t$ and $\widehat{r}_t$ are displayed graphically in the left panel of Figure 11. The right panel displays analogous estimates for the exponential function. Gaps in either panel's time series represent lack of convergence. As indicated in the figure, logistic parameters fail to converge for several days early in the outbreak, and then once again when the estimates have started to settle down in the beginning of May. The exponential model, by contrast, converges on every day in the sample period.

[21] Counts were released every weekday. These data can be downloaded from https://www.who.int/csr/sars/country/en/. A timeline of WHO activities related to SARS events can be found at https://www.who.int/csr/don/2003_07_04/en/.

[22] Reported cases for China are plotted in appendix Figure A.2.

CEPR PRESS

Figure 11: Parameter Estimates for SARS

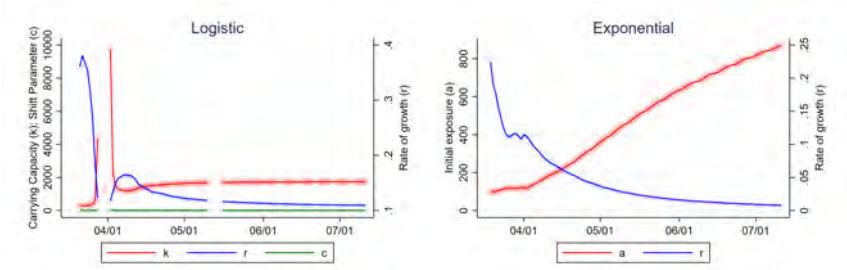

Source: World Health Organization and authors' calculations. The left panel plots the sequence of logistic parameters, $\widehat{k}_t$, $\widehat{c}_t$ and $\widehat{r}_t$, estimated using the information up to each day t on the cumulative reported cases for Hong Kong displayed in Figure 10. Right panel Figure plots the analogous sequence of exponential parameters, $\widehat{a_i}_t$ and $\widehat{r_i}_t$, using the same data. Missing estimates indicate lack of convergence (see text). Circles represent estimates. Solid lines connect estimates.

In the left panel of Figure 12, we compare the predictions of the two models. In each case, parameter estimates from day $t-1$ are used to predict the cumulative number of cases for day t. Shading represents 95 percent confidence intervals. As indicated in the panel, predicted infections under the two models (left axis) are similar through the first week in April, but diverge thereafter. Interestingly, this divergence coincides with a stabilization of the estimated inflection point of the logistic curve (right axis), which, as illustrated by the dashed grey line in the panel, hovers between April 5 and 7 from April 5 onward.[23]

Figure 12: Daily Predictions ($\widehat{C_t^{t-1}}$) for SARS

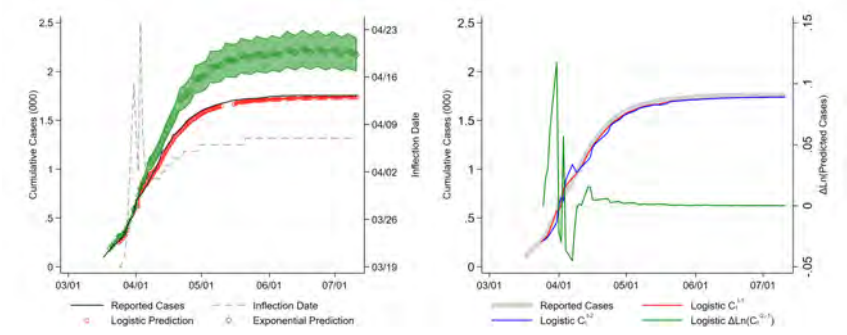

Source:World Health Organization and authors' calculations. Left panel displays predicted cumulative cases for each day t, $\widehat{C_t^{t-1}}$, information as of day $t-1$, based on parameter estimates reported in Figure 11. Shading spans 95 percent confidence intervals. Dashed line (right scale) traces out the estimated of the logistic curve's inflection point $(ln(\widehat{c}_t)/\widehat{r}_t)$. Right panel reports day t predicted cumulative cases under the logistic model using information as of day $t-1$, $\widehat{C_t^{t-1}}$, and day $t-2$, $\widehat{C_t^{t-2}}$, as well as the log difference between these predictions, $\Delta ln(\widehat{C_t^{-2,-1}})$. Missing estimates in left panel indicate lack of convergence (see text).

We use the predictions of the logistic model for the remainder of the analysis. The right panel

[23]The inflection point is given by $ln(\widehat{c}_t)/\widehat{r}_t$.

Covid Economics 4, 14 April 2020: 2-24

Covid Economics 4, 14 April 2020: 2-24

of Figure 12 compares the logistic model predictions for day t using information as of day $t-1$, $\widehat{C_t^{t-1}}$, versus day $t-2$, $\widehat{C_t^{t-2}}$, as well as the log difference between these predictions, $\Delta ln(\widehat{C_t^{-2,-1}})$.[24] We find that $\Delta ln(\widehat{C_t^{-2,-1}})$ exhibits wide swings in value during the early stages of the outbreak, before settling down in late April. As illustrated in Figure 13, these swings have a noticeably negative correlation with aggregate stock market performance in Hong Kong, as identified via daily log changes in the Hang Seng Index.[25]

We explore this relationship formally in an OLS estimation of equation 4. Coefficient estimates and robust standard errors are reported in Table 4. In the first column, we find a negative and statistically significant relationship using the raw data displayed in Figure 13. In column 2, we account for weekends and holidays by dividing both the left- and right-hand side variables by the number of days over which the returns are calculated, so that the regression coefficient represents a daily change in market value for a given log change in predicted cases. Here, too, the coefficient estimate is negative and statistically significant at conventional levels, and higher in absolute magnitude.

Figure 13: Changes in Predicted SARS Cases ($\Delta\widehat{C_t^{-2,-1}}$) vs Hang Seng Index Returns

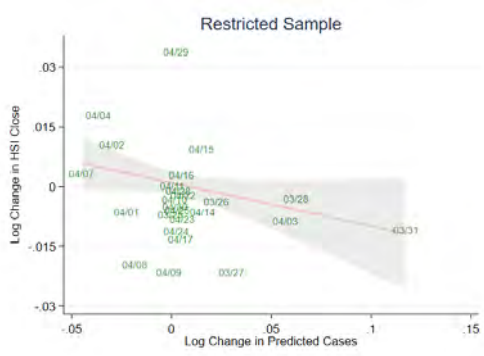

Source: World Health Organization, Yahoo Finance and authors' calculations. Figure displays the daily log change in the Hang Seng Index against the daily log change in predicted cases for day t based on information as of day $t-1$ versus day $t-2$, $\Delta ln(\widehat{C_t^{-2,-1}})$.

In column 3, we examine whether the explanatory power of $\Delta ln(\widehat{C_t^{-1,-2}})$ remains after controlling for a simple, local proxy of outbreak severity, the difference in cumulative *reported* infections between days $t-1$ and $t-2$, $\Delta ln(C_t^{-1,-0})$. As indicated in the table, the coefficient of interest remains negative and statistically significant at conventional levels, though of lower magnitude in absolute terms. The coefficient for $\Delta ln(C_t^{-2,-1})$ is also negative and statistically significant.

Finally, in column 4, we repeat the specification for column 3 but include month fixed effects to account for potential secular movements in the market unrelated to SARS. Esimate are essentially unchanged.

Overall, the estimates in Table 4 suggest investors may have used simple epidemiological models to update their beliefs about the economic severity of the outbreak in Hong Kong, in real time.

[24] We use the last available parameter estimates for days on which logistic parameters do not converge.
[25] Data for the Hong Seng index are downloaded from Yahoo Finance.

Table 4: Changes in Predicted SARS Cases vs Hang Seng Index Returns

	(1) ΔLn(Close)	(2) ΔLn(Close)	(3) ΔLn(Close)	(4) ΔLn(Close)
$\Delta Ln(\widehat{C^{-2,-1}})$	-0.0752***	-0.1095***	-0.0891**	-0.0923*
	(0.0241)	(0.0396)	(0.0427)	(0.0537)
$\Delta Ln(C^{-2,-1})$			-0.0445**	-0.0483
			(0.0200)	(0.0294)
Constant	0.0018	0.0010	0.0019*	0.0025
	(0.0013)	(0.0011)	(0.0011)	(0.0051)
Daily Adjustment	N	Y	Y	Y
Month FE	N	N	N	Y
Observations	70	70	70	70
R^2	0.108	0.060	0.103	0.111

Source: World Health Organization,Yahoo Finance and authors' calculations. $\Delta Ln(Close_t)$ is the daily log change (i.e., day $t-1$ to day t) closing values Hang Seng Index. $\Delta ln(\widehat{C_t^{-2,-1}})$ is the change in predicted cases for day t using information from days $t-1$ and $t-2$. $\Delta ln(C_t^{-2,-1})$ is the change in reported cases between days $t-1$ and t. Robust standard errors in parenthesis. Columns 2-4 divide all variables by the number of days since the last observation (i.e. over weekends). Column 4 includes month fixed effects.

Across specifications, coefficient estimates indicate an average decline of 8 to 11 percent in response to a doubling of predicted cumulative infections.

5 Conclusion

This paper shows that day-to-day changes in the predictions of standard models of infectious disease forecast changes in aggregate stock returns in Hong Kong during the SARS outbreak and the United States during the COVID-19 pandemic. In future updates to this paper, we plan to extend the analysis to other countries and pandemics, and to investigate the link between individual firms' returns and their exposure to public health crises via domestic and international input and output linkages as well as the demographics and occupations of their labor forces.

Covid Economics 4, 14 April 2020: 2-24

Covid Economics 4, 14 April 2020: 2-24

References

Atkeson, A. (2020, March). What will be the economic impact of covid-19 in the us? rough estimates of disease scenarios. Working Paper 26867, National Bureau of Economic Research.

Baker, S. R., N. Bloom, S. J. Davis, K. J. Kost, M. C. Sammon, and T. Viratyosin (2020, April). The unprecedented stock market impact of covid-19. Working Paper 26945, National Bureau of Economic Research.

Ball, R. and P. Brown (1968). An empirical evaluation of accounting income numbers. *Journal of accounting research*, 159–178.

Barro, R. J., J. F. Ursua, and J. Weng (2020, March). The coronavirus and the great influenza pandemic: Lessons from the "spanish flu" for the coronavirus's potential effects on mortality and economic activity. Working Paper 26866, National Bureau of Economic Research.

Berger, D., K. Herkenhoff, and S. Mongey (2020). A seir infectious disease model with testing and conditional quarantine. *Working Paper*.

Campbell, J. Y. and R. J. Shiller (1988). The dividend-price ratio and expectations of future dividends and discount factors. *The Review of Financial Studies 1*(3), 195–228.

Fama, E. and J. D. MacBeth (1973). Risk, return, and equilibrium: Emprirical tests. *Journal of Political Economy*.

Fama, E. F., L. Fisher, M. C. Jensen, and R. Roll (1969). The Adjustment of Stock Prices to New Information. *International Economic Review 10*.

Fama, E. F. and K. R. French (1988). Dividend yields and expected stock returns. *Journal of financial economics 22*(1), 3–25.

Gormsen, N. J. and R. S. Koijen (2020). Coronavirus: Impact on stock prices and growth expectations. *University of Chicago, Becker Friedman Institute for Economics Working Paper* (2020-22).

Greenland, A., M. Ion, J. Lopresti, and P. K. Schott (2019). Using equity market reactions to infer exposure to trade liberalization. Technical report, Working Paper.

Kermack, W. O. and A. G. McKendrick (1927). A contribution to the mathematical theory of epidemics. *Proceedings of the royal society of london. Series A, Containing papers of a mathematical and physical character 115*(772), 700–721.

Kermack, W. O. and A. G. McKendrick (1937). Contributions to the mathematical theory of epidemics iv. analysis of experimental epidemics of the virus disease mouse ectromelia. *Journal of Hygiene 37*(2), 172–187.

Keynes, J. M. (1937). The general theory of employment. *The quarterly journal of economics 51*(2), 209–223.

Knight, F. H. (1921). Risk, uncertainty and profit. *Library of Economics and Liberty*.

Li, R., S. Pei, B. Chen, Y. Song, T. Zhang, W. Yang, and J. Shaman (2020). Substantial undocumented infection facilitates the rapid dissemination of novel coronavirus (sars-cov2). *Science*.

Lucas, R. E. (1976). Econometric policy evaluation: A critique. In *Carnegie-Rochester conference series on public policy*, Volume 1, pp. 19–46.

Piguillem, F. and L. Shi (2020). The optimal covid-19 quarantine and testing policies. *Working Paper*.

Ramelli, S. and A. F. Wagner (2020). Feverish stock price reactions to covid-19. *Swiss Finance Institute Research Paper* (20-12).

Richards, F. J. (1959, 06). A Flexible Growth Function for Empirical Use. *Journal of Experimental Botany 10*(2), 290–301.

Ross, R. (1911). *The Prevention of Malaria*. John Murray.

Sharpe, W. F. (1964a). Capital Asset Prices: A Theory of Market Equilibrium Under Conditions of Risk.

Sharpe, W. F. (1964b). Capital Asset Prices: A Theory of Market Equilibrium Under Conditions of Risk.

Wang, Y.-H., F.-J. Yang, and L.-J. Chen (2013). An investor's perspective on infectious diseases and their influence on market behavior. *Journal of Business Economics and Management 14*(sup1), S112–S127.

WHO (2006). *SARS: how a global epidemic was stopped*. Manila: WHO Regional Office for the Western Pacific.

Covid Economics 4, 14 April 2020: 2-24

CEPR PRESS

Figure A.1: Actual COVID-19 Cases, By Country

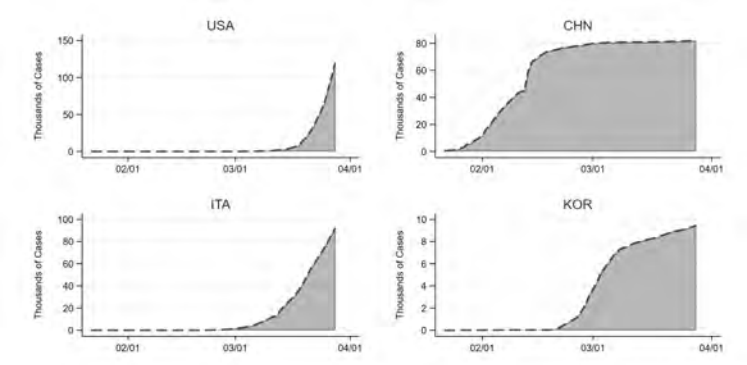

Source: Johns Hopkins Coronavirus Resource Center and authors' calculations. Figure displays the COVID-19 up to March 28.

Figure A.2: SARS Infections in China and Worldwide During 2003

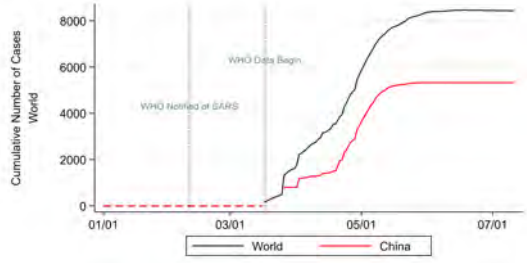

Source: World Health Organization and authors' calculations. Figure displays the cumulative reported SARS infections in China and the rest of the world from January 1, 2003 to July 11, 2003.

Covid Economics 4, 14 April 2020: 2-24

Covid Economics 4, 14 April 2020: 2-24

Figure A.3: Changes in Predicted SARS Cases vs HSI Index

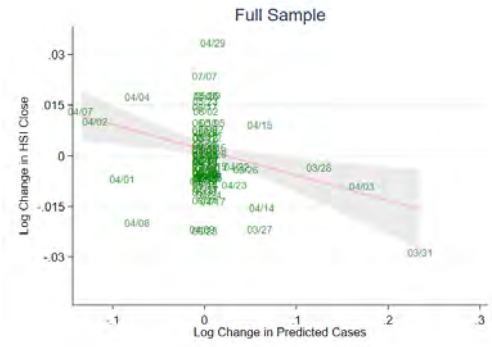

Source: Johns Hopkins Coronavirus Resource Center, Yahoo Finance and authors' calculations. Figure displays the daily log change in the Hang Seng Index against the log change in projected cases for day t based on day $t-1$ and day $t-2$ information.

CEPR PRESS

Covid Economics **Issue 4, 14 April 2020**

A note on efficient mitigation policies[1]

Callum Jones,[2] Thomas Philippon[3] and Venky Venkateswaran[4]

Date submitted: 5 April 2020; **Date accepted:** 7 April 2020

We study the response of an economy to an unexpected epidemic and we compare the decentralised equilibrium with the efficient allocation. Households mitigate the spread of the disease by reducing consumption and hours worked. A social planner worries about two externalities: an infection externality and a healthcare congestion externality. Private agents' mitigation incentives are too weak, especially at early stages while the planner implements drastic and front-loaded mitigation policies. In our calibration, assuming a CFR of 1% and an initial infection rate of 0.1%, private mitigation leads to a 10% drop in consumption and reduces the cumulative death rate from 2.5% of the initially susceptible population to about 2%. The planner reduces the death rate to 0.2% at the cost of an initial drop in consumption of around 40%.

Covid Economics 4, 14 April 2020: 25-46

1 We are grateful for comments from seminar participants at the University of Chicago. The views expressed herein are those of the authors and should not be attributed to the IMF, its Executive Board, or its management. First version: March 31, 2020.

2 Economist, IMF.
3 Max L. Heine Professor of Finance, New York University, Stern School of Business and CEPR Research Fellow.
4 Associate Professor of Economics, New York University, Stern School of Business.

CEPR PRESS

A Note on Efficient Mitigation Policies*

Callum Jones† Thomas Philippon‡ Venky Venkateswaran§

First version: March 31, 2020; this version: April 7, 2020

Abstract

We study the response of an economy to an unexpected epidemic and we compare the decentralized equilibrium with the efficient allocation. Households mitigate the spread of the disease by reducing consumption and hours worked. A social planner worries about two externalities: an infection externality and a healthcare congestion externality. Private agents' mitigation incentives are too weak, especially at early stages while the planner implements drastic and front-loaded mitigation policies. In our calibration, assuming a CFR of 1% and an initial infection rate of 0.1%, private mitigation leads to a 10% drop in consumption and reduces the cumulative death rate from 2.5% of the initially susceptible population to about 2%. The planner reduces the death rate to 0.2% at the cost of an initial drop in consumption of around 40%.

Keywords: contagion, containment, covid 19, recession, R_0, social distancing, SIR model, mitigation, suppression, vaccine.

Covid Economics 4, 14 April 2020: 25-46

1 Introduction

The response to the Covid-19 crisis highlights the tension between health and economic outcomes. The containment measures that can help slow the spread of the virus are likely to reinforce the economic downturn. Policy makers have naturally recognized this trade off and we hope to contribute to ongoing effort to provide quantitative models to guide their decisions.

*We are grateful for comments from seminar participants at the University of Chicago. The views expressed herein are those of the authors and should not be attributed to the IMF, its Executive Board, or its management. First version: March 31, 2020.

†International Monetary Fund, jonescallum@gmail.com
‡New York University, CEPR and NBER, tphilipp@stern.nyu.edu
§New York University, NBER, vvenkate@stern.nyu.edu

Covid Economics 4, 14 April 2020: 25-46

We propose a simple extension of the neoclassical model to quantity the tradeoffs and guide policy. We are particularly interested in understanding the design of the policy response. When will the private sector engineer the right response, and when is there a need for policy intervention? Which measures should be front-loaded and which ones should ramp up as the contagion progresses?

Our model has two building blocks: one for dynamics of contagion, and one for consumption and production. Our starting point is the classic SIR model of contagion used by public health specialists. Atkeson (2020b) provides a clear summary of this class of model. In a population of initial size N, the epidemiological state is given by the numbers of Susceptible (S), Infected (I), and Recovered (R) people. By definition, the cumulative number of deaths is $D = N - S - I - R$. Infected people transmit the virus to susceptible people at a rate that depends on the nature of the virus and on the frequency of social interactions. Containment, testing, and social distancing reduce this later factor. The rates of recovery (transitions from I to R), morbidity (I becoming severely or critically sick) and mortality (transition form I to D) depend on the nature of the virus and on the quality of health care services. The quality of health services depends on the capacity of health care providers (ICU beds, ventilators) and the number of sick people.

On the economic side of the model we use a standard model where members of large households jointly make decisions about consumption and labor supply. We assume that the consumption of (some) goods and services increases the risk of contagion, and that going to work also increases the risk of contagion.

We can then study how the private sector reacts to the announcement of an outbreak and how a government should intervene. Upon learning of the risks posed by the virus, households change their labor supply and consumption patterns. They cut spending and labor supply in proportion to the risk of infection, which – all else equal – is proportional to the fraction of infected agents I/N. Households only take into account the risk that they become infected, not the risk that they infect others, therefore their mitigation efforts are lower than what would be socially optimal. This infection externality is well understood in the epidemiology literature. The other important externality is the congestion externality in the healthcare system. When hospitals are overwhelmed the risk of death increases but agents do not internalize their impact on the risk of others.

We obtain interesting results when we compare the timing of mitigation. The planner wants to front load these efforts compared to the private sector. The risk of future contagion and of congestion in the health care system also drives an important wedge between private decisions and the socially

efficient allocation. If a private agent knows that she is likely to be infected in the future, this reduces her incentives to be careful today. We call this effect the fatalism effect. The planner on the other hand, worries about future infections and future congestion.

Literature Our paper relates to the literature on contagion dynamics (Diekmann and Heesterbeek, 2000). We refer to the reader to Atkeson (2020b) for a recent discussion. Berger et al. (2020) show that testing can reduce the economic cost of mitigation policies as well as reduce the congestion in the health care system. Baker et al. (2020) document the early consumption response of US households.

The most closely related papers are Barro et al. (2020), Correia et al. (2020), Eichenbaum et al. (2020) and Alvarez et al. (2020). Barro et al. (2020) and Correia et al. (2020) draw lessons from the 1918 flu epidemic. Barro et al. (2020) find a high death rate (about 40 million people, 2% of the population at the time) and a large but not extreme impact on the economy (cumulative loss in GDP per capita of 6% over 3 years). The impact on the stock market was small. Correia et al. (2020) find that early interventions help protect health and economic outcomes.

Our model shares with Eichenbaum et al. (2020) and Alvarez et al. (2020) the idea of embedding SIR dynamics in a simple DSGE model. The SIR model is the same, but there are some key differences in the DSGE model. Eichenbaum et al. (2020) consider hand-to-mouth agents who know their true status (infected or susceptible) while we work within a representative shopper/worker household framework à la Lucas and Stokey (1987). We explain the dynamic tension between the planner and the private sector and we describe an endogenous fatalism bias in private incentives. In terms of results, we find that optimal interventions are more front-loaded in our setting than in Eichenbaum et al. (2020). In their benchmark case, they find that the optimal policy is to gradually ramp up containment policies as the number of infected people rises, while congestion externalities in the healthcare system induce more aggressive, albeit still gradual, containment. Front-loading seems to become optimal only when agents anticipate the arrival of a vaccine in the future. In our setting, front-loading is optimal in almost all cases.

Alvarez et al. (2020) study a lockdown planning problem under SIR dynamics. They assume risk neutral agents and a linear lockdown technology. They find that the congestion externality plays an important role in shaping the policy response and that the planner front-loads the effort. Our planner has similar incentives but takes into account the desire for consumption smoothing. Jones et al. (2020) study optimal policies in a pandemic, including the option of working from home.

Covid Economics 4, 14 April 2020: 25-46

Covid Economics 4, 14 April 2020: 25-46

2 Benchmark Model

2.1 Households

There is a continuum of mass N of households. Each household is of size 1 and the utility of the household is

$$U = \sum_{t=0}^{\infty} \beta^t u\left(c_t, l_t; i_t, d_t\right),$$

where c_t is per-capita consumption and l_t is labor supplied by those who are alive and not sick. The household starts with a continuum of mass 1 of family members, all of them susceptible to the disease. At any time $t > 0$ we denote by s_t, i_t and d_t the numbers of susceptible, infected and dead people. The size of the household at time t is therefore $1 - d_t$. If per capita consumption is c_t then household consumption is $(1 - d_t)\, c_t$. Among the i_t infected members, κi_t are too sick to work. The labor force at time t is therefore $1 - d_t - \kappa i_t$, and household labor supply is $(1 - d_t - \kappa i_t)\, l_t$. The number of household members who have recovered from the disease is $r_t = 1 - s_t - i_t - d_t$. In the quantitative applications below we use the functional form

$$u\left(c_t, l_t; i_t, d_t\right) = (1 - d_t - \kappa i_t)\left(\log\left(c_t\right) - \frac{l_t^{1+\eta}}{1+\eta}\right) + \kappa i_t\left(\log\left(c_t\right) - u_\kappa\right) - u_d d_t,$$

where u_κ is the disutility from being sick and u_d the disutility from death which includes lost consumption and the psychological cost on surviving members.[1] For simplicity we assume that sickness does not change the marginal utility of consumption therefore c is the same for all alive members of the household. The variables s, i and d evolve according a standard SIR model described below. We use a Lucas and Stokey (1987) approach to model households. At the beginning of period t the household decides how much to consume c_t (per capita) and how much each able-bodied member should work l_t. Then the shoppers go shopping and the workers go to work. Notice that we have normalized the disutility of labor so that $l = c = 1$ before the epidemic starts.

Households understand that they can become infected by shopping and by going to work. We compute infection in two steps. First we define exposure levels for shoppers and for workers. Then we aggregate these into one infection rate at the household level. Finally we take into account the stochastic arrival of a vaccine by adjusting the discount factor β. Formally, we assume an exogenous arrival rate for a cure to the disease. By a cure we mean both a vaccine and a treatment for the

[1] Formally $u_d = PsyCost - \log\left(c_d\right)$ where c_d is the consumption equivalent in death. Technically we cannot set $c_d = 0$ with log preferences but u_d is a large number.

currently sick. Under this simplifying assumption the economy jumps back to $l = c = 1$ when a cure is found. We can therefore focus on the stochastic path before a cure is found. Let $\tilde{\beta}$ be the pure time discount rate and ν the likelihood of a vaccine. We define $\beta = \tilde{\beta}(1 - \nu)$ along the no-cure path.

2.2 Shopping

Household members can get infected by shopping. We define consumption (shopping) exposure as

$$e^c c_t C_t,$$

where e^c measures the sensitivity of exposure to consumption and C_t is aggregate consumption, all relative to a steady state value normalized to one. The idea behind this equation is that household members go on shopping trips. We assume that shopping trips scale up with consumption and that, for a given level of aggregate consumption, exposure is proportional to shopping trips. This functional form captures the notion of crowds in shopping mall as well as in public transportation.

2.3 Production

Exposure at work for household members working is given by

$$e^l l_t L_t,$$

where e^c measure the sensitivity of exposure to labor and L_t is aggregate labor supply. Effective labor supply, $\hat{l}_t$, is given by

$$\hat{l}_t = (1 - d_t - \kappa i_t)\, l_t.$$

This equation captures the fact that the number of valid household member is decreased by death and sickness. Production is linear in effective labor

$$Y_t = \hat{L}_t = N\hat{l}_t.$$

In our basic model we ignore the issue of firm heterogeneity and market power. Therefore price is equal to marginal cost

$$P_t = W_t = 1,$$

Covid Economics 4, 14 April 2020: 25-46

where W is the wage per unit of effective labor, which we normalize to one.

2.4 Income and Contagion

At the end of each period, household members regroup and share income, consumption and exposure. Household labor income is $W_t\hat{l}_t = \hat{l}_t$ and the budget constraint is

$$(1-d_t)\,c_t + \frac{b_{t+1}}{1+r_t} \leq b_t + \hat{l}_t$$

Household exposure is

$$e_t = \bar{e} + (1-d_t)\,e^c c_t C_t + (1-d_t-\kappa i_t)\,e^l l_t L_t,$$

where $\bar{e}$ is baseline exposure, independent of market activities. Contagion dynamics follow an SIR model. From the perspective of one household, this model is:

$$\begin{aligned} s_{t+1} &= s_t - \gamma e_t \frac{I_t}{N} s_t \\ i_{t+1} &= \gamma e_t \frac{I_t}{N} s_t + (1-\rho)\,i_t - \delta_t \kappa i_t \\ d_{t+1} &= d_t + \delta_t \kappa i_t \\ r_{t+1} &= r_t + \rho i_t \end{aligned}$$

where γ is the infection rate per unit of exposure, ρ the recovery rate, κ the probability of being sick conditional on infection, and δ_t the mortality rate of sick patients. In the standard SIR model γ is constant. In our model it depends on exposure and therefore on mitigation strategies. The parameter δ_t increases when the health system is overwhelmed, as discussed below.

2.5 Market Clearing and Aggregate Dynamics

Infection dynamics for the the entire population are simply given by the SIR system above with aggregate variable $I_t = Ni_t$, and so on. The aggregate labor force is $N\,(1-\kappa i_t - d_t)\,l_t$ and total consumption is $N\,(1-d_t)\,c_t$. Goods market clearing requires

$$(1-d_t)\,c_t = \hat{l}_t,$$

Covid Economics 4, 14 April 2020: 25-46

and bond market clearing requires

$$b_t = 0.$$

Finally we capture the limited capacity of the healthcare system with the increasing function

$$\delta_t = \delta\left(I_t\right).$$

Note that $\delta\left(I_t\right)$ should really be written as $\delta\left(\kappa I_t, H_t\right)$ where κI_t is the number of sick people and H_t is the capacity of the healthcare system. Since we assume that both κ and H are constant we write simply $\delta\left(I_t\right)$. We call the fact that δ is increasing the congestion externality.

Covid Economics 4, 14 April 2020: 25-46

3 Decentralized equilibrium

Our main goal is to compare the decentralized equilibrium with the planner's solution.

3.1 Equilibrium Conditions

Since our model reduces to a representative household model and since $b = 0$ in equilibrium, we simply omit b from the value function. The household's recursive problem is

$$V_t\left(i_t, s_t, d_t\right) = \max_{c_t, l_t, m_t} u\left(c_t, l_t; i_t, d_t\right) + \beta V_{t+1}\left(i_{t+1}, d_{t+1}, s_{t+1}\right),$$

where the flow utility is

$$u\left(c_t, l_t; i_t, d_t\right) = \left(1 - d_t\right)\log\left(c_t\right) - \left(1 - d_t - \kappa i_t\right)\frac{l_t^{1+\eta}}{1+\eta} - u_\kappa \kappa i_t - u_d d_t$$

Using the definition of effective labor $\hat{l}_t = \left(1 - d_t - \kappa i_t\right) l_t$, we can write the Lagrangian as

$$\begin{aligned}
V_t = {} & u\left(c_t, l_t; i_t, d_t\right) + \beta V_{t+1} + \lambda_t\left(\hat{l}_t + b_t - \left(1 - d_t\right)c_t - \frac{b_{t+1}}{1 + r_t}\right) \\
& + \lambda_{e,t}\left(e_t - \bar{e} - \left(1 - d_t\right)e^c c_t C_t - \left(1 - d_t - \kappa i_t\right)e^l l_t L_t\right) \\
& + \lambda_{i,t}\left(i_{t+1} - \gamma e_t \frac{I_t}{N} s_t - \left(1 - \rho\right) i_t + \delta_t \kappa i_t\right) \\
& + \lambda_{s,t}\left(s_{t+1} - s_t + \gamma e_t \frac{I_t}{N} s_t\right) \\
& + \lambda_{d,t}\left(d_{t+1} - d_t - \delta_t \kappa i_t\right)
\end{aligned}$$

We highlight in red the externalities, from infection and from congestion. The first order conditions for consumption and labor are then

$$c_t: \ c_t^{-1} = \lambda_t + \lambda_{e,t} e^c C_t$$
$$l_t: \ l_t^{\eta} = \lambda_t - \lambda_{e,t} e^l L_t$$

The remaining first order conditions are

$$e_t: \lambda_{e,t} = (\lambda_{i,t} - \lambda_{s,t}) \gamma \frac{I_t}{N} s_t$$
$$i_{t+1}: \lambda_{i,t} = -\beta V_{i,t+1}$$
$$s_{t+1}: \lambda_{s,t} = -\beta V_{s,t+1}$$
$$d_{t+1}: \lambda_{d,t} = -\beta V_{d,t+1}$$

The envelope conditions are

$$V_{i,t} = \kappa \frac{l_t^{1+\eta}}{1+\eta} - \kappa u_\kappa - \kappa \lambda_t l_t + \lambda_{e,t} \kappa e^l l_t L_t - (1-\rho) \lambda_{i,t} + \delta_t \kappa (\lambda_{i,t} - \lambda_{d,t})$$
$$V_{s,t} = (\lambda_{s,t} - \lambda_{i,t}) \gamma e_t \frac{I_t}{N} - \lambda_{s,t}$$
$$V_{d,t} = \frac{l_t^{1+\eta}}{1+\eta} - \log(c_t) - u_d - \lambda_t (l_t - c_t) + \lambda_{e,t} \left(e^c c_t C_t + e^l l_t L_t \right) - \lambda_{d,t}$$

3.2 Equilibrium with Exogenous Infections

Economy before the pandemic To simplify the notation we normalize $N = 1$, so we should think of our values as being per-capita pre-infection. When there is no risk of contagion, i.e., when $i_t = 0$ and $\lambda_{e,t} = 0$, optimal consumption and labor supply implies $c_t^{-1} = l_t^{\eta}$. We have $\hat{l}_t = l_t$ so market clearing is simply $c_t = l_t$. Combining these two conditions we get

$$c_t = l_t = 1.$$

The pre-infection economy is always in steady state.

Covid Economics 4, 14 April 2020: 25-46

Exogenous infections Consider now an economy with exogenous SIR dynamics: $e^c = e^l = 0$. The SIR system is then independent from the economic equilibrium. In the SIR system, the share of infected agents I_t increases, reaches a maximum and converges to 0 in the long run. Assuming a constant δ, the long run solution solves

$$\log\left(\frac{S_\infty}{1-I_0}\right) = -\frac{\gamma\bar{e}}{\rho+\delta\kappa}\left(\frac{1-S_\infty}{N}\right),$$

and

$$D_\infty = \frac{\delta\kappa}{\delta\kappa+\rho}\left(1-S_\infty\right).$$

When the congestion externality arises and δ_t increases, then we cannot obtain a closed-form solution for the long run death rate but the qualitative results are unchanged. Since $e^c = e^l = 0$ we have $m_t = 0$ and $c_t^{-1} = l_t^\eta$. Market clearing requires $(1-d_t)\,c_t = (1-d_t-\kappa i_t)\,l_t$ therefore labor supply is

$$l_t^{1+\eta} = 1 + \frac{\kappa i_t}{1-d_t-\kappa i_t}.$$

The labor supply of valid workers increases to compensate for the reduced productivity of the sick. Per capita consumption is

$$c_t = \left(\frac{1-d_t}{1-d_t-\kappa i_t}\right)^{-\frac{\eta}{1+\eta}}$$

As long as $\eta > 0$ consumption per capita decreases. Aggregate GDP decreases because of lost labor productivity and deaths. The following proposition summarizes our results.

Proposition 1. *When contagion does not depend on economic activity* $\left(e^c = e^l = 0\right)$*, the share of infected agents* I_t *increases, reaches a maximum and converges to* 0 *in the long run. The long run death rate is given by* $D_\infty = \frac{\delta\kappa}{\delta\kappa+\rho}\left(1-S_\infty\right)$ *where the long run share of uninfected agents solves* $\log\left(\frac{S_\infty}{1-I_0}\right) = -\frac{\gamma\bar{e}}{\rho+\delta\kappa}\left(\frac{1-S_\infty}{N}\right)$*. Along the transition path, labor supply of able-bodied workers follows the infection rate while per-capita consumption moves in the opposite direction as* $c_t = \left(1-\frac{\kappa i_t}{1-d_t}\right)^{\frac{\eta}{1+\eta}}$.

3.3 Private Incentives for Mitigation

Let us focus on consumption by setting $e^l = 0$. Optimal private consumption is

$$c_t^{-1} = \lambda_t + \lambda_{e,t} e^c C_t,$$

Covid Economics 4, 14 April 2020: 25-46

so the temptation to cut consumption depends on $\lambda_{e,t} = (\lambda_{i,t} - \lambda_{s,t})\,\gamma \frac{I_t}{N} s_t$ which is high when $\gamma \frac{I_t}{N} s_t$ is high, which is exactly when new infections are high and S is quickly decreasing. So holding constant $\lambda_{i,t} - \lambda_{s,t}$ the private incentives to cut consumption are proportional to the number of new cases. The other important element is

$$\lambda_{i,t} - \lambda_{s,t} = \beta\,(V_{s,t+1} - V_{i,t+1})$$

The right-hand-side of this expression represents the value of avoiding an infection. This reflects the future disutility of avoiding sickness and death. One problem is that when agents anticipate large infections in the future this value can fall. Jones et al. (2020) call this the fatalism effect.

4 Planner's Problem

We normalize $N = 1$ for simplicity. The planner solves

$$\max U = \sum_{t=0}^{\infty} \beta^t u\,(C_t, L_t; I_t, D_t)$$

subject to

$$u\,(C_t, L_t; I_t, D_t) = (1 - D_t)\log(C_t) - (1 - D_t - \kappa I_t)\,\frac{L_t^{1+\eta}}{1+\eta} - u_\kappa \kappa I_t - u_d D_t$$

and

$$(1 - D_t)\,C_t = (1 - D_t - \kappa I_t)\,L_t.$$

The first order conditions for consumption and labor are then (highlighted in red the difference with the decentralized equilibrium)

$$C_t:\ C_t^{-1} = \lambda_t + 2\lambda_{e,t} e^c C_t,$$
$$L_t:\ L_t^{\eta} = \lambda_t - 2\lambda_{e,t} e^l L_t.$$

The marginal utilities of the planner with respect to exposure are twice as high as those of the private sector because of the contagion externalities: private agents only care about how their behavior affect

Covid Economics 4, 14 April 2020: 25-46

their own infection risk. They do not care about how their behavior affects the infection risk of others. The envelope condition that differs from that of private agents is

$$V_{I,t} = \kappa \frac{L_t^{1+\eta}}{1+\eta} - \kappa u_\kappa - \kappa \lambda_t L_t + \lambda_{e,t} \kappa e^l L_t^2 - (1-\rho)\lambda_{i,t} - \gamma e_t S_t \lambda_{i,t} - \left(\delta_t \kappa + \delta_t' \kappa^2 I_t\right)(\lambda_{d,t} - \lambda_{i,t}).$$

This equation highlights the congestion externality. These externalities determine the planner's incentives to reduce consumption today.

Incentives to Mitigate Let us focus on consumption by setting $e^l = 0$ to understand the incentives to mitigate.

$$C_t^{-1} = \lambda_t + 2\lambda_{e,t} e^c C_t = \lambda_t + 2 e^c C_t \gamma I_t S_t (\lambda_{i,t} - \lambda_{s,t})$$

The contemporaneous impact depends on $\gamma I_t S_t$ but the impact is twice as high as in the private case because of the infection externality. As in the decentralized equilibrium, the forward looking effect depends on $\lambda_{i,t} - \lambda_{s,t} = \beta (V_{S,t+1} - V_{I,t+1})$, the future disutility of avoiding sickness and death, which is magnified in the planner solution compared to the decentralized equilibrium because of the potential for congestion in the healthcare system.

5 Calibration

The lack of reliable data to calibrate the contagion model creates a serious challenge and an important limitation. Atkeson (2020a) discusses these difficulties. We calibrate our model at the weekly frequency.

Contagion The SIR block of the model is parameterized as follows. The recovery parameter is set to $\rho = 0.35$. The fraction of infected people who are sick is $\kappa = 0.15$. We normalize $\bar{e} + e^c + e^l = 1$. In our baseline calibration, we set the exposure loading parameters $e^c = e^l = \frac{1}{3}$ which is consistent with the estimation in Ferguson (2020). These parameters imply $e = 1$ at the pre-pandemic levels of consumption and labor (the calibration of production and utility parameters will be described later). The parameter γ is then chosen to target the basic reproduction number (i.e. the average number of people infected by a single infected individual) of $\mathcal{R} = 2$, yielding an estimated value of $\gamma = 0.7$. Finally, to parameterize the fatality rate and the congestion effects, we adopt the following functional form for $\delta(\cdot)$:

$$\delta(\kappa I_t) = \bar{\delta} + \exp(\phi I_t) - 1$$

Covid Economics 4, 14 April 2020: 25-46

where the parameter ϕ indexes the strength of the congestion externality. We set $\bar{\delta}$ and ϕ to match two targets for the case fatality rate: a baseline value (i.e. the fraction of infected people who die even in the absence of congestion) of 1% and an 'extreme' value (the fraction of people who die $\kappa I = 0.15\,(0.2)$, i.e. 3% of the population requires medical attention) of 5%. This procedure yields $\bar{\delta} = 0.023$ and $\phi = 3.15$.

Preferences and technology The utility parameter u_d is set to a baseline value of 2. This implies a *flow* disutility from death that is roughly 7 times per capita income. Such large non-monetary costs associated with loss of life are consistent with estimates in the literature and with values used by government entities like the EPA. For example, Greenstone and Nigam (2020) use an estimated value of a statistical life of $11.5 million (in 2020 dollars) to the household from death. Assuming a rate of return of 5%, this translates into an annual flow value of $575,000, or roughly 10 times per capita GDP. The flow disutility from sickness $u_s$is set to equal one-fourth of u_d, i.e. a value of 0.5.

Initial Conditions, Vaccine, and Robustness A time period is interpreted as a week. The discount factor β captures both time discounting and the discovery of a cure/vaccine. We assume for simplicity that a cure and a vaccine arrive randomly together with a constant arrival rate. This is then exactly equivalent to adjusting β. We take a relatively pessimistic case as our baseline, where the combined effect of time discounting and the vaccine is to yield an annual β of 0.8 and a weekly beta of $\beta = (0.8)^{\frac{1}{52}} = 0.9957$.

6 Quantitative Results

Our benchmark exercise uses a large initial infection rate of $i_0 = 1\%$ because it makes the figures easier to read, but this is a large shock. It seems likely that agents and policy makers become aware of the epidemic much earlier so we report simulations starting at $i_0 = 0.1\%$.

Private Response The figures show the results of simulations. We start with the decentralized solution. Figure 1 shows the behavior of the contagion and macro variables in the decentralized equilibrium, under two different assumptions about exposure. The blue line solid shows a situation where infection rates are exogenous, i.e. do not vary with the level of economic activity. Since infection is assumed to be exogenous, agents do not engage in mitigation, i.e., they ignore the pandemic. In fact, labor input rises (the solid line, left panel in the third row in Figure 1), while per-capita consumption

Covid Economics 4, 14 April 2020: 25-46

Covid Economics 4, 14 April 2020: 25-46

falls by about 2.5% (the dashed line), as able-bodied workers work harder to compensate for the workers who are sick. This is of course not a realistic assumption, but it serves as a useful benchmark for the worst case scenario. In this scenario, eventually about 80% of the population is infected and about 2.5% of the population succumbs to the virus (left panel in the second row in Figure 1). The case mortality rate peaks at 4% roughly 15 weeks after the initial infection because, at the peak, about 15% of the population is infected and the healthcare system is overwhelmed.

The red line describes the case where exposure is endogenous and the household can reduce exposure by cutting back on its consumption and labor supply. As we would expect, this leads to a sharp reduction in economic activity (third row, left panel in Figure 1) by about 10%. Importantly, however, the reduction is gradual, tracking the overall infection rate (it takes almost 17 weeks for consumption and labor to hit their trough). Intuitively, when the fraction of infected people is low (as is the case in the early stages), a reduction in exposure has a small effect on infection risk, relative to the resulting fall in consumption. And since each household does not internalize the effect it has on the future infection rate, it has little incentive to indulge in costly mitigation early on. This dynamic is reflected in the hump-shaped pattern in λ_e (the bottom, left panel in Figure 1). As we will see, this is drastically different in the planner's problem. The mitigation behavior does lower the cumulative infection and death rates (relative to the exogenous infection risk) down do about 2%.

Optimal Response We now turn to the planner's solution, depicted in Figures 2. As before, the blue and red lines show the cases of exogenous infection and mitigation. As the red curve in Figure 2 clearly shows, the planner finds it optimal to "flatten the curve" rather dramatically. The peak infection and mortality rates are only slightly higher than their initial levels and well below the decentralized equilibrium levels, as are cumulative fatalities (approximately 0.8%, compared to 2% in the decentralized equilibrium). To achieve this, the planner has to reduce exposure drastically by more than 40% (recall that, in the decentralized equilibrium, exposure bottomed out at 0.8), keeping the basic reproduction number $\mathcal{R}$ from rising much above 1. Of course, this pushes the economy into a deep recession with consumption falling by as much as 40% (third row, left panel in Figure2). More interestingly, the planner chooses to step on the brakes almost immediately, rather wait for infection rates to rise. In fact, the shadow value of exposure (bottom left panel in Figure 2) spikes upon impact and then slowly decays over time, as the number of susceptible people declines.

Early Warning What is the value of an early warning? Suppose agents become aware of the disease at $i_0 = 0.1\%$ instead of 1% as assumed above. This simulation highlights even more the gap between the decentralized outcome and the planner's solution. The private sector response continues to follow the infection curve. As a result, the outcome barely changes. Private agents do not have the proper incentives to use the early warning.

The planner, on the other hand, continues to front-load her effort and achieves a much better outcome when it receives an early warning. The cumulative fatality rate is only 0.2% instead of 0.8% when it reacts to the disease at a later stage.

7 Conclusions

We propose an extension of the neoclassical model to include contagion dynamics, to study and quantify the tradeoffs of policies that can mitigate the Covid-19 pandemic. Our model reveals two key insights. The first insight is that externalities are massive. The planner acts much more forcefully than private agents. Roughly speaking, under SIR dynamics, the planner's incentives are twice as high as those of private agents. The risk of congestion increases the difference even further. Thus, when private incentives would yield a 10% drop in consumption, the planner engineers an optimal decline of 30% to 40%. One reason why the planner is willing to tolerate such a large decline in consumption is the assumption of complete risk-sharing, i.e. the recession affects all agents equally. Heterogeneity and incomplete markets might make the recession more costly, especially if the the burden of the recession falls disproportionally on low-income, low-wealth households, as in Kaplan et al. (2020). Our neoclassical setting also abstracts from demand-related amplifications, as in Guerrieri et al. (2020).

The second key difference is that the planner optimally chooses to front-load her mitigation strategies. As a result, a planner with an early warning does much better than a planner without an early warning. Private agents, on the other hand, waste the value of the early warning because their mitigation efforts are essentially proportional to the current infection rate.

As we write the first draft of this paper there is much uncertainty about the parameters of the disease, and yet decisions must be made. Some of our results speak directly to this dilemma. Atkeson (2020a) points out that, when one does not know the initial number of active cases, it is difficult "to distinguish whether the disease is deadly (1% fatality rate) or milder (0.1% fatality rate)." In our simulations we have considered a deadly disease with a low initial infection rate of $i_0 = 0.1\%$, and a

Covid Economics 4, 14 April 2020: 25-46

milder disease with a high initial infection rate of $i_0 = 0.1\%$. Interestingly, in both cases, the planner should implement immediately a strong suppression policy. The main difference is that in the mild case it is optimal to release the lockdown sooner. Assuming that there is enough data 20 weeks after the outbreak to correctly estimate the fatality rate, the planner could implement an optimal response despite the large uncertainty in the key parameter. Jones et al. (2020) study extensions of our baseline setup.

Covid Economics 4, 14 April 2020: 25-46

References

Alvarez, Fernando, David Argente, and Francesco Lippi, "A Simple Planning Problem for COVID-19 Lockdown," March 2020. Working Paper.

Atkeson, Andrew, "How Deadly is COVID-19? Understanding the Difficulties with Estimation," March 2020. NBER Working Paper No. 26867.

_ , "What Will Be the Economic Impact of COVID-19 in the US? Rough Estimates of Disease Scenarios," March 2020. NBER Working Paper No. 26867.

Baker, Scott R., R.A. Farrokhnia, Steffen Meyer, Michaela Pagel, and Constantine Yannelis, "How Does Household Spending Respond to an Epidemic? Consumption During the 2020 COVID-19 Pandemic," *University of Chicago, Working Paper*, 2020.

Barro, Robert J, Jose Ursua, and Joanna Weng, "The coronavirus and the Great Influenza epidemic: Lessons from the "Spanish Flu" for the coronavirus' potential effects on mortality and economic activity," March 2020. AEI Economics Working Paper 2020-02.

Berger, David, Kyle Herkenhoff, and Simon Mongey, "An SEIR Infectious Disease Model with Testing and Conditional Quarantine," March 2020. Working Paper.

Correia, Sergio, Stephan Luck, and Emil Verner, "Pandemics Depress the Economy, Public Health Interventions Do Not: Evidence from the 1918 Flu," March 2020. Working Paper.

Diekmann, Odo and J. Heesterbeek, *Mathematical Epidemiology of Infectious Diseases: Model Building, Analysis and Interpretation*, John Wiley, 2000.

Eichenbaum, Martin, Sergio Rebelo, and Mathias Trabandt, "The Macroeconomics of Epidemics," March 2020. Working Paper NWU.

Ferguson, Neil, "Impact of non-pharmaceutical interventions (NPIs) to reduce COVID- 19 mortality and healthcare demand," March 2020. Imperial College Report.

Greenstone, Michael and Vishan Nigam, "Does Social Distancing Matter?," *University of Chicago, Becker Friedman Institute for Economics Working Paper*, 2020, (2020-26).

Covid Economics 4, 14 April 2020: 25-46

Guerrieri, Veronica, Guido Lorenzoni, Ludwig Straub, and Iván Werning, "Macroeconomic Implications of COVID-19: Can Negative Supply Shocks Cause Demand Shortages?," April 2020. NBER Working Paper No. 26918.

Jones, Callum, Thomas Philippon, and Venky Venkateswaran, "Optimal Mitigation Policies in a Pandemic," March 2020. NYU Working Paper.

Kaplan, Greg, Benjamin Moll, and Gianluca Violante, "Pandemics according to HANK," April 2020. Working Paper.

Lucas, Robert E. Jr. and Nancy L. Stokey, "Money and Interest in a Cash-in-Advance Economy," *Econometrica,*, 1987, *55* (3), 491–513.

Covid Economics 4, 14 April 2020: 25-46

Covid Economics 4, 14 April 2020: 25-46

Figure 1: Decentralized Equilibrium

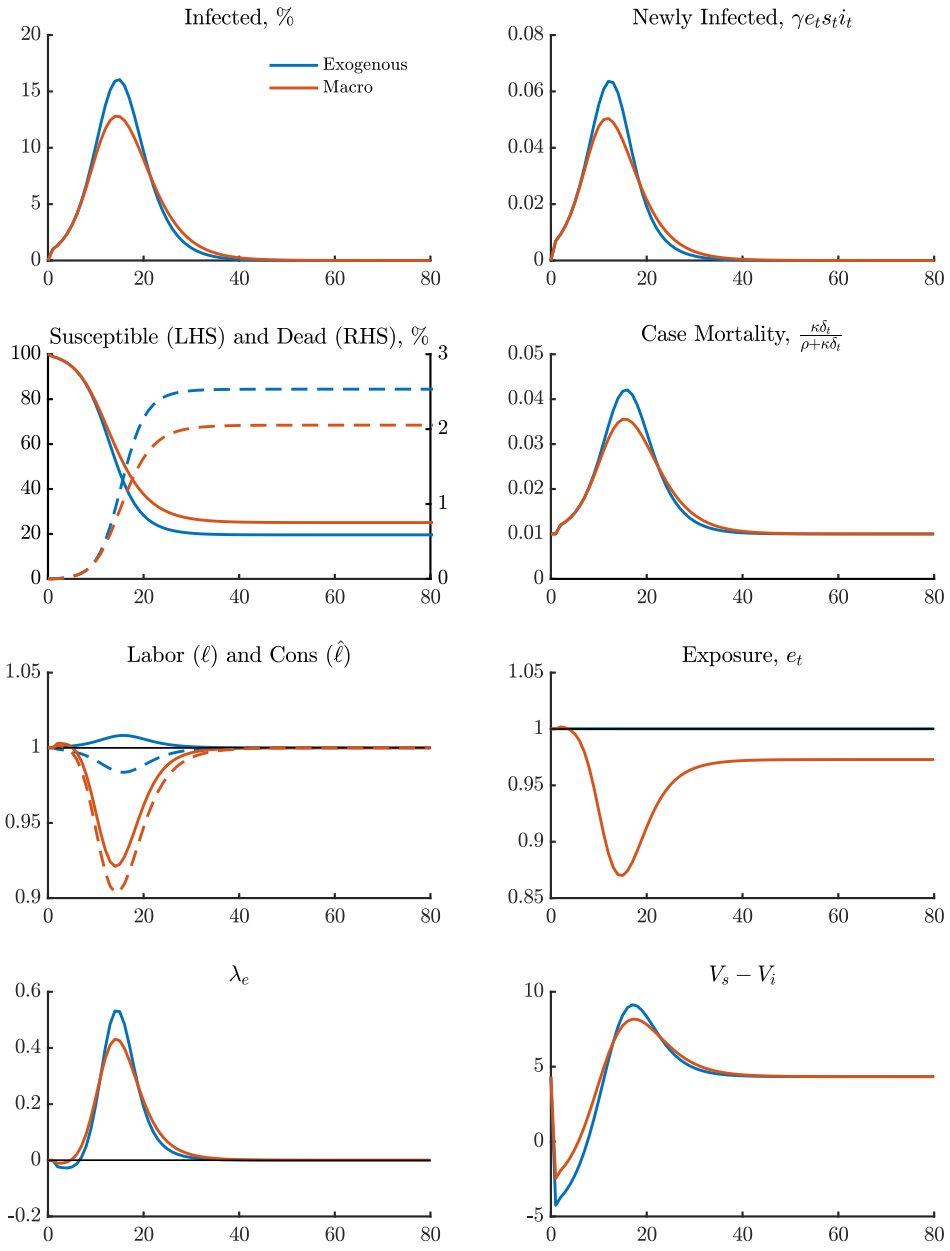

Figure 2: Planner Equilibrium

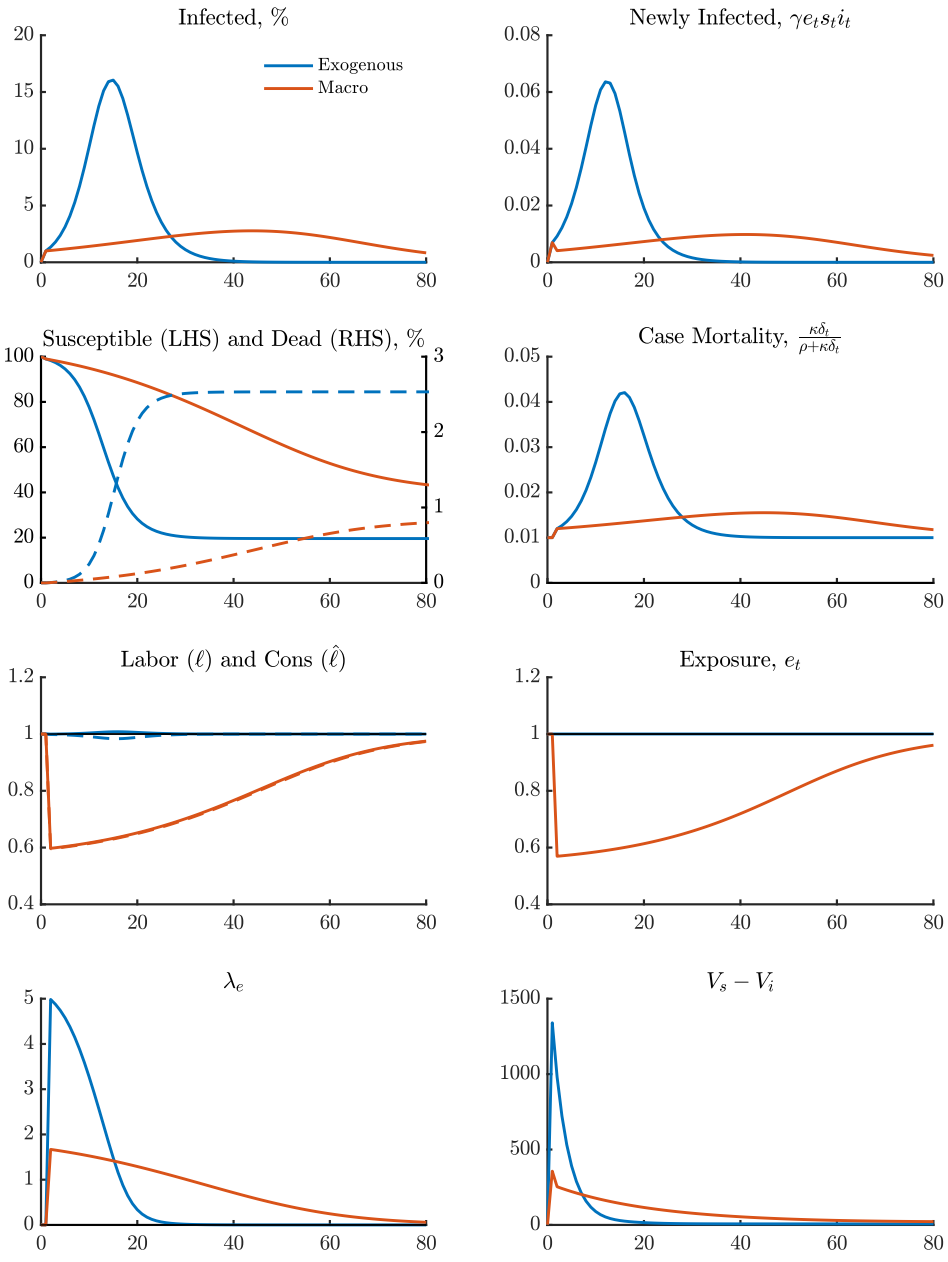

Covid Economics 4, 14 April 2020: 25-46

Figure 3: Decentralized Equilibrium, 0.1% Initial Infected

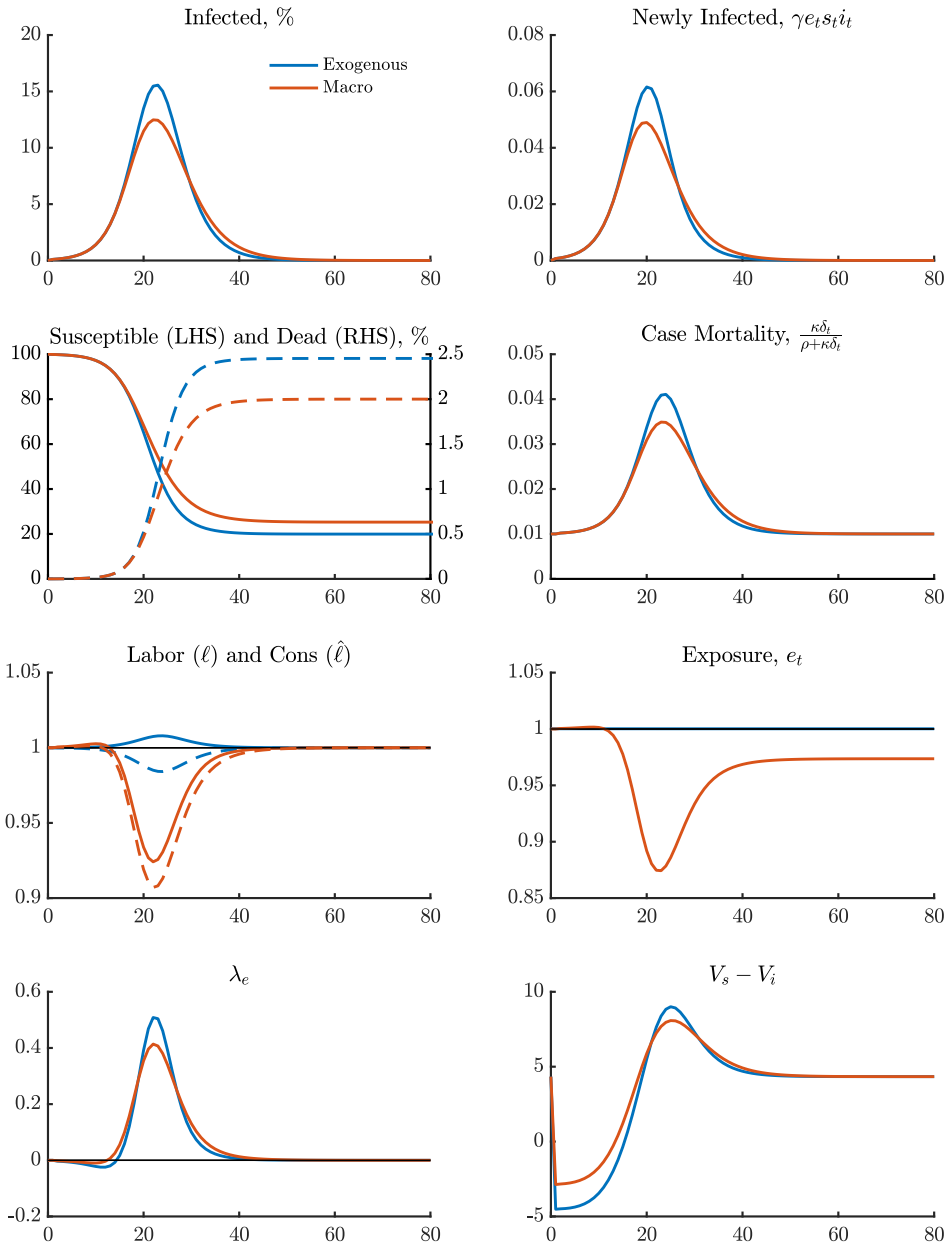

Covid Economics 4, 14 April 2020: 25-46

Covid Economics 4, 14 April 2020: 25-46

Figure 4: Planner Solution, 0.1% Initial Infected

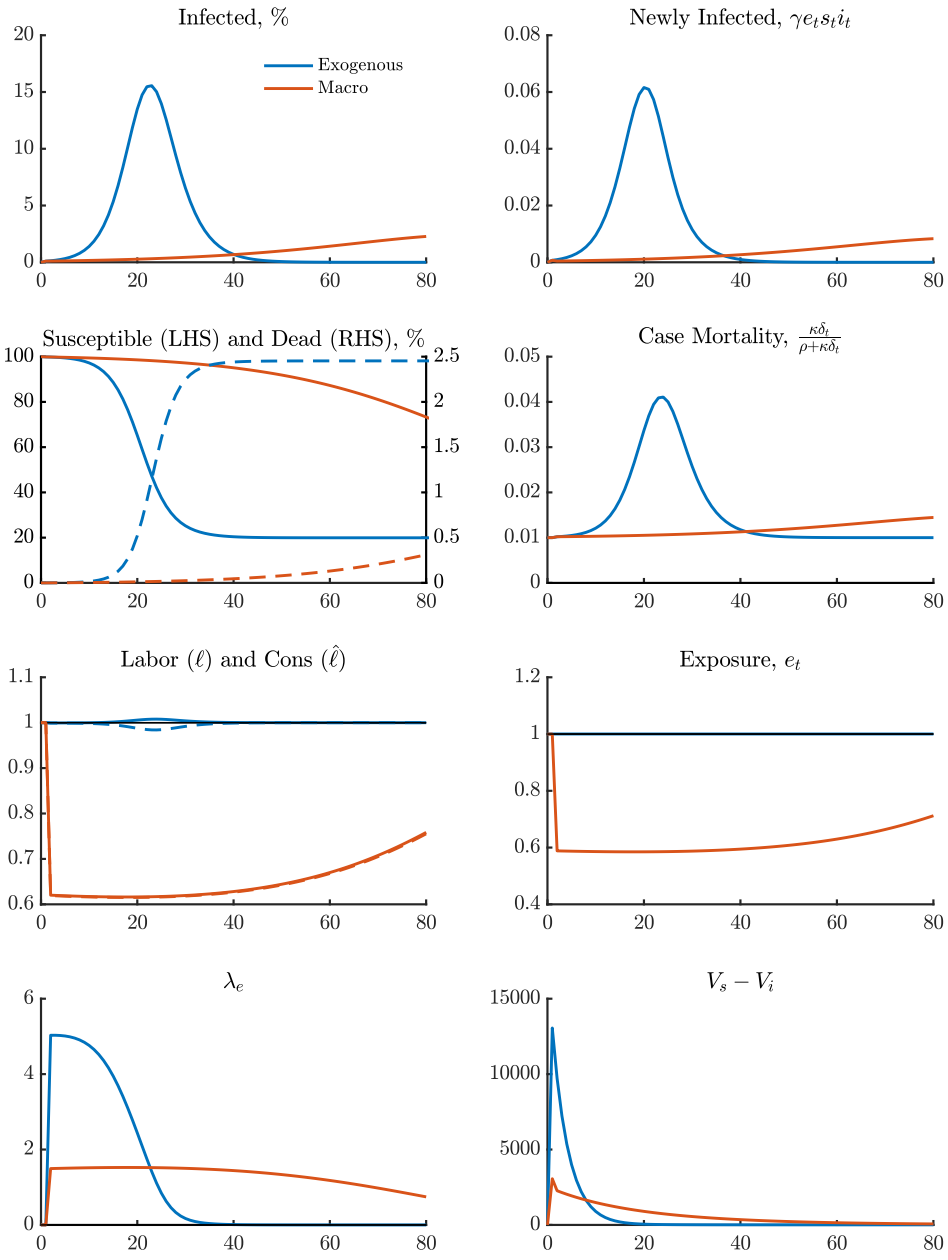

Covid Economics **Issue 4, 14 April 2020**

Why is Covid-19 mortality in Lombardy so high? Evidence from the simulation of a SEIHCR model[1]

Carlo Favero[2]

Date submitted: 3 April 2020; **Date accepted:** 7 April 2020

The standard SEIR model based on a parameterisation consistent with the international evidence cannot explain the very high Covid-19-related mortality in Lombardy. This paper proposes an extension of the standard SEIR model that is capable of solving the puzzle. The SEIR model features exogenous mortality: once susceptible individuals are first exposed, and then infected, they succumb with a given probability. The extended model inlcudes a hospitlisation process and the possibility that hospitalised patients, who need to resort to an intensive care unit, cannot find availability because the ICU is saturated. This constraint creates an additional increase in mortality, which is endogenous to the diffusion of the disease. The SEIHCR model (H stands for hospitalisation and C stands for constraint) is capable of explaining the dynamics of Covid-19-related mortality in Lombardy with a paramerisation consistent with the international evidence.

1 I thank the editor, Charles Wyplosz and an anonymous referee for their useful comments. I also thank Yakov Amihud,Francesco Corielli, Francesco Giavazzi, Luigi Guiso, Andrea Ichino, Marco Olivari, Fausto Panunzi, Franco Peracchi, Carlo Pinardi, Aldo Rustichini, Guido and Marco Tabellini for many useful comments and discussion. Giovanni Favero brought my attention to SEIR models. I worked on this project full-time during the Milan lockdown. The fact that I was stuck at home while my daughter Vittoria, who is a young doctor, was everyday on the front line gave me an enormous motivation. I dedicate this effort of mine to the hospital personnel in Lombardy, they deserve it fully.

2 Deutsche Bank Professor of Asset Pricing and Quantitative Finance, Bocconi University and CEPR Research Fellow.

Covid Economics 4, 14 April 2020: 47-61

Covid Economics 4, 14 April 2020: 47-61

1 Introduction

COVID-19 related mortality in Lombardy is way above COVID-related mortality everywhere else. Using data made available by the Civil Protection, https://github.com/pcm-dpc/COVID-19 , Figure 1 illustrates the ratio of deaths (morti) to total cases (casi_totali) observed daily over the period February 24th 2020-April 8th 2020 which shows a reported lethality growing rather steadily from an initial 4 per cent to a value reaching 16 per cent at the end of the sample (9722 Fatalities for 53414 total observed cases).

INSERT FIGURES 1 HERE

This pattern of lethality cannot be replicated by standard SEIR model, which has been successfully applied to the analysis of COVID-19 diffusion in China [Wu, et. al, Kucharski et. al.]. The second line in the graph reports the pattern of the ratio of fatalities to the sum of Exposed, Recovered and Removed as Fatalities generated by a SEIR model with an internationally consistent CFR of 0.0138 (see, for example, Verity et al(2020)) which is nowhere near the observed data.

Two possible explanations can be considered for a discrepancy between observed data and model simulated data: either the model is wrong or the data are wrong. As matter of fact, the data can be wrong the total observed cases observe do not include patients with mild symptoms, which were not hospitalized and were therefore not tested.

In this paper we explore the possibility that the standard model misses an important dimension that is instead reflected in the data.

Figure 2 reports daily fatalities in Lombardy and Veneto, nearby region with about half of the population (4.9 millions inhabitants versus about 10 millions in Lombardy), which witnessed a remarkably lower number of deaths per day. Figure 3 illustrates another interesting feature of the data from Lombardy and Veneto: the share of hospitalized patients in ICU has been much higher in Veneto than in Lombardy, hinting at the possibility of an important mismatch between the demand of ICU beds and their supply in Lombardy.

INSERT FIGURES 2-3 HERE

The mismatch between data and model prediction in Lombardy and the heterogenous pattern of mortality observed in Lombardy and Veneto can be related to a specific feature of the SEIR model: mortality is exogenously given by a constant parameter. In the SEIR specification Infectious patients are divided in three groups, Mild, Severe and Fatal,

Covid Economics 4, 14 April 2020: 47-61

and the destiny of each patient is written at the time their are exposed to the disease. After some heterogenous duration, Mild and Severe patients inevitably recover, while fatal patients inevitably die. What if what happened in Lombardy can be described as follows: infectious patients are still divided in the three standard groups, but the Severe do not inevitably recover. In fact, some of them need assistance in Intensive Care Unit and if there are no available ICU positions, then their status changes from Severe to Fatal . There is therefore a time-varying endogenous component of mortality that cannot be captured by the standard SEIR model.

Note that Ferguson et al. (2020) when providing estimates of the simulated effect on US and UK of an unmitigated epidemic featuring a basic reproduction number R_o of 2.4 clearly state "... In total, in an unmitigated epidemic, we would predict approximately 510,000 deaths in GB and 2.2 million in the US, **not accounting for the potential negative effects of health systems being overwhelmed on mortality**...."

This paper extends the SEIR model to a SEIHCR that follows patients in their pattern of Hospitalization and endogeneize the possible Constraint of ICU availability and its impact on lethality.

The model is calibrated to the data from Lombardy to illustrate that it is capable to replicate the observed pattern of lethality in Lombardy with a parametrization fully in line with the international evidence.

2 The SEIHCR Model: Description

The SEIHCR model is a system of differential equations for the dynamics of a virus across different groups of the population.

The exact specification of the equations is reported in the Appendix, Figure 4 reports the Dependency Graph of the Model, while this section describes its structure and fundamental elements.

INSERT FIGURE 4 HERE

The model allows to simulate the dynamics of the virus diffusion starting from an initial period in which the total **Population** (N_t) of N individuals is divided in 1 **Infectious** (I_t) and N-1 **Susceptible** (S_t)**.** In each period (day) some Susceptible become **Exposed** (E_t)**,** their number is determined by the basic reproduction number R_0,that determines the number of secondary infections each infected individual produces, by the probability with which Susceptible meets Infectious, $\left(\frac{I_{t-1}}{N_{t-1}}\right)$, and by the average duration of the period in which a patient is infectious

Covid Economics 4, 14 April 2020: 47-61

T_{inf}. Exposed after an incubation period of length T_{inc}, become Infectious. The outflows from Susceptible is the inflows into Exposed in each period, and the outflows from Exposed is the inflows into Infectious. Infectious falls into three groups: those with mild symptoms ($MILD_t$), those with severe symptoms (SEV_t), and those with fatal symptoms (FAT_t). The allocation to these groups is controlled by three probabilities: $\left(1-p^{sev}-p^{fat}\right)$, p^{sev}, p^{fat}. Patients with mild symptoms recover after a recovery period, T_{srec}. Patients with severe and fatal are **Hospitalized.** All patients with symptoms that require hospitalization, are hospitalized after a period of average duration T_{shosp}, some hospitalized patients require intensive care unit with probability p^{ic}. Patient with fatal symptoms succumb notwithstanding hospitalization, even in intensive care, after the mean duration from the onset of symptoms to death, T_{sd}. Patient with severe symptoms either recover or become fatal. The recovered, with a mean duration of from the onset of symptoms to hospital discharge of T_{shd}, are those who do need intensive care unit and those who need intensive care unit and find a place. The patients with severe symptoms that need ICU and do not find availability are **Constrained** and become fatalities. At the end of each period the population decreases because of the fatalities, while the stock of recovered grows as a consequence from the new additions of recovered with mild and severe symptoms.

After calibration, we shall compare model simulated data with observed data from Lombardy to assess the potential of the model and its explanation of the mortality in Lombardy.

.

3 The SEIHCR Model: a Calibration to data from Lombardy

Model simulation requires numerical values for all the relevant parameters. Given the availability of a sample of sufficient size of reliable data, parameters can be estimated (see Cereda et al.(2020)). The daily data made available on Lombardy by Protezione Civile cover a short sample of about forty observations and are affected by a change in regime. In fact, on March 8 2020 a full lockdown was legislated for the region and the entire country.

Moreover, estimation of the model in a conventional sense, that is, deriving parameter values by fitting equations using time series data, is not possible because there are no data on Exposed, Infectious and Recovered. In fact, there are no patients are not tracked and those with Severe symptoms are recorded as positive only if they are tested and with a lag. This lag depends on the duration of the time elapsed between

Covid Economics 4, 14 April 2020: 47-61

symptoms and hospitalization, between hospitalization and testing, and between the moment in which the swab is taken and the results become available. Obtaining estimates of the Infectious would require ongoing random testing of the population, which has not happened so far in Lombardy. Similarly, the Recovered are underestimated because the only Recovered observed are those Recovered from hospital. In principle estimates of the total recovered could be obtained by ongoing random sampling of tests for serum antibodies in response to the coronavirus, however such tests are currently under development but not yet available.

Measurement error in the data has strong implications for the estimation of the crucial model parameters and for the design of optimal policies for them (see Stock(2020)).

These considerations led to the design and implementation of a calibration strategy based on the exploitation of the data on hospitalization, that we regard as the observed variable with the closest distance from the theoretical variables in the model.

Our procedure allowed to select the dating of the lockdown in the sample of simulated data and to estimate the impact of the lockdown on the basic reproduction number R_0. R_0 was set initially at 2.2 in line with the international evidence, reflected in the baseline parameterization in the epidemic calculator available online (https://gabgoh.github.io/COVID/index.html).

Also all the other parameters that determines the transmission dynamics and the clinical dynamics were chosen in line with the international evidence. The calibration of these parameters is summarized in Table 1.

INSERT TABLE 1 HERE

To set the value of R_0 after the intervention the model was simulated first in a pre-lockdown scenario, when the capacity constraint in terms of ICU was still irrelevant, with an initial population of 10 millions, and all duration parameters set in line with the international evidence. The lockdown was then dated in the model simulated data to match the number of hospitalized patients observed on the March 8 2020. This procedure dates March 8th as day 95 of our 730 (2 years) of simulated data. Having dated the lockdown, the post lockdown R_0 was calibrated to match the observed number of hospitalized patients two weeks after the lockdown. This procedure delivered a R_0 post lockdown of 0.95.

Finally, the probability with which of an hospitalized patient needs intensive care was calibrated at 0.2. As Figure 2-3 suggest, this is the value around which the share of hospitalized patients in ICU stabilizes over time in Veneto, the nearby region that recorded a much lower daily deaths than Lombardy.

Covid Economics 4, 14 April 2020: 47-61

4 The SEIHCR Model: Simulations

The model has been simulated under two scenarios. In the baseline scenario the IC capacity is set to 400 beds before the lockdown (the maximum of the observed utilization) and to the observed number of occupied ICU beds reported by Protezione civile that grows constantly to reach a total size of 1500, with a batch of 200 new units released simultaneously toward the end of the sample (this jump in the series is generated by the availability of the new Fiera Hospital in Milan). In the alternative scenario the capacity constraint has been removed, making counterfactually available to Lombardy a number of ICU beds equal to 20 per cent of hospitalized patients.

The most interesting results from the model extension is reported in Figure 5. Figure 5 clearly illustrates that the capacity constraint is essential to replicate the pattern of mortality observed in Lombardia. The model with the ICU constraint imposed generates a number of simulated daily deaths very close to the number of observed daily deaths in Lombardy. When the constraint is counterfactually removed, the simulated data provide a very close match for the pattern of daily deaths observed in Veneto and are nowhere near to the daily deaths observed in Lombardy.

INSERT FIGURE 5 HERE

The results of these simulations point to a crucial role for the expansion of ICU capacity to save lives in Lombardy and to the importance of the NPI policy implemented in Venteto. These policies were capable of keeping the diffusion of the disease under control and therefore the hospitalization rate much lower than that observed in Lombardy .

Figure 6 reports the pattern of model simulated total recovered, model simulated hospital recovered and tracked patients recovered (guariti).

INSERT FIGURE 6 HERE

The model based variables that tracks well the observed recovered patient is the patients recovered from hospital while the effective number of recoveries is much higher because of the relevance of patients with mild symptoms which were not tested. However, the model simulated number of total recovered patients at the end of May 2020 is of about half a million, which is five per cent of the total population in Lombardy.

Finally Figure 7.1 and 7.2 report the pattern of model based exposed and observed exposed (total cases- death-fatalities), looking at their level and their daily changes.

INSERT FIGURE 7.1-7.2 HERE

The figure shows that the observed daily exposed are also in line with the model prediction. In fact, while Susceptible becomes Exposed instantaneously in the model, their observation in the data requires testing which is implemented only some time after hospitalization. The model based pattern of the change in Exposed, which again is followed with a lag by the actual data, might be of help in designing optimal interpolant for reduced form data based prediction of the dynamics of the virus.(Peracchi(2020))

5 Conclusions and Policy Implications

A SEIHCR Model used for simulation of the fatality of the COVID disease in Lombardy is capable of explaining the high mortality rate observed in this region.

The main innovation of the model is the endogeneization of the fatality rate, that becomes higher than the CFR of 0.0138 when the demand of ICU beds exceeds their available supply.

Data simulated from the model with endogenous mortality can explain the high number of deaths observed in Lombardy and the striking difference in observed COVID mortality bewteen Lombardy and Veneto.

The impact of different NPI approaches to reduce hospitalization is amplified when mortality increases because of excess demand of ICU beds.

The cost of not implementing NPI interventions aimed at "flattening the curve" becomes higher when the curve becomes "more humpy" as a consequence of the strain on healthcare and Intensive Unit Care capacity.

The model also shows that the number of actual recovered patients in Lombardy is much higher than the observed number of patients recovered from hospitalization. However, the estimate of model simulated recovered subjects by the end of May 2020 stands only half a million individuals (under a parameterization in which the lockdown has brought R_0 to 0.95).

The importance of the ICU constraint in increasing fatality should be taken into account in the design of exit strategies from the lockdown.

NPI measures that have brought R_0 close to one have greatly relieved the strain of healthcare capacity. In their removal strategy the benefits of a growing proportion of the immune indivduals in the population should be carefully weighted against the risk that the number of new infections saturates again healthcare capacity.

Covid Economics 4, 14 April 2020: 47-61

Covid Economics 4, 14 April 2020: 47-61

6 Appendix: The SEIRHC Model Specification

We report in this appendix the full model specification equation by equation. The model is made of 16 equations. It allows to simulate the dynamics of the virus diffusion starting from an initial period in which the total **Population** (N_t) of N individuals is divided in 1 **Infectious** (I_t) and N-1 **Susceptible** (S_t)**.** In each period (day) some Susceptible become **Exposed** (E_t)**,** their number is determined by the basic reproduction number R_0,that determines the number of secondary infections each infected individual produces, by the probability with which Susceptible meets Infectious, $\left(\frac{I_{t-1}}{N_{t-1}}\right)$, and by the average duration of the period in which a patient is infectious T_{inf}. Exposed after an incubation period of length T_{inc}, become Infectious. The outflows from Susceptible is the inflows into Exposed in each period, and the outflows from Exposed is the inflows into Infectious. Infectious falls into three groups: those with mild symptoms ($MILD_t$), those with severe symptoms (SEV_t), and those with fatal symptoms (FAT_t). The allocation to these groups is controlled by three probabilities: $\left(1-p^{sev}-p^{fat}\right)$, p^{sev}, p^{fat}. Patients with mild symptoms recover after a recovery period, T_{srec}. The daily change in **Mild** patients stock is determined by the share $\left(1-p^{sev}-p^{fat}\right)$ of the outflows from Infectious, and the outflows from the share of Mild who recover that depends on the average duration form symptoms to recovery for mild patients, T_{srec} . Patients with severe and fatal symptoms require hospitalization, both these group are hospitalized after a period between developing symptoms and hospitalization of average duration T_{shosp}, hospitalized. The daily change in **Fatal** patients is determined by the share p^{fat} of the outflows from Infectious and the outflows by the share of Fatal who are hospitalized. Patient with fatal symptoms succumb notwithstanding hospitalization, even in intensive care, after the mean duration from the onset of symptoms to death, T_{sd}. The daily change in **Severe** patients is determined by the share p^{sev} of the outflows from Infectious and the outflows by the share of Severe who are hospitalized. Patients in hospital, independently from their initial status, require intensive care p^{sev} unit with probability p^{ic}. Patient with severe symptoms either recover or become fatal. The recovered, with a mean duration of from the onset of symptoms to hospital discharge of T_{shd} , are those who do need intensive care unit and those who need intensive care unit and find a place. The patients with severe symptoms that need ICU and do not find availability become fatal. At the end of each period the population decreases because of the fatalities, while the stock of recovered grows as a consequence from the new additions of recovered with mild and severe symptoms.

Covid Economics 4, 14 April 2020: 47-61

$$\Delta S_t = \left(-\frac{R_0}{T_{\inf}}\frac{I_{t-1}}{N_{t-1}}\right) S_{t-1}$$

$$\Delta E_t = \left(\frac{R_0}{T_{\inf}}\frac{I_{t-1}}{N_{t-1}}\right) S_{t-1} - \left(\frac{1}{T_{inc}}\right) E_{t-1}$$

$$\Delta I_t = \left(\frac{1}{T_{inc}}\right) E_{t-1} - \left(\frac{1}{T_{\inf}}\right) I_{t-1}$$

$$\Delta MILD_t = p^{mild}\left(\frac{1}{T_{\inf}}\right) I_{t-1} - \left(\frac{1}{T_{srec}}\right) MILD_{t-1}$$

$$\Delta REC\_MILD_t = \left(\frac{1}{T_{srec}}\right) MILD_{t-1}$$

$$\Delta SEV_t = p^{sev}\left(\frac{1}{T_{\inf}}\right) I_{t-1} - \left(\frac{1}{T_{shosp}}\right) SEV_{t-1}$$

$$\Delta SEV\_H_t = \left(\frac{1}{T_{shosp}}\right) SEV_{t-1} - \left(\frac{1}{T_{shd} - T_{\inf} - T_{shosp}}\right) SEV\_H_{t-1} - \Delta SEV\_FAT_t$$

$$\Delta SEV\_FAT_t = I_t^{ICCS}(S_t)\left(p^{ic}SEV\_H_t - \left(ICC_t - p^{ic}FAT\_H\right)\right)\frac{SEV\_H_t}{HOSPITALIZED_t}$$

$$\Delta REC\_SEV_t = \left(\frac{1}{T_{shd} - T_{\inf} - T_{shosp}}\right) SEV\_H_{t-1}$$

$$\Delta FAT_t = p^{fat}\left(\frac{1}{T_{\inf}}\right) I_{t-1} - \left(\frac{1}{T_{shosp}}\right) FAT_{t-1}$$

$$\Delta FAT\_H_t = \left(\frac{1}{T_{shosp}}\right) FAT_{t-1} - \left(\frac{1}{T_{sd} - T_{\inf} - T_{shosp}}\right) FAT\_H_{t-1}$$

$$\Delta REM\_FAT_t = \left(\frac{1}{T_{sd} - T_{\inf} - T_{shosp}}\right) FAT\_H_{t-1}$$

$$HOSPITALIZED_t = SEV\_H_t + FAT\_H_t$$

$$EFF\_FAT_t = REM\_FAT_t + SEV\_FAT_t$$

$$RECOVERED_t = REC\_MILD_t + REC\_SEV_t$$

$$\Delta N_t = -\Delta EFF\_FAT_t$$

$$I_t^{ICCS}(ED_t) = \left\{\begin{array}{ll} 1 & if \quad ED_t > 0 \\ 0, & otherwise \end{array}\right\}$$

$$ED_t = p^{ic}SEV\_H_t + p^{ic}FAT\_H_t - ICC_t$$

7 Table and Figures

Table1: Calibration of the SEIRHC model for Lombardy

Parameter	Pre-lockdown	Post-Lockdown	Source PreL	Source PostL
R_0	2.2	0.95	EC	Calibrated[1]
T_{inf}	2.9 days	2.9 days	EC	EC
T_{inc}	5.2 days	5.2 days	EC	EC
T_{srec}	11.1 days	11.1 days	EC	EC
T_{shosp}	5 days	5 days	EC	EC
T_{sd}	17.8 days	17.8 days	Verity et al.	Verity et al.
T_{shd}	22.6 days	22.6 days	Verity et al.	Verity et al.
p^{fat}	0.0138	0.0138	Verity et al.	Verity et al.
p^{sev}	0.1	0.1	IE	IE
p^{ic}	0.2	0.2	PC	PC

EC (Epidemic Calculator): https://gabgoh.github.io/COVID/index.html
IC (International Evidence) https://www.worldometers.info/coronavirus/#countries
PC (Protezione Civile data on Lombardy) https://github.com/pcm-dpc/COVID-19

[1] The value is chosen to generate a match between model simulated hospitalization and observed hospitalization in Lombardy two weeks after the lockdown date.

Covid Economics 4, 14 April 2020: 47-61

Covid Economics 4, 14 April 2020: 47-61

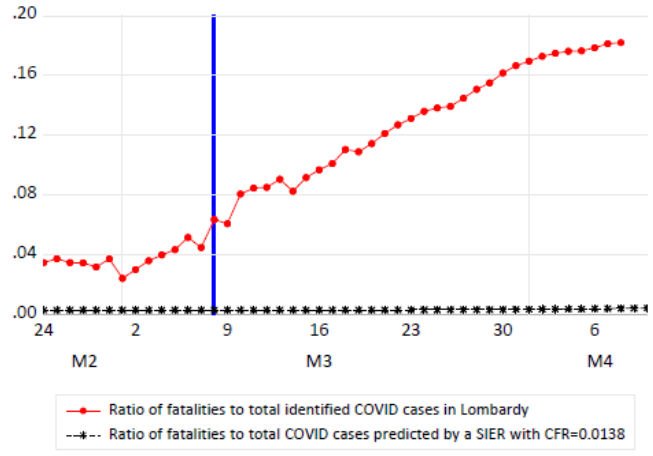

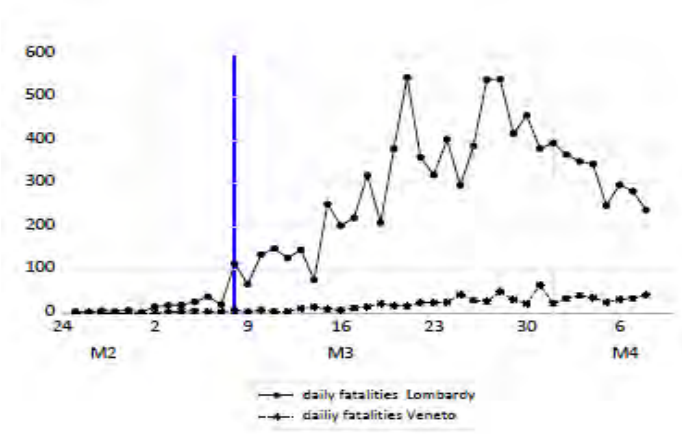

Figure 2: COVID in Lombardy and Veneto. Daily Fatalities

Covid Economics 4, 14 April 2020: 47-61

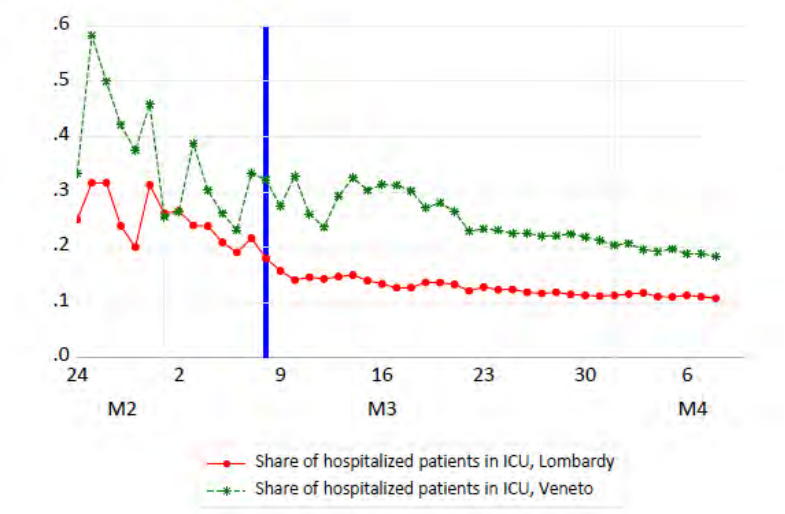

Figure 3: COVID in Lombardy and Veneto. Share of total COVID hospitalized patients in ICU

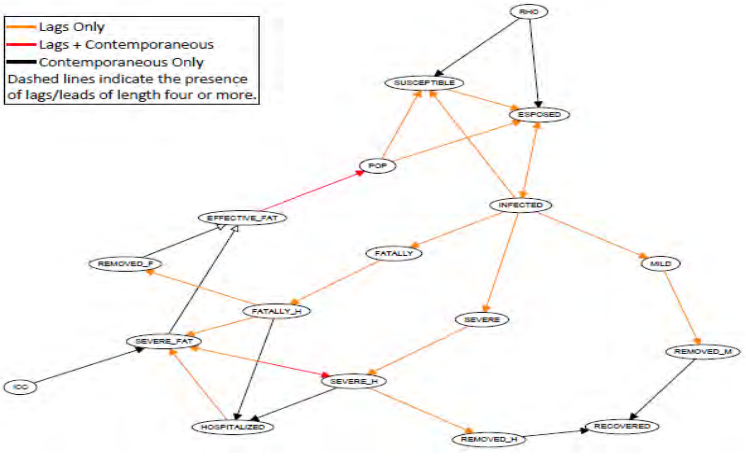

Figure 4: The SEIRHC model dependency graph

Covid Economics 4, 14 April 2020: 47-61

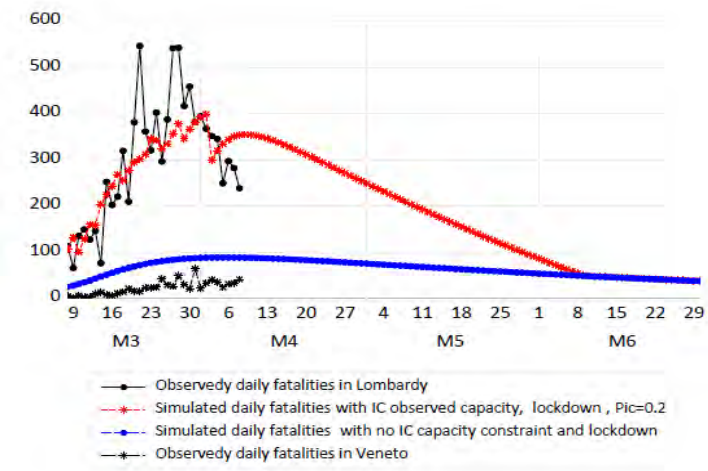

Figure 5: Actual and Simulated Fatalities in Lombardy and Veneto

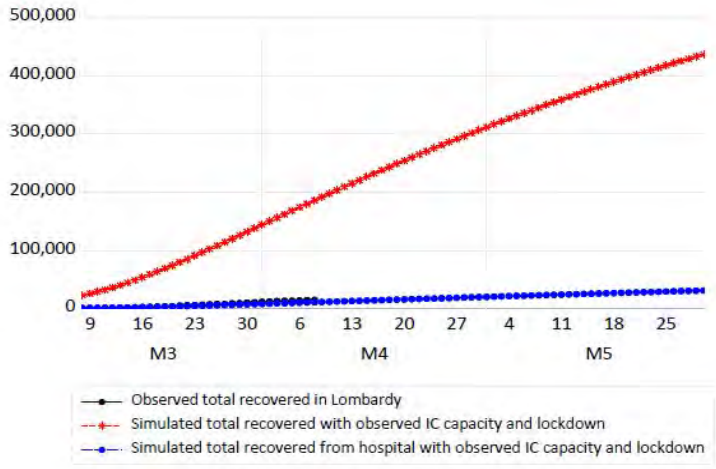

Figure 6: Model Simulated Recovered patients and observed recovered (guariti)

Covid Economics 4, 14 April 2020: 47-61

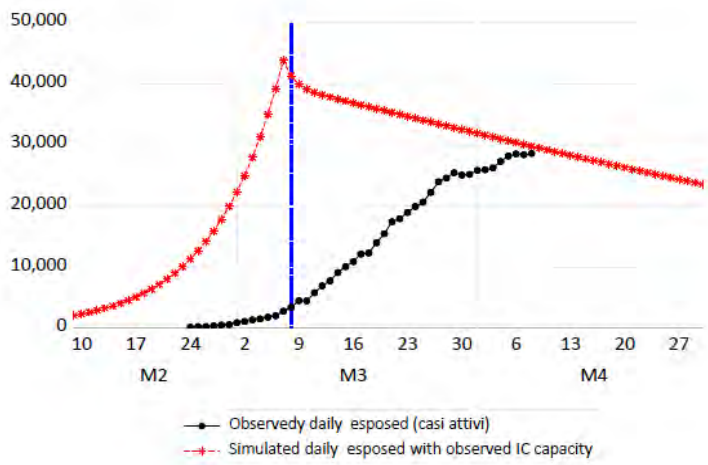

Figure 7.1: model simulated and observed exposed

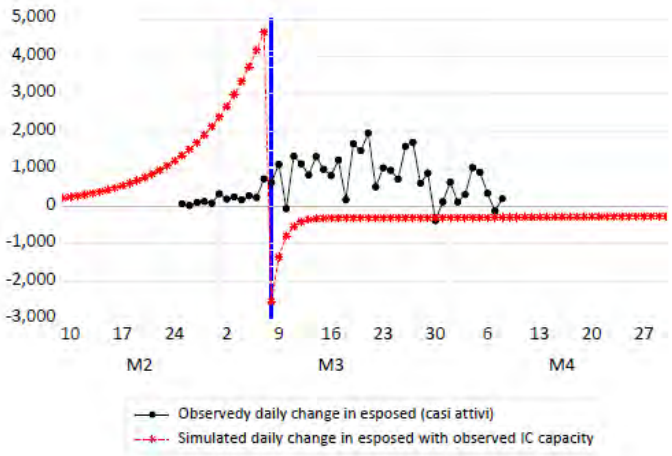

Figure 7.2: Model Simulated and Observed Change in Esposed

Covid Economics 4, 14 April 2020: 47-61

8 References

Allen, L.J.S. (2017). "A primer on stochastic epidemic models: Formulation, numerical simulation, and analysis." Infectious Disease Modeling 2(2), 128-142.

Cereda et al.(2020) "The early phase of COVID-19 outbreak in Lombardy", mimeo

Ferguson et a.(2020) "Impact of non-pharmaceutical interventions (NPIs) to reduce COVID-19 mortality and healthcare demand",

https://www.imperial.ac.uk/media/imperial-college/medicine/sph/ide/gida-fellowships/Imperial-College-COVID19-NPI-modelling-16-03-2020.pdf

Goh Gabriel, the Epidemic Calculator, https://gabgoh.github.io/COVID/index.html

Kucharski et al. (2020) Analysis and projections of transmission dynamics of nCoV in Wuhan, https://cmmid.github.io/topics/covid19/current-patterns-transmission/wuhan-early-dynamics.html

Peracchi F.(2020), The Covid-19 pandemic in Italy, mimeo EIEF Rome

Stock J. (2020) Coronavirus Data Gaps and the Policy Response to the Novel Coronavirus, Harvard Mimeo

Verity et a.(2020), Estimates of the Severity of the COVID-19 disease, https://www.medrxiv.org/content/10.1101/2020.03.09.20033357v1

Wu., Leung and Leung (2020) Nowcasting and forecasting the potential domestic and international spread of the 2019-nCoV outbreak originating in Wuhan, China: a modelling study, VOLUME 395, ISSUE 10225, P689-697, The Lancet, https://www.thelancet.com/journals/lancet/article/PIIS0140-6736(20)30260-9/fulltext

Covid Economics Issue 4, 14 April 2020

The impact of Covid-19 on gender equality[1]

Titan Alon,[2] Matthias Doepke,[3] Jane Olmstead-Rumsey[4] and Michèle Tertilt[5]

Date submitted: 3 April 2020; **Date accepted:** 7 April 2020

Covid Economics 4, 14 April 2020: 62–85

The economic downturn caused by the current Covid-19 outbreak has substantial implications for gender equality, both during the downturn and the subsequent recovery. Compared to 'regular' recessions, which affect men's employment more severely than women's employment, the employment drop related to social distancing measures has a large impact on sectors with high female employment shares. In addition, closures of schools and daycare centers have massively increased child care needs, which has a particularly large impact on working mothers. The effects of the crisis on working mothers are likely to be persistent, due to high returns to experience in the labour market. Beyond the immediate crisis, there are opposing forces which may ultimately promote gender equality in the labour market. First, businesses are rapidly adopting flexible work arrangements, which are likely to persist. Second, there are also many fathers who now have to take primary responsibility for child care, which may erode social norms that currently lead to a lopsided distribution of the division of labour in house work and child care.

1 We thank Fabrizio Zilibotti for early discussions that helped shape some of the ideas in this paper. Financial support from the German Science Foundation (through CRC-TR-224 (project A3) and the Gottfried Wilhelm Leibniz-Prize) and the National Science Foundation (grant SES-1949228) is gratefully acknowledged.
2 Assistant Professor of Economics, University of California San Diego.
3 HSBC Research Professor, Northwestern University and CEPR Research Fellow.
4 PhD candidate in Economics, Northwestern University.
5 Professor of Economics, University of Mannheim and CEPR Research Fellow.

Covid Economics 4, 14 April 2020: 62-85

1 Introduction

It has by now become clear that the COVID-19 pandemic is not only a global health emergency, but is also leading to a major global economic downturn. In this paper, we provide some first results on how this economic downturn is going to affect women and men differently, and what the main long-run repercussions for gender equality may be.

We start by providing evidence that the effects of the current crisis on women versus men are likely to be sharply distinct from those of other economic downturns. In recent recessions such as the one in 2008, job losses for men were much higher than for women. One reason is that relatively more men work in industries heavily affected by a "standard" downturn (such as manufacturing and construction), while women's employment is concentrated in less cyclical sectors such as health care and education. In contrast, the current crisis has a big impact on service occupations with high female employment shares, such as restaurants and hospitality.

An even more important channel for differential impacts on women and men is that in the course of the pandemic, most US states along with other countries have decided to close schools and daycare facilities. Worldwide more than 1.5 billion children are out of school right now.[1] This has dramatically increased the need for childcare. In addition, grandparent-provided childcare is now discouraged due to the higher mortality rate for the elderly, and given social distancing measures, sharing childcare with neighbors and friends is very limited also. Thus, most families have no choice but to watch their kids themselves. Based on the existing distribution of child care duties in most families, mothers are likely to be more affected than fathers. Single mothers, of which there are many in the United States, and who are often in a disadvantaged economic position to begin with, will take the biggest hit.

Taken together, these factors suggest that the COVID-19 pandemic will have a disproportionate negative effect on women and their employment opportunities.[2] The effects of this shock are likely to outlast the actual epidemic. A sizeable

[1] Estimated by UNESCO, as of March 25, 2020.

[2] In terms of mortality from the disease itself, it appears men are slightly more at risk than

literature documents that earnings losses from job losses are highly persistent (Stevens 1997) and much more severe when they occur in recessions (Davis and von Wachter 2011). Workers who lose jobs now forgo returns to experience and are likely to have less secure employment in the future (Jarosch 2015). The consequences are not just limited to those who lose jobs, but also those who were about to enter the labor market for the first time.[3]

Despite this gloomy outlook, we also believe that the COVID-19 crisis can bring about some changes that have the potential to reduce gender inequality in the labor market in the long term. We start by noting that today, a large part of gender inequality in the labor market is related to an unequal division of labor in the household. Even though the labor force participation rate of women is now close to or equal to that of men in most industrialized countries, women continue to provide a disproportionate share of housework (such as cooking and cleaning) and childcare. A recent literature in labor economics has documented that the gender pay gap is closely related to (expected and actual) child birth.[4] From this perspective, long-run progress towards more gender equality is likely to stem primarily from changes in social norms and expectations that lead towards a more equal division of labor within the home.

We can identify at least two channels through which the COVID-19 pandemic is likely to accelerate changing social norms and expectations. One is on the side of employers. Many businesses are now becoming much more aware of the childcare needs of their employees and responding by rapidly adopting more flexible work schedules and telecommuting options. Through learning by doing and changing norms, some of these changes are likely to prove persistent. As a result, in many places mothers and fathers alike will gain flexibility in meeting the combined demands of having a career and running a family. Since currently women are more exposed to these competing demands, they stand to benefit disproportionately.

women (Global Health 50/50). If current efforts to contain the spread of the epidemic are successful, however, many more people will be affected by the economic repercussions of the pandemic rather than the disease itself.

[3]See, for example, Altonji, Kahn, and Speer (2016), Oreopoulos, von Wachter, and Heisz (2012), and Schwandt and von Wachter (2019).

[4]See, for example, Kleven, Landais, and Søgaard (2019), Kleven et al. (2019), and Gallen (2018).

Covid Economics 4, 14 April 2020: 62-85

Covid Economics 4, 14 April 2020: 62-85

A second channel runs through social norms and role models in individual families. While in many cases mothers will pick up a large share of the additional childcare (and home schooling) during the crisis, there will also be a sizeable fraction of families where role models will be reversed. Many medical doctors are women, as are most nurses. Other critical businesses that will continue operating during the crisis include grocery stores and pharmacies, both of which feature high female employment shares. A sizeable fraction of women working in such areas are married to men who will either lose employment during the crisis or will be able to work from home (e.g., many office workers). In such families, many men will inevitably turn into the main providers of child care. The literature on policy changes that engineer a similar change (e.g., "daddy months" and other forms of paternity leave) suggest that such a reallocation of duties within the household is likely to have persistent effects on gender roles and the division of labor.[5]

In this paper, we use data on the distribution of women, men, and couples across occupations as well as time-use data on the division of labor in the household to shed more light on the channels through which the COVID-19 pandemic affects gender inequality. Even though we identify at least some channels that could ultimately have beneficial effects, we emphasize that the short-run challenges posed by the crisis are severe, and especially so for single mothers and other families with a lack of ability to combine work with caring for children at home. We conclude by discussing policy options that could be used to deal with these specific challenges.

2 The Effect of COVID-19 on Employment

The social distancing measures and stay-at-home orders imposed in many US states and other countries during the COVID-19 crisis are having a large impact on employment, leading to a sharp rise in unemployment and other workers being given reduced hours or temporarily furloughed.

[5]See for example Farré and González (2019) for evidence from Spain and for evidence from Tamm (2019) for Germany that paternity leave leads a persistent increase in fathers' involvement in childcare. However, Ekberg, Eriksson, and Friebel (2013) do not find an effect of "daddy months" in Sweden in father's likelihood to take medical leave to care for children.

Covid Economics 4, 14 April 2020: 62-85

In economic downturns preceding the current crisis, including the financial crisis of 2007–2009, the employment of male workers was affected more strongly than the employment of female workers. Doepke and Tertilt (2016) summarize evidence on how employment varies over the business cycle for women and for men. They show that in the period 1989–2014, men account for more than three quarters of overall cyclical fluctuations in employment (i.e., the component of overall volatility in employment that is correlated with aggregate economic fluctuations), and women for less than one quarter.[6]

One reason for the lower cyclical volatility of female employment is insurance in the family—women's employment may be less affected by downturns precisely because some married women increase their labor supply to compensate for unemployment or higher unemployment risk of their husbands.[7] A second important channel is the different sectoral composition of female and male employment. In typical recessions, sectors such as manufacturing and residential construction are much more severely affected compared to, say, education and health care. Men's employment is on average more concentrated in sectors with a high cyclical exposure, whereas women are highly represented in sectors with relatively stable employment over the cycle.[8]

2.1 Gender Differences Based on Sectors Most Affected by COVID-19

The evidence suggests that the impact of the current downturn during the COVID-19 pandemic on women's versus men's employment will be unlike previous recessions. A principal difference is which sectors of the economy are likely to be most affected. Two factors are especially important:

1. Whether demand for the sector's output is affected by stay-at-home orders (e.g., no impact on sectors deemed "critical," such as pharmacies and grocery stores; large negative effect on sectors such as travel and hospitality).

[6] The role of women in aggregate fluctuations has changed substantially over time due to rising female labor force participation; see, e.g., Albanesi (2020) and Fukui, Nakamura, and Steinsson (2019).

[7] See Ellieroth (2019) for a study documenting the quantitative importance of this mechanism.

[8] These facts are documented in a recent paper by Coskun and Dalgic (2020).

2. Whether the nature of the work in the sector allows for telecommuting or not (e.g., larger impact on manufacturing vs. higher education and business services).

To assess how women and men in the labor market are exposed to the crisis, Table 1 provides an overview of how the dimensions of "critical" and "telecommutable" matter for male and female workers. Using data from the American Time Use Survey (ATUS) in 2017 and 2018, the table gives the fraction of workers in a given occupation that say that they are able to telecommute and whether they actually do telecommute. Occupations vary immensely by whether people say they are able to telecommute—ranging from 3% for *transportation and material moving* to 78% for *computer and mathematical*. The effective actual time that people do telecommute in normal times is small, however, as the third column in the table shows. For the current situation, however, the ability to telecommute is a lot more relevant than past behavior.

To get a sense of what fraction of men and women work in telecommutable jobs, consider occupations where at least 50 percent of workers state they are able to telecommute. We find that that 28 percent of male workers but only 22 percent of female workers are employed in these highly telecommutable occupations. These numbers suggests that in terms of their occupations, more men than women will easily adapt to the changed work environment during the crisis. Conversely, more women will potentially face loss of employment, which is the opposite of the pattern in normal economic downturns.

The picture is less clear if we use a lower threshold for telecommutable jobs. For example, consider occupations where at least 25 percent of workers state that they are able to telecommute. 49 percent of male employees but 63 percent of female workers work in these occupations. Thus, if all workers in these occupations could carry on during the crisis, women would have the advantage. In reality, in each occupation only a fraction of jobs will be able to continue remotely, and this fraction is likely to correlate with the fraction of workers who stated in the pre-crisis survey that they have the ability to telecommute.

We also classified occupations by whether they are critical in the current situation, especially health care workers. According to this (rough) classification, 17

Covid Economics 4, 14 April 2020: 62-85

CEPR PRESS

Table 1: Labor Force Across "Critical" and "Telecommutable" Occupations.

Occupation	Able to TC	Effective Annual TC	Employed Men	Employed Women	Critical Occupation
Transportation and Material Moving	3%	1	10%	2%	✓
Food Preparation and Serving	4%	2	4%	6%	
Building and Grounds Cleaning and Maintenance	4%	4	4%	3%	
Production	4%	4	8%	3%	
Healthcare Support	8%	13	1%	4%	✓
Construction	10%	4	8%	0%	
Farming, Fishing, and Forestry	11%	1	1%	0%	✓
Installation, Maintenance, and Repair	11%	10	6%	0%	✓
Extraction	13%	1	0%	0%	
Personal Care and Service	13%	21	2%	6%	
Protective Service	14%	4	3%	1%	✓
Healthcare Practitioners and Technicians	16%	17	3%	10%	✓
Technicians	18%	3	0%	0%	
Office and Administrative Support	26%	24	7%	19%	
Sales and Related	33%	35	10%	10%	
Education, Training, and Library	37%	36	3%	10%	
Community and Social Services	46%	46	1%	2%	
Life, physical, and social science	54%	24	1%	1%	
Arts, Design, Entertainment, Sports, and Media	57%	45	2%	2%	
Management,business, science, and arts	63%	44	13%	9%	
Legal	64%	35	1%	1%	
Business operations specialists	66%	60	2%	3%	
Architecture and engineering	67%	36	3%	1%	
Financial specialists	68%	37	2%	3%	
Computer and Mathematical	78%	66	4%	2%	

Note: The table reports the share of individuals in each occupation reporting they were able to work from home (column 1); the effective total days a year they actually did work from home (column 2); the share of all employed men and women in each occupation (column 3-4); and whether the occupation seems critical during the COVID-19 crisis. Data Source: American Time Use Survey 2017-2018; American Community Survey 2017-2018.

percent of employed women work in critical occupations, compared to 24 percent of all employed men. Hence, this second channel suggests once again that, unlike in usual economic downturns, women will be less protected from employment loss during the downturn. It is possible that this classification overstates women's exposure. The true share for women in critical occupations is likely higher once grocery store clerks are taken into account. The true share of men, on the other hand, may be somewhat smaller since we classified men working in "transportation and material moving" as critical. Clearly, some transportation is needed to provide basic necessities such as food, and employment in food and online business delivery is rising. But public transportation is being scaled back in many places.

Covid Economics 4, 14 April 2020: 62-85

The bottom line is that based on ability to telecommute and working in critical occupations, we do not observe the pattern of usual recessions that women are more protected than men from employment loss. In fact, there are indications that women's employment will suffer more during the crisis based on these two factors. Even if the exposure of women and men in terms of their current occupations should turn out to be about the same, this would still be a big deviation from other recessions, where the employment consequences fell much more heavily on men.

3 The Effect of COVID-19 on Child Care Needs

The effect of the COVID-19 pandemic on a worker's employment depends on factors beyond sector and occupation. Another salient aspect of the COVID-19 crisis is that it involves large-scale closures of daycare centers and schools, implying that children stay at home, where they have to be cared for and (if possible) educated. This poses particularly severe challenges for single parents. For parents who raise their children together, the division of childcare will depend on how much work flexibility each parent has in terms of working from home while also taking care of children. It will likely also depend on the current division of childcare within each family. These factors suggest that women's employment will be affected more severely by the sudden rise in child care needs.

3.1 Household Arrangements and Single Mothers' Exposure to School and Daycare Closures

To assess how many households are affected by the rise in childcare needs, Tables 2 and 3 summarize the distribution of living arrangements prior to the crisis. There are almost 130 million households in the United States. Slightly less than half are married couples (with and without children), 17 percent are single-parent households (i.e., "Family, Female Householder" and "Family, Male Householder") and 35 percent are non-family households, who are mostly singles living by themselves. There are around 15 million single mothers, accounting for just under 70 percent of all single parent households.[9]

[9]Note that in Table 2 the "Family" categories include families with children of all ages, including those over 18 years old, as long as children live in the same household as the parent.

Covid Economics 4, 14 April 2020: 62-85

CEPR PRESS

Table 2: Households by Type in United States

Total # of Households	128,579	100%
Married Couples	61,959	48%
Family, Male Householder	6,480	5%
Family, Female Householder	15,043	12%
Non-family, Male Householder	21,582	17%
Non-family, Female Householder	23,515	18%

Note: Thousands in 2019. Source: US Census Bureau, Table HH-1.

The sudden spike in childcare needs during the crisis will affect all households with school-age children or below. Single parents (17 percent of all households) will be particularly hard hit, and as Table 2 shows, there are more than 8.5 million more single mothers than single fathers in the United States today.

Table 3: Living Arrangements of Children in the United States

Total children under 18	73,525	100%
Two parents	51,561	70%
Mother only	15,764	21%
Father only	3,234	4%
Other relatives	2,319	3%
Non-relatives	647	1%

Note: Thousands in 2019. Source: US Census Bureau, Table ch1.

To get a clearer picture of the importance of school closures, note that there are currently 73.5 million children under 18 in the United States (see Table 3). Of these, 70 percent live in two-parent families, while most of the others live in single-parent households. 21 percent of all children live only with their mother, compared to 4 percent living with their father only. Thus, the current crisis will affect mothers disproportionately. If all schools in the US are closed for a prolonged period, so that single mothers cannot work, then 21 percent of all children are at risk of living in poverty. In normal times, many alternative forms of

Covid Economics 4, 14 April 2020: 62-85

childcare arrangements are used. However, many daycare centers have been ordered closed. Informal care performed by grandparents, other relatives, friends, or neighbors is being discouraged or prevented by shelter-in-place orders to slow down the spread of the virus. There is little room for alternative arrangements in the COVID-19 crisis.

3.2 Childcare Provision Within Married Couples

Among married couples, who is likely to bear the majority of increased childcare needs due to school and daycare closures? First, the current work arrangements of married couples (i.e., single vs. dual earner) will play a role. Second, the division of the increased childcare needs will also likely mirror existing disparities between men and women in hours spent on childcare. Third, among dual-earner couples, the ability to telecommute and whether one or both members of the couple work in critical sectors will also matter.

Table 4 summarizes the distribution of family types across work arrangements in the American Community Survey for married couples with children. Dual full-time earner couples account for 44 percent of all couples with children. This group is heavily affected by the rise in child care needs. Families with the traditional division of labor of the husband having a full-time job and the wife staying at home will have to make fewer adjustments to respond to the school closures. However, today this group accounts for only 25 percent of married couples with children. Only 5 percent of couples are in the opposite arrangement of the husband staying at home and the wife working full time, underlining once again that more women than men will be strongly affected by the rise in child care needs.

Even among couples who both work, one spouse often provides the majority of child care. It is likely that any increase in child care needs will fall disproportionately on this main provider. Survey data from the ATUS shows that married women provide more childcare than married men on average. Among all married couples with children, the husbands provide 7.4 hours of child care per week on average, versus 13.3 hours for the wives.[10] Households with young children have higher childcare needs, but the male vs. female ratio is almost the same:

[10]These numbers are based on time use data for the 16–65 population.

Covid Economics 4, 14 April 2020: 62-85

Table 4: Distribution of couples with children by employment status

Married Couples		Wives		
		Not Employed	*Part-Time*	*Full-Time*
Husbands	*Not Employed*	4%	1%	5%
	Part-Time	1%	1%	2%
	Full-Time	25%	15%	44%

Note: The table reports the share of couples by employment and full-time, part-time status of each spouse. Not Employed includes unemployed individuals and those not in the labor force. Source: American Community Survey, 2017-2018.

Covid Economics 4, 14 April 2020: 62-85

conditional on children up to the age of 5, married men provide 10.9 hours of childcare, versus 19.8 hours per week for married women. Of course, some of this gap arises because there are more stay-at-home moms than stay-at-home dads. But even if we condition on both spouses being employed full time, a large gap remains. Among the full time employed, married men provide 7.2 hours of child care per week versus 10.3 hours for married women. Conditional on having at least one child up to the age of 5, the numbers are 10.6 hours for married men versus 16.8 hours for married women. Thus, married women provide close to 60 percent of child care even among couples who work full time, and an even higher share if they have young children, when childcare needs are the highest.[11] Similarly, if attention is restricted to the division of childcare hours performed during typical working hours for children of all ages (8AM-6PM, Monday through Friday), women provide an even larger fraction, around 70 percent, of childcare during working hours (Schoonbroodt 2018).

It is likely that this uneven distribution of the burden of childcare will persist during the current crisis; many of the factors that initially led to this arrangement (which could include relative income, relative bargaining power, and the influence of traditional social norms and role models) will continue to apply. If the relative distribution of the burden stays at 60-40 and childcare needs rise by

[11] The observation that women provide the majority of childcare even if both spouses are working holds true across industrialized countries. However, the size of the gap between women's and men's contributions varies substantially (Doepke and Kindermann 2019).

20 hours/week during the crisis, full-time working women would need to increase their childcare hours by 12 hours vs. 8 for men. In the absence of flexible work arrangements, another likely outcome is that one spouse will temporarily have to quit work, which based on the existing division of labor would again be much more likely to be the wife.

3.3 Employment Flexibility for Men vs. Women

In addition to the existing division of the burden of childcare, the impact of the crisis will also depend on the relative flexibility of men's and women's work arrangements, in particular the ability to telecommute. Table 5 shows that among all individuals with kids, married women spent the most time telecommuting in 2017 and 2018, averaging 41 days per year. Married men are best-equipped to telecommute (45% are able to) but spend fewer days actually telecommuting than married women. Married women are the group most likely to report working from home for personal reasons, which includes managing childcare. Single parents, both women and men, are much less able to telecommute, driving home our earlier point that school closures will be extremely difficult for single parents, most of whom are women, to navigate while continuing to work.

Table 5: Telecommuting, for those with children by marital status and gender

	Can Telecommute	Did Telecommute	Days Telecommute
single men	17%	14%	15
single women	21%	18%	19
married men	45%	39%	30
married women	42%	38%	41

Note: Table reports those who said they are able to telecommute (column 1); those that were able and did telecommute (column 2); and the approximate days per year telecommuting, for those which were able. Source: American Time Use Survey, 2017-2018.

In summary, the evidence suggests that women will be vastly more affected by the rise in childcare needs that follows from closures of schools and daycare centers during the crisis. The 15 million single mothers in the United States will be the most severely affected, with little potential for accessing other sources of

Covid Economics 4, 14 April 2020: 62-85

childcare under social isolation orders, and little possibility to continue working during the crisis.

Even among couples raising their children together, there are clear indications that women will be much more affected by rising childcare requirements. There are already many more married women than men who are stay-at-home parents and who are likely to pick up most of the increase in the workload. And among the many couples with children who both work full time (44 percent of the total), the women provide about 60 percent of childcare hours. In times of high childcare needs (i.e. when children are young), the women's share is even higher. It is likely that much of this division of labor will persist. For some working married women, this will mean that they will temporarily drop out of the labor force. Others will continue to work from home—including, for example, mothers on the tenure track at an academic institution—but they will be more impaired in their ability to actually get work done compared to married men in the same situation. While these women are in a more favorable situation compared to single mothers, they may still face severe setbacks in terms of career progression and their future earnings potential.

4 The Effect of COVID-19 on Workplace Flexibility and Gender Norms

The discussion so far shows that the COVID-19 shock is likely to place a disproportionate burden on women. Nevertheless, there are also countervailing forces that may promote gender equality during the recovery from the current crisis. We believe that two channels are likely to be important:

1. **More flexible work arrangements:** Many businesses are currently adopting work-from-home and telecommuting options at a wide scale for the first time. It is likely that some of these changes persist, leading to more workplace flexibility in the future. Given that mothers currently carry a disproportionate burden in combining work and child care duties, they stand to benefit relatively more than men from these changes. Goldin (2010) points to lack of flexibility in work arrangements and hours, particularly in financial and business services, as one of the last sources of the gender pay gap.

Covid Economics 4, 14 April 2020: 62-85

2. **Changes in social norms and role models:** Many fathers will now also shoulder additional child care and home-schooling responsibilities. In a sizeable number of families, fathers will temporarily turn into primary child care providers. These changes are likely to push social norms towards more equality in the provision of child care and house work.

4.1 The Role of Workplace Flexibility

Consider the role of more flexible work arrangements. If there is a persistent increase in the ability to work from home for women and men alike, how will the division of labor in the household change? We can get a sense of the potential impact by comparing the time spent on child care between parents who can work from home and those who cannot. Table 6 provides evidence on this by comparing the average weekly childcare hours of husbands and wives conditional on the occupation type of each spouse. Occupations are split into “Critical" (same classification as Table 1), “Tele", non-critical occupations where at least 50% of ATUS respondents reported being able to telecommute, and “Non-Tele", non-critical occupations where fewer than 50% reported being able to telecommute.

We observe that if husbands who don’t work are married to women who do, they carry the majority of childcare duties in their households (first three rows of the last panel). They do a lot less childcare than women in the same situation (rows 4, 8, 12)—social norms still matter—but still, the result shows that availability for child care has a large impact on the actual distribution.

More importantly, we observe a similar effect when we look at the impact of telecommuting. Consider couples where the wife is not able to telecommute and is either in the “Non-Tele” or “Critical” groups. In this case, if the husband is in an occupation with a high ability to telecommute, weekly childcare hours of the husband are about two hours higher per week compared to husbands in “Non-Tele” occupations (6 vs. 4 hours, i.e. a 50 percent difference). Notice that being in such an occupation does not imply that most of these men actually telecommute on a regular basis. Nevertheless, the added flexibility of these jobs is reflected in a much higher participation of men in childcare, as long as their wives do not have the same flexibility.

Covid Economics 4, 14 April 2020: 62-85

Covid Economics 4, 14 April 2020: 62-85

Table 6: Childcare by Family Occupational Group

Family Group (*husband, wife*)	**Husbands Childcare** (*weekly hours*)	**Wives Childcare** (*weekly hours*)	**Husbands High Childcare** (*percent of group*)
(Non-Tele, Non-Tele)	4	7	17%
(Non-Tele, Tele)	6	8	20%
(Non-Tele, Critical)	4	7	20%
(Non-Tele, Not Employed)	6	12	26%
(Tele, Non-Tele)	6	8	21%
(Tele, Tele)	6	7	23%
(Tele, Critical)	6	5	24%
(Tele, Not Employed)	6	12	24%
(Critical, Non-Tele)	3	5	12%
(Critical, Tele)	6	7	18%
(Critical, Critical)	5	8	18%
(Critical, Not Employed)	4	17	14%
(Not Employed, Non-Tele)	8	6	25%
(Not Employed, Tele)	9	6	27%
(Not Employed, Critical)	9	4	21%
(Not Employed, Not Employed)	4	11	13%

Note: The table reports the average childcare hours per week by spouse for each family occupation group for all married couples. Groups are reported in column one as (husband, wife) pairs. The final column ("High Husband Childcare") reports the share of husbands in this family group which provide childcare hours in excess of the average married woman in the economy. TC classifications by 50% cutoff, see Table 1. Source: American Time Use Survey 2017-2018; American Community Survey 2017-2018.

Covid Economics 4, 14 April 2020: 62-85

Right now, many businesses are adopting work-from-home options on a large scale. It is likely that a sizeable fraction of this additional flexibility will stay in place after the actual crisis. Once businesses have invested in remote-working technology and the learning-by-doing that is involved in the transition has taken place, going back all the way to the status quo is not attractive. As a result, many workers will benefit from added flexibility in combining career and child care needs. This change will be a benefit to both mothers and fathers, but given that currently mothers carry the majority of the burden of child care, in relative terms they are likely to gain more, both because of added flexibility in their own work and because of more contributions from their husbands.

4.2 Existing Evidence on Persistent Changes to Gender Norms

One central force behind the uneven division of the burden of childcare between women and men is persistent social norms. Is there a possibility that the COVID-19 shock will push these norms towards more gender equality? To assess this possibility, we can draw a parallel between the COVID-19 crisis and the last major shock to women in the labor market, namely World War II. During the war, millions of women entered the labor force to replace men in factories and other workplaces. The impact of the war shock was particularly large for married women with children, who in the pre-war economy had very low labor force participation rates. A large literature documents that the shock of World War II had a large and persistent effect on female employment.[12]

While some of this impact was at the individual level (i.e., women who entered the labor force during the war increased their employment also after the war), another component works through shifting cultural norms. Fernández, Fogli, and Olivetti (2004) show that boys who grow up in a family where the mother is working are more likely to eventually be married to women who also work (they use the World-War-II shock to identify the size of this effect). This observation is suggestive of an impact on social norms: these boys observed a more equal sharing of duties at home and in the labor market between their parents com-

[12]See for example Acemoglu, Autor, and Lyle (2004) and Goldin and Olivetti (2013). Doepke, Hazan, and Maoz (2015) argue that the persistent impact of World War II on the female labor market was also one of the root causes of the post-war baby boom.

pared to single-earner families, which had repercussions for which they desired in their own families.[13] There is also evidence that shifting social norms and beliefs were one cause of the secular rise in the labor force participation of married women from the 1960s to the 1990s. Fernández (2013) and Fogli and Veldkamp (2011) argue that women gradually learned, by observing other working women in their family and neighborhoods, about the true costs and benefits of being in the working force (including potential effects of working on children). As more women worked, there were more observations to learn from, which accelerated the transition to higher levels of female labor force participation.

4.3 Fathers' Childcare Responsibilities During the COVID-19 Crisis and the Evolution of Gender Norms

The example of World War II suggests that temporary changes to the division of labor between the sexes have long-run effects. How is this likely to play out during the COVID-19 crisis? Here an important question is how much fathers' child care responsibilities will increase. Many fathers will be working from home during the crisis while also taking on child care responsibilities. The mere fact of being at home rather than at a workplace is likely to increase men's child care responsibilities. This effect is likely to be large during the crisis, because given that schools and daycare centers are closed, the overall need for child care is much higher. Hence, even if (as is likely) on average women will shoulder the majority of the increase, many fathers will still experience a large increase in their child care hours. It is likely that this higher exposure will have at least some persistent effect on future contributions to child care, be it through learning by doing, more information about what kids are actually doing all day, or through increased attachment to children.

We would expect even bigger effects within families where the COVID-19 crisis also results in a shift in the relative distribution of childcare hours towards men. One group for which this is likely to be the case is families where the mother is already staying at home, but the father previously worked out of the house and is now either working at home or not employed. The biggest impact on the division

[13] See Grosjean and Khattar (2018) for evidence of persistence in gender norms over even longer periods.

Covid Economics 4, 14 April 2020: 62-85

CEPR PRESS

of labor will occur among couples where, because of the COVID-19 crisis, fathers temporarily turn into the main provider of child care. This is likely to be the case for couples where both parents are currently in the labor force, and where the father is able/forced to work from home during the crisis, while the mother is not. An example are couples where the mother is in a "critical" occupation (such as a medical doctor or other healthcare professional who can't work from home), whereas the father is in an occupation that switches to telecommuting during the crisis (such as education and a lot of non-critical office work).

Table 7: Employment Flexibility of Married Couples with Children

	Wife Non-Tele	Wife Tele	Wife Crit	Wife Non-Emp	*Total*
Husb Non-Tele	17%	5%	5%	11%	38%
Husb Tele	9%	7%	3%	8%	28%
Husb Critical	8%	2%	4%	6%	21%
Husb Non-Emp	4%	1%	1%	7%	13%
Total	38%	16%	13%	33%	100%

Note: The table reports the share of couples by husband-wife occupation types. Telecommuting classifications are made according to the TC 50% cut-off. Source: American Time Use Survey 2017-2018; American Community Survey 2017-2018.

Table 7 provides an impression of the magnitudes involved. The table describes the distribution of married couples with children among employment vs. non-employment for each spouse, where employment is further broken down in critical occupations and, among the non-critical ones, occupations with a low and high ability to telecommute. During a stay-at-home order with only critical occupations exempt, we expect all non-critical workers to be at home. In nine percent of households, the wife is in a critical occupation (such as medical doctor) while the husband is not. In these households, we expect the husbands to temporarily turn into the main providers of childcare. While this group is obviously a minority, it still consists of millions of households, suggesting that during the height of the crisis seeing men as the main providers of child care will be much more common than previously.

We can also consider what happens if workplaces resume but schools remain

Covid Economics 4, 14 April 2020: 62-85

closed. In this case, we would expect most workers with the ability to telecommute to continue working from home. We see that in 12 percent of married couples with children the husband is in an occupation with a high ability to telecommute, while the wife is not ("Non-Tele" or "Critical"). Hence, in this scenario the number of men turning into main providers of child care is even higher.

We therefore see that the crisis is likely to generate a large, if temporary, upward shift in men's participation in child care, with a sizeable fraction of married men taking the main responsibility, in most cases for the first time. Based on the persistent effects of other shocks to the household distribution of labor in the past, we expect this shift to lead to a substantial increase in men's future participation in child care.

In assessing these effects, it bears emphasizing that the changes imposed on households by the current crisis are very large. The existing literature on the effects of paternity leave (i.e., parental leave reserved exclusively for fathers) finds effects for relatively small changes; for example, Farré and González (2019) provide evidence that the introduction of just two weeks of paternity leave for fathers in Spain had persistent effects on the division of labor within couples. During the current crisis, many millions of men are on a form of forced paternity leave for a much longer period, and a sizeable fraction will be the main providers of childcare during this time. Hence, even while women carry a higher burden during the crisis, it is still highly likely that we will observe a sizeable impact of this forced experiment on social norms, and ultimately on gender equality, in the near future.

5 Outlook and Policy Options

We conclude with thoughts on policy options. Although in the last section we pointed out channels that may ultimately lead to a reduction in gender inequality, we should keep in mind that the challenges for families during the current crisis are unprecedented, severe, and falling disproportionately on those least able to respond, such as low-income single mothers. The immediate challenge is to formulate policy responses that acknowledge the specific challenges women are likely to face during the coming crisis.

Covid Economics 4, 14 April 2020: 62-85

We therefore recommend the following policies:

1. Government subsidies to replace 80% of employee pay for workers who need to provide child care during the crisis due to school and daycare closures and are therefore unable to work, conditional on a continued employment relationship (i.e., workers can return to work immediately after the crisis).

2. Work requirements for government assistance programs such as Temporary Assistance for Needy Families (TANF) and Medicaid should be removed until school and daycare centers re-open, and time off work now should not count towards future work requirements. Unemployment insurance should remove the requirement to be actively seeking work over the same period.

3. Unemployment benefits should be extended to workers voluntarily separating from employment to provide child care.

4. Universities should extend tenure clocks for faculty members with children under age 14, with similar provisions for other employers with up-or-out promotion systems.

5. Companies should be encouraged to waive billable hours targets tied to bonus pay for 2020 for women with children under age 14.

This is not a comprehensive list, but it deals with some of the specific challenges posed by the COVID-19 crisis. Items (1), (4), and (5) deal with women who can retain their jobs during the crisis but will lose many hours due to shouldering the majority of childcare provision for very young children and children out of school. Item (1) is particularly important in light of the evidence that job loss has large, persistent negative effects on human capital accumulation and earnings. Allowing women to keep their jobs will avoid these consequences that would otherwise follow them for many years. Countries like Germany and Denmark have already taken aggressive steps along this line to allow workers to remain on their employers' payrolls during the crisis despite working zero or reduced

Covid Economics 4, 14 April 2020: 62-85

hours. In the United States, the Families First Coronavirus Response Act also includes provisions for paid family leave, but is limited to certain employers (private employers with 50–500 employees).

Many universities are already extending tenure clocks for both mothers and fathers. But recent evidence from Antecol, Bedard, and Stearns (2018) suggests that gender blind tenure clock extensions actually reduce female tenure rates and increase male tenure rates, likely because of differences in time spent on childcare. Given the unavailability of other forms of childcare, during the crisis the gap between the ability of junior faculty with and without children to get research done will be extremely large. While faculty without children may still suffer from stress during this period, their time available to work is likely to actually increase, given that time use for other activities, such as socializing with others, declines during social isolation.[14] Extending the tenure clock indiscriminately for all current junior faculty, as a number of universities have already implemented, will not address this disparity, which hits women stronger than men. Similar mechanisms are at work in corporate settings where bonuses are tied to hours worked: mothers will likely find it harder to meet these targets because of childcare provision during the crisis while most men will not, exacerbating the gender wage gap.

Section 2.1 argues that women are more likely to become unemployed during this crisis than previous ones. Policies (2) and (3) are meant to address this group. Some women, especially single mothers, will have no choice but to leave their jobs to care for their children and should be eligible for unemployment benefits. California has already taken this step by extending UI to cover parents who stop working due to school closures. While caring for children, unemployed parents will not be able to resume working so the requirement to be actively seeking employment should be waived. Work requirements for other social assistance programs such as food stamps and Medicaid in some states should be lifted for the same reason and time limits on duration of receipt of these services should be lifted.

Finally, there will be other consequences of the current crisis that will fall dis-

[14] Aguiar et al. (2018) report that young men spend about eight hours per week socializing.

Covid Economics 4, 14 April 2020: 62-85

proportionately on women that are outside the scope of this paper that we leave to future research. In normal recessions, incidents of domestic violence increase (Siflinger, Tertilt, and van den Berg 2012). With families cooped up inside, these risks will further increase and women are much more likely than men to be the victims of domestic violence. Further, some states are restricting access to abortions during the crisis, and the impact of the pandemic on fertility more broadly remains to be seen. We plan to expand our analysis to some of these dimensions in future research.

References

Acemoglu, Daron, David H. Autor, and David Lyle. 2004. "Women, War, and Wages: The Effect of Female Labor Supply on the Wage Structure at Midcentury." *Journal of Political Economy* 112 (3): 497–551.

Aguiar, Mark, Mark Bils, Kerwin Kofi Charles, and Erik Hurst. 2018. "Leisure Luxuries and the Labor Supply of Young Men." Unpublished Manuscript, University of Chicago.

Albanesi, Stefania. 2020. "Changing Business Cycles: The Role of Women's Employment." NBER Working Paper 25655.

Altonji, Joseph G., Lisa B. Kahn, and Jamin D. Speer. 2016. "Cashier or Consultant? Entry Labor Market Conditions, Field of Study, and Career Success." *Journal of Labor Economics* 34 (S1): S361–S401.

Antecol, Heather, Kelly Bedard, and Jenna Stearns. 2018. "Equal but inequitable: Who benefits from gender-neutral tenure clock stopping policies?" *American Economic Review* 108 (9): 2420–2441.

Coskun, Sena, and Husnu Dalgic. 2020. "The Emergence of Procyclical Fertility: The Role of Gender Differences in Employment Risk." CRC TR 224 Discussion Paper Series No. 142.

Davis, Steven J., and Till von Wachter. 2011. "Recessions and the costs of job loss." *Brookings Papers on Economic Activity*, no. 2:1–72.

Doepke, Matthias, Moshe Hazan, and Yishay D. Maoz. 2015. "The Baby Boom

Covid Economics 4, 14 April 2020: 62-85

and World War II: A Macroeconomic Analysis." *Review of Economic Studies* 82 (3): 1031–1073.

Doepke, Matthias, and Fabian Kindermann. 2019. "Bargaining over Babies: Theory, Evidence, and Policy Implications." *American Economic Review* 109 (9): 3264–3306.

Doepke, Matthias, and Michèle Tertilt. 2016. "Families in Macroeconomics." Chapter 23 of *Handbook of Macroeconomics, Vol. 2*. North Holland.

Ekberg, John, Rickard Eriksson, and Guido Friebel. 2013. "Parental leave: A policy evaluation of the Swedish "Daddy-Month" reform." *Journal of Public Economics* 97:131 – 143.

Ellieroth, Kathrin. 2019. "Spousal Insurance, Precautionary Labor Supply, and the Business Cycle." Unpublished Manuscript, Indiana University.

Farré, Lídia, and Libertad González. 2019. "Does Paternity Leave Reduce Fertility?" *Journal of Public Economics* 172:52–66.

Fernández, Raquel. 2013. "Cultural Change as Learning: The Evolution of Female Labor Force Participation over a Century." *American Economic Review* 103 (1): 472–500.

Fernández, Raquel, Alessandra Fogli, and Claudia Olivetti. 2004. "Mothers and Sons: Preference Formation and Female Labor Force Dynamics." *Quarterly Journal of Economics* 119 (4): 1249–99.

Fogli, Alessandra, and Laura Veldkamp. 2011. "Nature or Nurture? Learning and the Geography of Female Labor Force Participation." *Econometrica* 79 (4): 1103–38.

Fukui, Masao, Emi Nakamura, and Jón Steinsson. 2019. "Women, Wealth Effects, and Slow Recoveries." Unpublished Manuscript, University of Berkeley.

Gallen, Yana. 2018. "Motherhood and the Gender Productivity Gap." Unpublished Manuscript, University of Chicago.

Global Health 50/50. "COVID-19 sex-disaggregated data tracker."

Covid Economics 4, 14 April 2020: 62-85

Goldin, Claudia. 2010. "How to achieve gender equality." *The Milken Institute Review*, pp. 24–33.

Goldin, Claudia, and Claudia Olivetti. 2013. "Shocking Labor Supply: A Reassessment of the Role of World War II on Women's Labor Supply." *American Economic Review* 103 (3): 257–62.

Grosjean, Pauline, and Rose Khattar. 2018. "It's Raining Men! Hallelujah? The Long-Run Consequences of Male-Biased Sex Ratios." *Review of Economic Studies* 86 (2): 723–754.

Jarosch, Gregor. 2015. "Searching for Job Security and the Consequences of Job Loss." Unpublished Manuscript, Princeton University.

Kleven, Henrik, Camille Landais, Johanna Posch, Andreas Steinhauer, and Josef Zweimüller. 2019. "Child Penalties across Countries: Evidence and Explanations." *AEA Papers and Proceedings* 109:122–26.

Kleven, Henrik, Camille Landais, and Jakob Egholt Søgaard. 2019. "Children and Gender Inequality: Evidence from Denmark." *American Economic Journal: Applied Economics* 11 (4): 181–209.

Oreopoulos, Philip, Till von Wachter, and Andrew Heisz. 2012. "The Short- and Long-Term Career Effects of Graduating in a Recession." *American Economic Journal: Applied Economics* 4 (1): 1–29.

Schoonbroodt, Alice. 2018. "Parental Child Care During and Outside of Typical Work Hours." *Review of the Economics of the Household* 16:453–476.

Schwandt, Hannes, and Till von Wachter. 2019. "Unlucky Cohorts: Estimating the Long-Term Effects of Entering the Labor Market in a Recession in Large Cross-Sectional Data Sets." *Journal of Labor Economics* 37 (S1): S161–S198.

Siflinger, Bettina, Michele Tertilt, and Gerard van den Berg. 2012. "Domestic Violence over the Business Cycle." Unpublished Manuscript, University of Mannheim.

Stevens, Ann Huff. 1997. "Persistent effects of job displacement: The importance of multiple job losses." *Journal of Labor Economics* 15 (1): 165–188.

Tamm, Marcus. 2019. "Fathers' parental leave-taking, childcare involvement and labor market participation." *Labour Economics* 59:184–197.

Covid Economics 4, 14 April 2020: 62-85

Covid Economics Issue 4, 14 April 2020

Staying at home: Mobility effects of Covid-19

Sam Engle,[1] John Stromme[2] and Anson Zhou[3]

Date submitted: 3 April 2020; **Date accepted:** 4 April 2020

We combine GPS data on changes in average distance travelled by individuals at the county level with Covid-19 case data and other demographic information to estimate how individual mobility is affected by local disease prevalence and restriction orders to stay at home. We find that a rise of local infection rate from 0% to 0.003%[4] is associated with a reduction in mobility by 2.31%. An official stay-at-home restriction order corresponds to reducing mobility by 7.87%. Counties with larger shares of population over age 65, lower share of votes for the Republican Party in the 2016 presidential election, and higher population density are more responsive to disease prevalence and restriction orders.

Covid Economics 4, 14 April 2020: 86-102

1 PhD student in Economics, University of Wisconsin-Madison.
2 PhD student in Economics, University of Wisconsin-Madison.
3 PhD student in Economics, University of Wisconsin-Madison.
4 This is the median infection rate (number of confirmed cases divided by county population) across counties with positive number of confirmed cases as of 20 March 2020.

Covid Economics 4, 14 April 2020: 86-102

1 Introduction

In the face of the rapidly growing threat posed by the COVID-19 pandemic, public health experts and economists alike are relying on epidemic models to make predictions and evaluate policies. In the standard SEIR model (e.g. Wang et al. (2020)), the effective reproduction rate R_t measures the actual average number of secondary cases per infected case at time t. It is widely acknowledged that R_t reflects both the nature of the virus (including the basic reproduction rate R_0), as well as the effectiveness of various protective measures taken by individuals and governments in response to available information. In the case of COVID-19, the key policy measure to reduce R_t is a restriction order to stay-at-home. To date, this policy has been promoted by governments across the globe. It is an open question, however, to what extent individuals alter their mobility in response to government orders. It is also little known how they adjust traveling behaviour when perceived risks of COVID-19 increases, but the government has not yet announced a restriction order.

Mobility statistics provide invaluable information as to whether people are actively reducing their exposure to COVID-19 by reducing distances traveled and avoiding social contact, and by how much. In this paper, we use a novel dataset from Unacast, a location data firm. Their dataset includes a measure of daily average changes in distance traveled (Δ_{it}) in every U.S. county. Their measurement of distance travelled is a relative change to a baseline measure of distance travelled based on historical data, so Δ_{it} is an important measure of changing behaviours in response to the COVID-19 pandemic. We use this data to estimate how the average change in distance traveled is related to perceived risk of contracting the disease (Ω_{it}) and restriction orders I_{it}. We also investigate how these relationships depend on demographic characteristics (X_i). The methodology here is similar to that in Auld (2006), where the author estimates elasticities of risky behavior to local prevalence of AIDS, and explored heterogeneity across observable characteristics.

The estimates obtained here contribute to the current discussion in three ways. First, our results provide an estimate of how much human behavior, in our case average distance

Covid Economics 4, 14 April 2020: 86-102

traveled, responds to perceived risks of contracting the disease. Second, the results give us a sense of how important government announcements are in affecting people's behaviour. Lastly, by considering demographics, political attitude and population density, we evaluate whether characteristics of the underlying population play a role in determining the effectiveness of restriction orders and responses to disease prevalence. In particular, since older individuals are at higher risk[2], we would be interested in whether counties with relatively high elderly populations have altered their behavior more than younger counties. There has also been some discussion that political partisanship is an indicator of skepticism in the legitimacy of the COVID-19 outbreak [3]. We also evaluate whether counties with higher population density adjust behavior more due to the fact that the virus is spreading mainly through interpersonal interactions. To summarize, the novel data and careful analysis in this paper contributes to the understanding of mobility changes amid COVID-19 epidemic while focusing on levels of travel distance and raw percentage change without considering confounding factors such as local disease prevalence and population density could paint an incomplete picture.[4]

Another paper in this issue, Painter and Qiu (2020), also investigates how political beliefs affect compliance with COVID-19 restriction orders. They define a social distancing measure using the fraction of mobile users completely staying at home with location data from SafeGraph Inc. Their panel regression results support our finding that counties with a lower share of votes for the Republican Party in the 2016 Presidential Election respond less to restriction orders. They also use party misalignment to argue that faith in the credibility of government officials affects adherence to those policies. Our paper differs from theirs in three ways. First, besides political affiliation, we also demonstrate the importance of other heterogeneities such as age structure and population density. Second, we focus on people's

[2]See, e.g. the CDC guidelines: https://www.cdc.gov/coronavirus/2019-ncov/need-extra-precautions/people-at-higher-risk.html

[3]e.g. https://www.nytimes.com/interactive/2020/03/21/upshot/coronavirus-public-opinion.html

[4]e.g. `https://www.nytimes.com/interactive/2020/04/02/us/coronavirus-social-distancing.html`

Covid Economics 4, 14 April 2020: 86-102

reduction in mobility to factors beyond restriction orders, such as confirmed cases in both local and neighboring counties. This is important since as we show in Figure 7, average mobility starts to decrease long before restriction orders were announced. Lastly, we build a model of individual behavior; our estimates aim at providing a benchmark value for individual responses to overall perceived COVID-19 risks that can be used in other studies (e.g. Kaplan et al. (2020)). We view Painter and Qiu (2020) as complementary to our paper.

In the rest of the paper, we outline a simple model in section 2. In section 3 we discuss our novel data source on daily travel patterns and how we have augmented it with COVID-19 data. In section 4 we present our preliminary results and argue that even the simple model provides a solid baseline. We finish with section 5 where we summarize our current progress and outline our plan for current and future work.

2 Simple Model

In this section, we present a simple model that relates an individual's travel decision to perceived disease prevalence. This model provides theoretical motivation for the estimation strategy in Section 4.

Consider an individual that derives utility $U(d) = d^\sigma/\sigma$ from distance traveled (d) with $0 < \sigma < 1$. The cost of traveling each unit of distance is composed of one component that is independent of the epidemic Π, and one component that is the product of a linear perceived risk index of contracting the disease ($\Omega > 0$) and the utility cost of contracting the disease (Z). An individual's utility is given by:

$$\begin{aligned} U(d) &= d^\sigma/\sigma - \Pi d - \Omega Z d \\ &= d^\sigma/\sigma - \Pi\left(1 + \Omega\frac{Z}{\Pi}\right)d \\ &\approx d^\sigma/\sigma - \Pi e^{\frac{Z}{\Pi}\Omega} d \end{aligned} \tag{1}$$

The solution of the utility maximization problem is therefore:

$$d^* = \left(\Pi e^{\frac{Z}{\Pi}\Omega}\right)^{\frac{1}{\sigma-1}} \tag{2}$$

As can be seen, when an individual perceives a higher risk level, corresponding to higher Ω, individuals decide to travel less, i.e. by reducing d. We will carefully define Ω later.

If we compare an individual's decision to travel at time t under perceived risk index Ω_t versus some benchmark date t_0 with Ω_0, we get a measure of change in distance traveled:

$$\Delta_t = \frac{d_t^*}{d_0^*} - 1 = e^{\frac{Z}{(\sigma-1)\Pi}(\Omega_t - \Omega_0)} - 1 \equiv e^{\kappa\Omega_t} - 1 \tag{3}$$

since before the outbreak $\Omega_0 = 0$.

Equation (3) is suggestive of a strategy to estimate how the index of perceived risk, Ω, affects the percentage change in distance traveled from date t relative to date 0. We propose to estimate κ via nonlinear least squares, after we consider an appropriate definition of Ω_t below in Section 4.[5]

3 Data

We construct a county-level panel data for the contiguous United States. with dates covering 2/24/2020 to 3/25/2020. Our data includes the following information:

1. Daily confirmed coronavirus cases compiled by The New York Times.[6]

2. Daily changes in average distance traveled relative to the same weekday pre-COVID-19, provided by Unacast. Unacast use GPS signals from mobile devices to calculate

[5]Since change in distance traveled (Δ_t) is large in the data, we do not approximate it by $\log(d_t^*/d_0^*)$.

[6]We also compared this data to case data compiled by the Johns Hopkins University Center for Systems Science and Engineering and found the data to be essentially identical. Our results are robust to both sources.

Covid Economics 4, 14 April 2020: 86-102

average distance traveled by device-holders in each county at a daily frequency.[7]

3. Enacted social-distancing policies (stay-at-home restriction orders) as of 3/28/2020 as compiled by the New York Times.

4. Demographic data is sourced from the MIT Election Data and Science Lab (MEDSL). MEDSL data conveniently matches demographic information from the 2012-2016 5-year ACS, to county-level 2016 Presidential Election Results.

In total, our data covers 3142 U.S. counties with 94,116 observations. The summary statistics are given in Table 1.

Figure 1 plots the changes in average distance traveled relative to the same weekday pre-COVID-19 on 2/24/2020. The overall light color in the figure indicates that at the beginning of the epidemic when there were very few cases confirmed (see Figure 3), there was not much change in population mobility.

When we turn to a more recent date, 3/23/2020, Figure 2 shows that average distance traveled decreases significantly in most counties across the U.S., with particularly large drop in New York, California, Colorado and Florida. Figure 4 shows that these are also places with relatively large number of reported COVID-19 cases.

Figure 5 and 6 show the share of counties and population that is under a stay-at-home order respectively. Both measures start to grow on 3/19 as national cases surpass 10,000. As of 3/25/2020, more than 30% of the counties and 55% of the national population is under government orders to stay-at-home unless for essential activities.

Figure 7 shows the 10th quantile, median, and 90th quantile of the changes in average distance traveled across counties in our sample. We can see that mobility starts to decrease for median counties at around 3/10, well before the announcements of restriction orders as shown in Figure 5 and 6.

[7]For more information on methods of data collection and aggregation, visit `unacast.com` and Unacast COVID-19 Social Distancing Scoreboard.

Covid Economics 4, 14 April 2020: 86-102

Covid Economics 4, 14 April 2020: 86-102

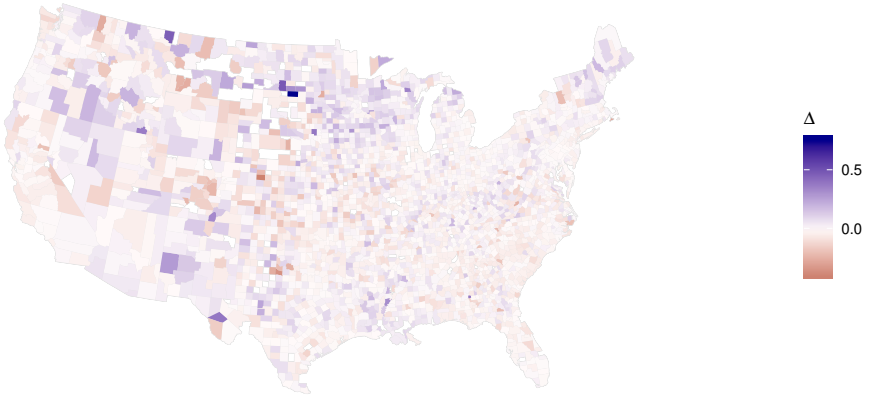

Figure 1: Change in distance traveled relative to the same weekday pre-COVID-19, 2/24/2020

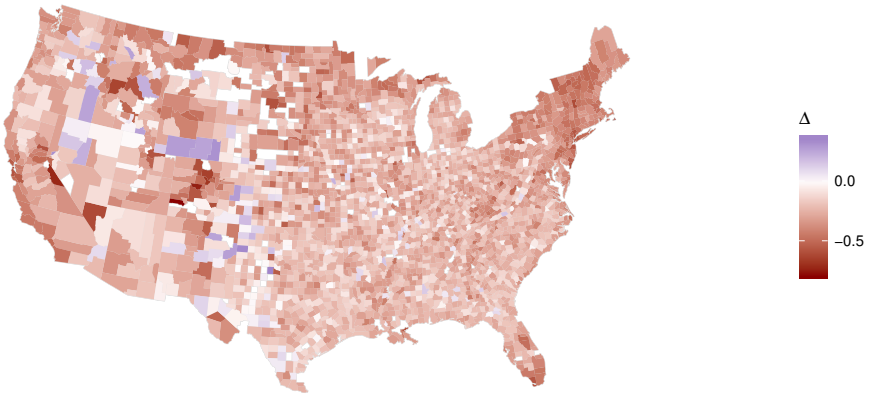

Figure 2: Change in distance traveled relative to the same weekday pre-COVID-19, 3/23/2020

Covid Economics 4, 14 April 2020: 86-102

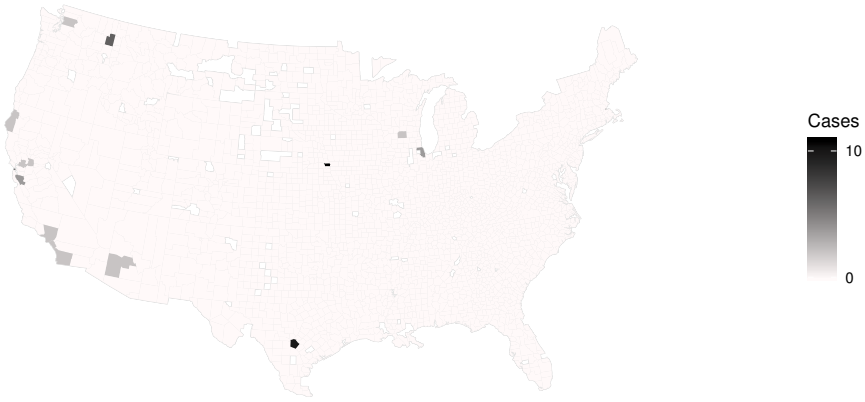

Figure 3: Number of confirmed cases, 2/24/2020

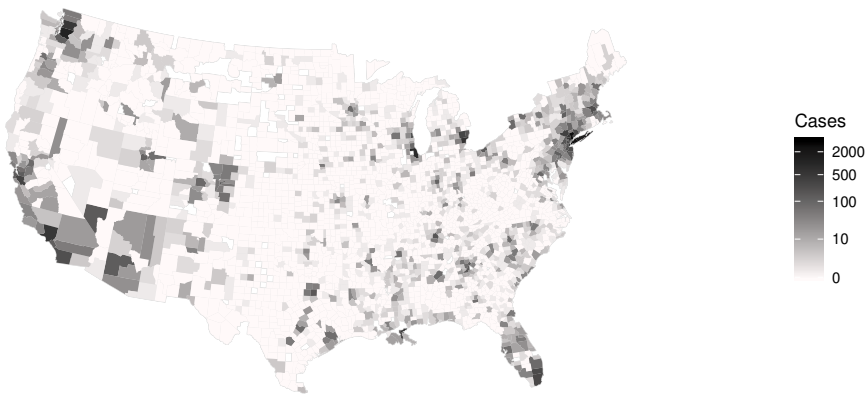

Figure 4: Number of confirmed cases, 3/23/2020

Covid Economics 4, 14 April 2020: 86-102

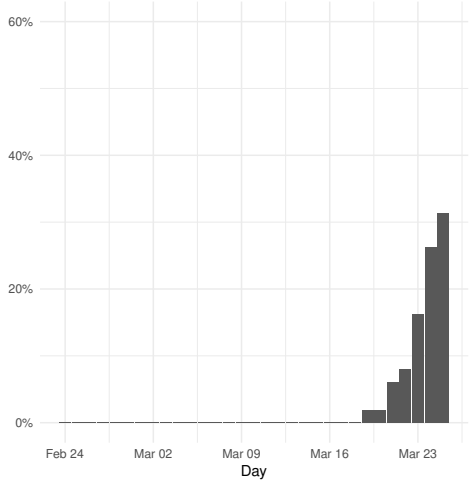

Figure 5: Share of Counties under Stay-at-Home

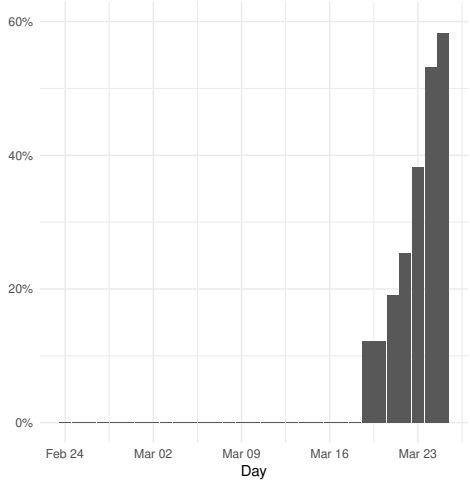

Figure 6: Share of Pop under Stay-at-Home

Covid Economics 4, 14 April 2020: 86-102

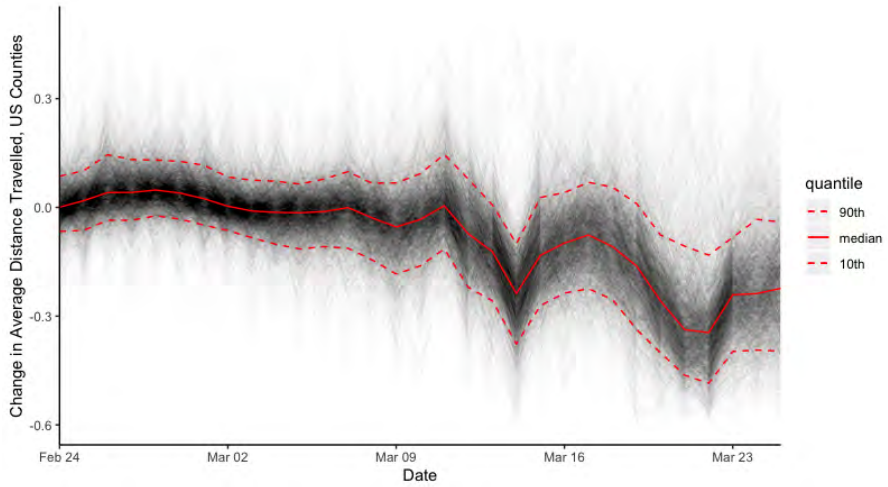

Figure 7: Quantiles of Changes in Average Distance Traveled Across Counties

Table 1: Summary Statistics of Pooled Dataset

Statistic	Mean	St. Dev.	Min	Max
Total Cases	3.004	61.546	0.000	6,154.000
Cases, Share of Pop	0.001%	0.01%	0.00%	0.5%
Neighbor Cases, Weighted	0.005%	0.01%	0.00%	0.2%
Pct Chg in Distance Travelled	−0.079	0.158	−0.879	1.388
Share of Pop Over Age 65	17.502	4.319	3.855	53.106
Share of Republican Votes, 2016	0.629	0.156	0.041	0.916
Population Size, Thousands	104.648	330.248	1.233	10,057.160
Density: Thousands per Sq. Mile	0.268	1.753	0.001	69.468

Note: See Section 4 for formal definition of the *Neighbor Cases* variable.

Covid Economics 4, 14 April 2020: 86-102

4 Empirical Results

Motivated by the model outlined in (3), our baseline regression model is given by:

$$\Delta_{it} = \beta_0 + \beta_1 \exp(\beta_2 \Omega_{it}) + \beta_3 I_{it} + \beta_4 \exp(\beta_2 \Omega_{it}) \times I_{it} + \beta_X I_{it} \times X_i + \rho \Delta_{i,t-1} + \epsilon_{it} \qquad (4)$$

where the variables are defined as follows:

Dependent variable (Δ_{it}) Mobility change is measured by the percentage difference in average daily distance in county i at time t, compared to the average in the four weeks before COVID-19 outbreak, by weekday.

Perceived risk index of contracting COVID-19 (Ω_{it}) We assume that individuals' perception of risk is affected by COVID-19 prevalence in both local and neighboring counties, as well as population demographics. We propose using a linear index, Ω_{it}, defined as:

$$\Omega_{it} = C_{i,t-1} + \gamma \sum_{j \neq i} w_{ij} C_{j,t-1} + \gamma_X X + \gamma_{CI} \left[C_{i,t-1}, \sum_{j \neq i} w_{ij} C_{j,t-1} \right] \times X \qquad (5)$$

where each term in (5) denotes

1. $C_{i,t-1}$, is total confirmed cases divided by population at county i at time $t-1$. To ease interpretation of coefficients, we then normalize the median prevalence level for counties with positive COVID-19 cases on 3/20/2020 to be one (0.003% - Mecklenburg, North Carolina).

2. $\sum_{j \neq i} w_{ij} C_{j,t-1}$, a weighted average of confirmed cases at neighboring counties measured at time $t-1$. For simplicity, we let weight be proportional to the inverse of distance between county centroids with $\sum_{j \neq i} w_{ij} = 1$.We adopted the same normalization as in $C_{i,t-1}$.

3. X_i, County-level demographics include age structure (share of population over 65), political attitude (share of the population that voted Republican in the 2016

Presidential Election), and population density (thousand people per square mile).

In this baseline model, we interpret Ω_{it} as a linear approximation perceived risk.

Restriction orders (I_{it}) Restriction order I_{it} is a dummy variable that takes the value of one if an order to stay-at-home is in effect in county i at date t; zero otherwise.

In (4), we allow individuals' response to perceived risk to differ depending on whether the government have announced restriction or not. We also consider the possibility that responses to a restriction order might vary based on demographic characteristics. In (5), perceived risk index Ω_{it} is affected by both local and neighborhood COVID-19 confirmed cases, as well as underlying population characteristics. We also include an interaction term to study how population characteristics affect individuals' perceived risks as the disease become more widespread. Note that the coefficient in front of $C_{i,t-1}$ in Equation (5) is normalized to 1, since the overall scale of the γ's cannot be separately identified from β_2 in Equation 4.

Our main results are shown in Table 2. The top-half of the table shows estimates of the parameters in Equation (4) while the bottom-half shows coefficients in the perceived risk equation (5). In subscripts of coefficients, we use $\{P, O, D\}$ to represent the share of population that voted Republican in the 2016 Presidential Election, share of population with age over 65, and population density (in thousands of people per square mile) respectively. Subscripts $\{L, N\}$ refer to the interaction terms of population characteristics with local confirmed cases $C_{i,t-1}$ and neighborhood confirmed cases $\sum_{j \neq i} w_{ij} C_{j,t-1}$.

We start the interpretation of the main results from the top. The positive value of $\hat{\beta}_1$ combined with negative $\hat{\beta}_2$ implies that an increase in perceived risk index Ω_{it} reduces leads to a decrease in Δ_{it}.

To get a sense of the magnitude of the effect of restriction orders on mobility, we consider the case where the government announces a stay-at-home order in a county with median demographic characteristics $(\bar{P}, \bar{O}, \bar{D})$ and our median estimate of perceived risk index, $\bar{\hat{\Omega}}$.

Covid Economics 4, 14 April 2020: 86-102

Covid Economics 4, 14 April 2020: 86-102

Table 2: Main Results

	Δ	
	Estimate	SE
β_0	-0.1222^{***}	(0.0011)
β_1	0.1349^{***}	(0.0031)
β_2	-1.5616^{***}	(0.2554)
β_3	-0.0685^{***}	(0.0106)
β_4	-0.0890^{*}	(0.0439)
β_{PI}	0.1810^{***}	(0.0141)
β_{DI}	-0.0025^{***}	(0.0006)
β_{OI}	-0.0034^{***}	(0.0005)
ρ	0.5141^{***}	(0.0029)
Ω		
γ	0.2132^{*}	(0.0952)
Political Affiliation		
γ_P	-0.0056	(0.0180)
γ_{PC}	-1.1557^{***}	(0.1118)
γ_{PN}	-0.4063^{***}	(0.1267)
Population Density		
γ_D	0.0034	(0.0029)
γ_{DC}	-0.0959^{*}	(0.0430)
γ_{DN}	0.5541^{***}	(0.1153)
At Risk Share		
γ_O	0.0033^{***}	(0.0008)
γ_{OC}	-0.0069	(0.0094)
γ_{ON}	0.0439^{***}	(0.0076)
$^{***}p < 0.001$, $^{**}p < 0.01$, $^{*}p < 0.05$		
Num. Obs = 91080		

Based on our estimates from Table 2, we find that the restriction order would reduce mobility by 7.87% for a county with characteristics $\bar{P}$, $\bar{O}$, $\bar{D}$, and perceived risk index $\bar{\bar{\Omega}}$.

The coefficients from interacting restriction order with population demographics tell an interesting story. We illustrate this point with the hypothetical county with characteristics $(\bar{P}, \bar{O}, \bar{D})$ and perceived risk index $\bar{\bar{\Omega}}$) as before. If we perturb the characteristics $\{P, O, D\}$ one at a time by increasing each in turn by one standard deviation of that characteristic, how would the effect of the restriction order change? Recall that this baseline effect is a 7.87% decrease. The estimates suggest that the effect of a restriction order would be of smaller magnitude, going to a 5.05% decrease with a 15.6 percentage point increase in the share of the population that voted Republican in the 2016 Presidential Election; the effects would be stronger when the share of the population over age 65 increases by 4.3 percentage points, with the effect size of a 9.33% decrease. Lastly, when population density increases by 1000 people per square mile, we would expect the effect of a restriction order to be stronger, an 8.30% decrease. These results suggests that the effects of restriction order are highly heterogeneous depending on the underlying population, with the direction of the effect being consistently negative, as expected.

The coefficient of the interaction between Ω and I, β_4, is negative with an absolute value smaller than β_1. This implies that an increase in perceived risk index of contracting the disease Ω still decreases mobility when restriction order is announced, but with a smaller impact.

Now we turn to the bottom half of Table 2 to interpret the estimates of coefficients in Equation (5) determining perceived risks. Parameter γ measures the relative importance of cases in neighboring counties relative to local cases. The estimate $\hat{\gamma}$ shows that an increase in COVID-19 confirmed cases in neighboring counties would indeed raise the perceived risk locally, but individuals discount that increase at rate 0.2. This implies that spillover of risks across regions are potentially important, but the magnitude is not very large in the data relative to local cases.

Covid Economics 4, 14 April 2020: 86-102

Covid Economics 4, 14 April 2020: 86-102

To study the magnitude of these estimates, we consider again the county with median characteristics $\{\bar{P}, \bar{O}, \bar{D}\}$. If the county starts out with zero confirmed cases locally, and with neighboring confirmed cases at the sample median, suppose there is a unit increase[8] in local cases. How much would individuals reduce traveling without government imposing any restriction order? By combining estimates of parameters, our results suggest that the mobility reduction is 2.31%. These estimates suggests that decreases in mobility could take place well before the official announcement of restriction orders, which is in line with the findings in Figure 7 and evidence from OpenTable reservations in Kaplan et al. (2020).

The direct effects of demographic characteristics, and their interactions with confirmed cases, on perceived risk, shown in the bottom half of Table 2, lead to a very similar conclusion to the one we reached on the their effects on restriction order. Counties with a lower share of the population that voted Republican in the 2016 Presidential Election, higher share of elderly population, and higher population density have higher perceived risk in levels, and are more responsive to increases of disease prevalence.

5 Discussion and Conclusion

In this paper, we combine a novel GPS location dataset with COVID-19 cases and population characteristics at the county level to estimate the effects of disease prevalence and restriction orders on individual mobility. We find that population mobility reacts strongly to changes in perceived disease prevalence and government stay-at-home announcements: a rise of local infection rate from 0% to 0.003% reduces mobility by 2.31%, and a government restriction order to stay-at-home reduces mobility by 7.87%. Additionally, we find that these effects of information on individual behaviour depends on characteristics of the underlying population. In particular, counties with larger shares of population over age 65, lower share of population voted Republican in the 2016 Presidential Election, and higher population density are more

[8]Due to the normalization, we could interpret the unit increase as a shift to the median prevalence level in counties with confirmed cases as of 3/20/2020, i.e. Mecklenburg, NC.

responsive to disease prevalence and restriction orders.

There are a couple of important limitations to our work in its current iteration. First, our perceived risk index Ω_{it} does not line up with the exact interpretation of Ω in the model; to be specific, we are providing a linear approximation to Ω, a strictly positive quantity. Our model fits the data well, as $\hat{\Omega}_{it}$ is positive in over 99.9% of cases. Future work could include a submodel for Ω so that we can directly interpret the estimated quantities as perceived risk. Second, we have not yet included a model of endogeneity. Presumably, travel decisions and perceived risk are simultaneously determined. We have begun to study how to incorporate this into an extended model. Lastly, we plan to include more demographic controls such as industry composition and share of workers in essential jobs. These could affect the substitutability between on-site work and work-from-home, hence affecting changes in mobility. and these will be included in future versions of the project being continuously updated on SSRN.

Covid Economics 4, 14 April 2020: 86-102

References

Auld, M. C. (2006). Estimating behavioral response to the aids epidemic. The BE Journal of Economic Analysis & Policy 5(1).

Hauck, K. (2018). The economics of infectious diseases. Oxford University Press.

Kaplan, G., B. Moll, and G. Violante (2020). Pandemics according to hank.

MIT Election Data + Science Lab (2020, Accessed: March 28th). 2018 election analysis dataset. https://github.com/MEDSL/2018-elections-unoffical.

Painter, M. and T. Qiu (2020). Political beliefs affect compliance with covid-19 social distancing orders. Covid Economics - A Real-Time Journal 2.

The New York Times (2020a, Accessed: March 30th). Coronavirus (covid-19) data in the united states. https://github.com/nytimes/covid-19-data.

The New York Times (2020b, Accessed: March 28th). See which states and cities have told residents to stay at home. https://https://www.nytimes.com/interactive/2020/us/coronavirus-stay-at-home-order.html.

Unacast (2020, Accessed: March 28th). Covid-19 location data. https://https://www.unacast.com/covid19.

Wang, H., Z. Wang, Y. Dong, R. Chang, C. Xu, X. Yu, S. Zhang, L. Tsamlag, M. Shang, J. Huang, et al. (2020). Phase-adjusted estimation of the number of coronavirus disease 2019 cases in wuhan, china. Cell Discovery 6(1), 1–8.

Covid Economics 4, 14 April 2020: 86-102

Political beliefs affect compliance with Covid-19 social distancing orders[1]

Marcus O. Painter[2] and Tian Qiu[3]

Date submitted: 5 April 2020; **Date accepted:** 6 April 2020

Social distancing is vital to mitigate the spread of the novel coronavirus. We use geolocation data to document that political beliefs present a significant limitation to the effectiveness of state-level social distancing orders. Residents in Republican counties are less likely to completely stay at home after a state order has been implemented relative to those in Democratic counties. We also find that Democrats are less likely to respond to a state-level order when it is issued by a Republican governor relative to one issued by a Democratic governor. These results are robust to controlling for other factors including time, geography, local Covid-19 cases and deaths, and other social distancing orders. We conclude that bipartisan support is essential to maximise the effectiveness of social distancing orders.

Covid Economics 4, 14 April 2020: 103-123

1 We thank SafeGraph Inc. for data access. Academics and others working for the public good can access the geolocation data used in this paper for free here: https://www.safegraph.com/covid-19-data-consortium.
2 Assistant Professor of Finance, Saint Louis University.
3 PhD student, University of Kentucky.

Covid Economics 4, 14 April 2020: 103-123

I. Introduction

Both the World Health Organization and Center for Disease Control have recognized social distancing as the most effective way to slow down the spread of the novel coronavirus. Early evidence from China and the 1918 US flu pandemic also highlight the importance of limiting travel time in fighting the disease (Kraemer et al. (2020); Correia et al. (2020)). Observing the universal effectiveness of social distancing from Asia and Europe, many regions in the US have also started to issue stay-at-home and shelter-in-place orders. Since March 19th of 2020, 33 states have issued explicit orders that urge their residents to stay home. As of this writing roughly 84% of Americans are now disciplined by some level of social distancing requirements.

It is important for the government to understand how effective these orders are for at least two reasons. First, there are states that have not issued statewide social distancing orders, and this analysis would help them make better-informed decisions going forward. Second, understanding the effectiveness of current policies may allow states that have a policy in place to make adjustments as necessary. In this paper, we leverage geolocation tracking data sourced from smartphones to analyze the effectiveness of state-level social distancing policies and show that political beliefs are an important limitation for whether people adhere to these orders.

Potentially due to the recent increase in political polarization in the US (Boxell, Gentzkow, and Shapiro, 2020), there are concerns regarding how political beliefs would heterogeneously affect compliance with social distancing orders. For instance, a pastor from Arkansas told the Washington Post that "in your more politically conservative regions, closing is not interpreted as caring for you. It's interpreted as liberalism, or buying into the hype." The same report also documents that people from more liberal areas show more distrust in President Trump's initial message and are more proactive about social distancing.[1] The press has also highlighted that

[1] "Without guidance from the top, Americans have been left to figure out their own coronavirus solutions." Washington Post. March 15, 2020.

President Trump initially downplayed the severity of the coronavirus pandemic, suggesting that Republicans may not take social distancing orders seriously.[2]

Does this media coverage solely pick up extreme observations that are not representative of how residents with differing political beliefs behave? Or is there some generalizability of these anecdotes? These are important questions as the answers could help policymakers understand the difference in the treatment effect of stay-home orders among different subpopulations and better allocate precious time and resources in this challenging time.

To analyze these questions, we create a measure of social distance based on the location of a sample of smartphones throughout the day. From this data we measure social distancing as the percentage of people who stay home for an entire day relative to all people identified in a census block group. This daily data covers February and most of March, 2020. We also collect data on government-sanctioned social distancing orders, county-level demographics, and county-level voting results from the 2016 presidential election. The union of these datasets allows us to study whether partisanship affects adherence to social distancing orders through a difference-in-differences framework.

We find that state-level social distancing orders are associated with a significant increase in social distancing. Specifically, the change in the proportion of people who completely stay at home is 5.1 percentage points (pps) higher in areas with a state-level policy relative to areas without a policy. This finding is robust to the inclusion of county and date fixed effects as well as controlling for other local policies (e.g., closing schools) and reports of county-level coronavirus cases and deaths.

Next, analyzing differential responses to state policies, we find that Republican counties respond less to social distancing orders relative to Democratic counties. A one standard deviation increase in the county-level share of votes for Donald Trump in the 2016 election is associated with a 3pps lower percentage of people who stay at home after a state social distancing order relative to the average county. This finding is robust to subsample tests

[2] "Analyzing the Patterns in Trump's Falsehoods About Coronavirus." New York Times. March 27, 2020.

Covid Economics 4, 14 April 2020: 103-123

designed to adjust for county population and density.

Our final tests focus on whether the political affiliation of the governor announcing a state-level social distancing order affects compliance. If Republican's lower response to social distancing orders is due to President Trump's early dismissal of the pandemic, we may likewise find that Democrats' response to orders may vary based on the political affiliation of who gives the order. We identify "aligned" counties as those with the same political affiliation as the governor and "misaligned" counties as those with conflicting political identities. We find that misaligned counties have a 2.9pps lower response to state policy social distancing orders relative to aligned counties. This difference is driven by misaligned democratic counties. These results suggest that the difference in compliance to social distancing orders based on partisanship is likely due to how credible residents find government officials and not an information transmission channel.

Taken together, our results suggest that political polarization is a major roadblock on the path to full compliance with social distance measures. Republicans and misaligned Democrats are less likely to adhere to these orders, suggesting that bipartisan support for social distancing measures is a key factor in how quickly we can mitigate the spread of the novel coronavirus.

Covid Economics 4, 14 April 2020: 103-123

II. Related Literature

Our findings are related to the literature examining how political beliefs can influence behavior. Examining politically-charged fake news, Long, Chen, and Rohla (2019) find that conservative-media dismissals of the dangers of hurricane Harvey and Irma led to lower evacuation rates for conservatives relative to liberals. Painter (2020) shows that consumers respond along partisan lines when firms issue political statements. There is also evidence that politics can influence economic expectations (Gerber and Huber (2010); McConnell et al. (2018)). We extend this literature to the recent pandemic setting, showing that information from political officials can influence responses to government orders.

Covid Economics 4, 14 April 2020: 103-123

In contemporaneous independent work, Engle, Stromme, and Zhou (2020) also use geolocation data to study how Americans respond to the threat of the coronavirus. Though similar in spirit, their study differs from ours regarding both research focus and methodology. Regarding focus, Engle et al. (2020) give a more general overview of factors associated with geographic mobility amid the pandemic (including past cases, age, and political beliefs), whereas we focus more in depth on the political beliefs factor and document more nuanced behavior in that respect.

Regarding methodology, there are two significant differences between our paper and Engle et al. (2020). First, we use data from SafeGraph and measure how often people stay completely at home as our social distancing measure while Engle et al. (2020) use data from Unacast and focus on how Americans change their average distance traveled. While informative, a distance traveled measure may be confounded by people driving to work and may also be upwardly biased in areas that have to drive further for essential goods like groceries. This bias is especially problematic when studying political divides as rural areas tend to be more Republican. Our social distancing measure is able to avoid these confounding effects as the SafeGraph data identifies devices which are likely traveling for work and the proportion of people who completely stay at home is not affected by how far they travel for essential goods and services. Second, our model includes fixed effects for county and date and double-clustering of standard errors by county and date. In contrast, the model of Engle et al. (2020) does not appear to include either fixed effects or standard error adjustments. Though they do include county-level controls for age, population, and density, their results may still be influenced by unobserved heterogeneity at the county level (e.g., local economic conditions like unemployment). In addition, the absence of clustering may lead to downward biased standard errors if those errors are correlated by county or date. Having established differences in our papers, we next turn to describing the data used in our study.

Covid Economics 4, 14 April 2020: 103-123

III. Data

The primary datasets we use in this study are (1) geolocation data from SafeGraph, (2) government-sanctioned social distancing orders, and (3) county-level election results from the 2016 Presidential election.

A. Geolocation Data

To create a measure of social distance compliance, we rely on anonymized location data from SafeGraph Inc. SafeGraph partners with mobile application services that have opt-in consent from users to collect location data. The partnerships allow SafeGraph to see location data from approximately 35 million unique devices in a given month. To preserve anonymity, the data is aggregated to the census block group (CBG) level and all CBG's with fewer than five observations are omitted. This geolocation data is advantageous as it allows us to see the movement behavior of a large sample of Americans. Further, prior studies using SafeGraph data find the data are generally representative of the US population (Chen, Haggag, Pope, and Rohla, 2019) and in particular representative of voting patterns in the US (Chen and Rohla, 2018).

From the SafeGraph data we create the following variable to track social distancing:

$$Social\ Distance_{c,t} = \frac{Completely\ Home_{c,t}}{Total\ Device\ Count_{c,t} - Working_{c,t}} \tag{1}$$

where $Completely\ Home_{c,t}$ is the number of devices in county c on day t that never left home. Home is measured as the common nighttime location of each mobile device over a 6 week period to a Geohash-7 granularity (about 153 square meters). $Total\ Device\ Count_{c,t}$ is the total number of devices identified in county c on day t, and $Working_{c,t}$ is the number of devices that leave home and go to another location for more than three hours during the period of 8 am to 6 pm local time.[3] A higher percentage of $Social\ Distance_{c,t}$ indicates more

[3]We use three hours in order to adjust for both part-time and full-time workers. Full documentation for the

residents in the area are complying with the social distancing order.

Though the SafeGraph data is extensive and is useful for our setting, it does have some limitations. The data is nationally representative but relies on smartphones to track location and as of 2018 23% of American adults did not own a smartphone.[4] Thus inferences can only be drawn about those who own smartphones. Finally, the data is generated through intermittent and somewhat random "pings" to smartphones and is not monitored continuously throughout the day. This means short trips outside the home may be missed if the phone is not pinged during that time. This could introduce bias as more densely populated areas - which tend to be Democratic - are able to make short trips out of the house whereas rural areas - which tend to be Republican - must make longer trips for daily necessities (e.g., groceries). We address this potential bias by analyzing subsamples of counties based on population and population density.

B. Government Social Distancing Orders

There are a few sources that track the social distancing policies at varying geographical levels. We choose to use the data assembled by the New York Times because it is comprehensive and provides precise information on both the timing and geography of the social distancing order.[5] Importantly for our study, it also provides official documentation for the order, allowing us to identify the policy announcer in each case. California, the most populous state, was the first to order a state-wide stay at home order effective March 19. Since then, a total of 33 states have issued social distancing orders[6]. We merge the political affiliation of all governors with the NYT data as it is not included in their report. We also gather daily data on the number of reported cases and deaths in each county from the NYT.[7]

There are also instances of governors who refrain from issuing state-wide social distancing

SafeGraph social distancing data can be found here: https://docs.safegraph.com/docs/social-distancing-metrics

[4] Mobile Fact Sheet. Pew Research Center. June, 2019.

[5] "See Which States and Cities Have Told Residents to Stay at Home." New York Times. April 2, 2020.

[6] As of the current draft, with Maine (April 2^{nd}) being the last on our list.

[7] "We're Sharing Coronavirus Case Data for Every U.S. County." New York Times. March 28, 2020.

Covid Economics 4, 14 April 2020: 103-123

orders. These refusals often cite concern on the economy as the main reason. For instance, Alabama Governor Kay Ivey said she will not issue a statewide order because she wanted to "balance the health of the state's residents with the health of the economy." In these cases, NYT also collects information at the city/county level. This data is not useful in our analysis however, as most city/county level orders are not made by political officers. For example, county level social distancing orders in Missouri have largely been made by public health officials. For this reason, we exclude all counties that have implemented a county-level social distancing order from our analysis.

C. Political Affiliation and Demographic Data

Our setting also requires a proxy for the political preference of US residents. We use the results of the 2016 US Presidential election to measure a county's political preference. Specifically, we collect county-level voting data from the MIT Election Data and Science Lab (MIT, 2018) and use the vote share won by Donald Trump to measure the degree to which a county leans Republican or Democrat. Lastly, we collect county-level demographic data - most notably population and population per square mile - from the 2018 American Community Survey database.

IV. Results

A. Summary Statistics

We report summary statistics of social distancing compliance in panel A of Table 1. Our social distancing data covers February 1st to March 29th of 2020. During this period, on average 33.1% of residents are identified as staying completely at home. We observe the univariate treatment effect of social distancing orders when we split this variable into before and after a state announces a social distancing policy. After having a policy in place, the completely at home rate increases to 46.4% from 32.6% (a 42% increase). Panel B of Table 1 reports summary statistics on county characteristics and highlights the importance of adjusting for population characteristics. There are fewer Democratic counties in the US

Covid Economics 4, 14 April 2020: 103-123

but they are both more populated and more densely populated than Republican counties. The average Democratic (Republican) county has 290,000 residents (46,000) and 293 (30) residents per square mile.

B. The Effects of State-Level Social Distancing Orders

We examine whether political beliefs affect the response to state-level social distancing orders using the following generalized difference-in-differences estimation:

$$Social\ Distancing_{c,t} = \beta * (State\ Policy \times Trump\ Vote) + \delta' * controls + \gamma_c + \gamma_t + \epsilon_{c,t} \quad (2)$$

Where $Social\ Distancing_{c,t}$ is the percentage of smart devices that were completely at home in county c on day t, $State\ Policy = 1$ if a state level social distancing order has gone into effect,[8] and $Trump\ Vote$ is the county level vote share that went to Donald Trump in the 2016 election. We z-score $Trump\ Vote$ to have a mean of zero and standard deviation of one. The β coefficient on the interaction term will capture the marginal response to social distancing orders based on how much a county leans Republican or Democrat. We include controls for the one-day lag of the cumulative number of cases and deaths due to the coronavirus in a county. We also include as controls dummy variables that identify when a state closed k-12 schools, day cares, gyms, and movie theatres and banned nursing home visits, non-essential business, and sit-in restaurants.[9] We include county fixed effects to control for time-invariant local factors like the performance of the local economy. We also include date fixed effects to control for common factors across time like the release of a coronavirus-related news on a certain day. We double-cluster standard errors at the county and date level.

While we have taken careful steps to mitigate confounding factors, there still exists some potential for endogeneity. In particular, the timing and strength of policy implementation

[8]We exclude from our analysis days where a state policy went into effect at 12pm or later.
[9]We thank Julia Raifman, Kristen Nocka, and their contributors for sharing this data.

Covid Economics 4, 14 April 2020: 103-123

Covid Economics 4, 14 April 2020: 103-123

may be endogenous to the expectations of politicians regarding the effectiveness of other social distancing strategies (e.g., loosely defined recommendations to practice social distancing). Though our day fixed effects adjust for timing issues, we cannot completely rule out this possibility.

We report the results of estimating equation (2) in Table 2. In column (1) we estimate a baseline specification to examine how much social distancing increases after a state-policy order at the aggregate level. We find that counties with state social distancing orders have a completely-at-home rate that is 5.1 pps higher (16% increase from the unconditional mean) than counties with no state policies in place. This finding highlights the importance of implementing state-level policies, especially when considering this effect is after controlling for county-level coronavirus cases and deaths as well as a host of other state-level business closures. We next estimate equation (2) to analyze how political partisanship affects adherence to social distancing orders (column 2). Consistent with the argument that Republicans were influenced by Trump's early dismissal of the pandemic, we find that a higher vote share to Trump is associated with a lower proportion of people staying completely at home. Specifically, a one standard deviation increase in the vote share to Trump is associated with a 3pps decrease in proportion of people staying completely at home after a state policy relative to a county with an average vote share to Trump.

We also analyze these effects in event-time in panels A and B of Fig. 1. We interact our state policy variable with indicator variables for how far away a date is from the state policy enactment and report the resulting coefficients. By construction, these coefficients capture the time-series of differences in social distancing compliance between treated and control counties. The baseline result (panel A) shows little difference between the social distancing in our treatment and control counties before state policies are enacted and a large jump in the difference once a state policy goes into effect. The partisan split event study (panel B) also shows a significant difference in the response to state-policies when comparing Republican counties (>50% Trump) and Democratic counties, with Democratic counties

responding more.

There is also evidence in panel B that Democrats begin adopting social distancing behavior prior to the announcement of state policies. To ensure that this difference in pre-trends is not driving our results in Table 2 column (2), we re-estimate equation (2) while excluding observations that occur greater than five days before a state policy is implemented. We also exclude all observations before March 15th in our control sample. We continue to find a significant difference in social distancing behavior based on the vote share to Trump (column 3), suggesting that pre-trends are not driving our results.

Because more populous areas are more at risk, there could be an increasing intensive margin effect based on the population of the area. To test this hypothesis, we repeat the previous regression but instead interact the state policy indicator with the population in a county (z-scored to mean 0 and standard deviation one) and report results in column (4) of Table 2. We find that population is indeed an important factor in social distancing compliance: A one standard deviation increase in county population is associated with 10 pps higher compliance rate. We find a similar - though somewhat muted - effect when including population density (the z-score population per square mile) as the interaction term. We also find that the population and density differences primarily occur on the date that the state-policies are implemented (panels C and D of Fig. 1).

The population results highlight the need to adjust for county population when examining differences in social distancing behavior in Republican and Democratic counties. This is particularly important as Republican counties tend to be less populated, rural areas and Democratic counties tend to be more populated, urban areas. To adjust for these differences, we estimate equation (2) on subsamples of counties sorted into quintiles based on population and population density and report results in Table 3.

Panel A of Table 3 reports results for the subsamples based on population. We find a significant negative coefficient on $State\ Policy \times Trump\ Vote$ in all subsamples, suggesting that the population of a county is not driving the difference in social distancing responses

Covid Economics 4, 14 April 2020: 103-123

between Republican and Democratic counties. When sorting by population density (panel B), we find a significant coefficient on the interaction term in the top three quintiles but no effect in the bottom two quintiles. The absence of a significant effect in more sparsely populated areas is intuitive as these areas are naturally less exposed to the quick spread of the coronavirus. Taken together, these results suggest that Republicans located in relatively densely populated areas are less like to adhere to social distancing orders relative to Democrats.

There are two possible channels that may explain our results thus far. First, an "information" channel would suggest that Democrats are more informed about the potential spread of coronavirus and thus react more intensely when government measures are put in place. Second a "credibility" channel would suggest that Republicans, who may rely on President Trump's word more than more local government officials, do not find the state policy warnings credible and therefore react less to social distancing orders.

To distinguish between these two potential channels, we create the variable *misalignment* which indicates whether the political affiliation of a county is misaligned with the political affiliation of the person who issues a state policy order. For example, $misalignment = 1$ for a Republican county in Colorado, where the Democratic Governor Jared Polis issued a stay at home order. On the other hand, $misalignment = 0$ for a Democratic county in Colorado. Our final tests examine equation (2) but instead interact the state policy indicator with the misalignment variable. If the results are driven by the information channel, we would expect to find no difference based on misalignment. If the results are driven by the credibility channel, we would expect a lower response in misaligned counties relative to aligned counties as the misaligned counties would find the social distancing order less credible.

Table 4 reports the misalignment results. Consistent with the credibility channel, we find that misaligned counties respond less to social distancing orders relative to aligned counties. After a state policy is enacted, the proportion of people who completely stay home is 2.9pps lower in misaligned counties relative to aligned counties. To further examine the credibility channel, we repeat the misalignment tests on subsamples of Republican and Democratic

Covid Economics 4, 14 April 2020: 103-123

counties. We find no difference in behavior between aligned and misaligned Republican counties (column 2) but a significant difference in behavior in Democratic counties (column 3).

We find consistent results when examining these subsamples in event time (Fig. 2). Interestingly, the event-time studies show that misaligned Democratic counties' social distancing difference is similar to those of all Republican counties and the difference in partisan response to social distancing orders is driven by Democratic counties responding to orders made by Democratic governors.

V. Conclusion

Social distancing is vital to mitigate the spread of the novel coronavirus. In this paper, we study political limitations to government-mandated orders intended to get people to practice social distancing. Our results suggest that faith in the credibility of officials issuing government orders affects adherence to those policies. In particular, Republican and politically-misaligned Democratic counties respond significantly less to social distancing policies. Our results highlight the need for bipartisan support of the effectiveness of social distancing in order to mitigate the spread of the coronavirus.

Covid Economics 4, 14 April 2020: 103-123

Covid Economics 4, 14 April 2020: 103-123

References

Boxell, Levi, Matthew Gentzkow, Jesse M Shapiro. 2020. Cross-country trends in affective polarization. Tech. rep., National Bureau of Economic Research.

Chen, M Keith, Kareem Haggag, Devin G Pope, Ryne Rohla. 2019. Racial disparities in voting wait times: Evidence from smartphone data. Tech. rep., National Bureau of Economic Research.

Chen, M Keith, Ryne Rohla. 2018. The effect of partisanship and political advertising on close family ties. *Science*, **360**(6392) 1020–1024.

Correia, Sergio, Stephan Luck, Emil Verner. 2020. Pandemics depress the economy, public health interventions do not: Evidence from the 1918 flu. *Working Paper*.

Engle, Samuel, John Stromme, Anson Zhou. 2020. Staying at home: Mobility effects of covid-19. *Working Paper*.

Gerber, Alan S, Gregory A Huber. 2010. Partisanship, political control, and economic assessments. *American Journal of Political Science*, **54**(1) 153–173.

Kraemer, Moritz U. G., Chia-Hung Yang, Bernardo Gutierrez, Chieh-Hsi Wu, Brennan Klein, David M. Pigott, Open COVID-19 Data Working Group†, Louis du Plessis, Nuno R. Faria, Ruoran Li, William P. Hanage, John S. Brownstein, Maylis Layan, Alessandro Vespignani, Huaiyu Tian, Christopher Dye, Oliver G. Pybus, Samuel V. Scarpino. 2020. The effect of human mobility and control measures on the COVID-19 epidemic in China. *Science*.

Long, Elisa F, M Keith Chen, Ryne Rohla. 2019. Political storms: Emergent partisan skepticism of hurricane risks.

McConnell, Christopher, Yotam Margalit, Neil Malhotra, Matthew Levendusky. 2018. The economic consequences of partisanship in a polarized era. *American Journal of Political Science*, **62**(1) 5–18.

MIT. 2018. County Presidential Election Returns 2000-2016. doi:10.7910/DVN/VOQCHQ.

Painter, Marcus. 2020. Consumer response to corporate political statements: Evidence from geolocation data. *Working Paper*.

Covid Economics 4, 14 April 2020: 103-123

Covid Economics 4, 14 April 2020: 103-123

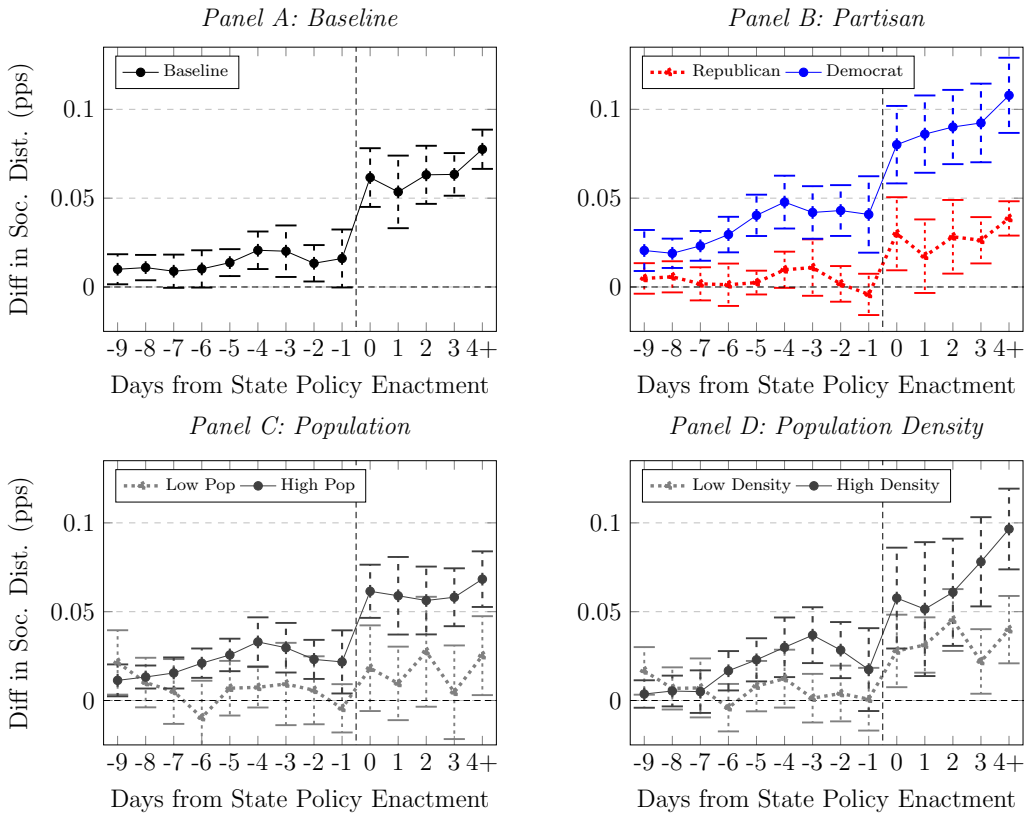

Fig. 1
Changes in Social Distancing around State Policies
This figure plots coefficients of β_j from the following regression of social distancing on the interaction of state policies for shelter in place in event time, where day 0 is the first date the state order went into effect. Panel A plots the entire sample. Panel B plots subsamples for Republican and Democratic counties, where Republican counties are those where Trump received over 50% of the vote in the 2016 Presidential election. Panel C plots the highest and lowest quintiles of counties based on population. Panel D plots the highest and lowest quintiles based on population density. Controls include the lag number of cases and deaths from COVID19 at the county level as well as state level indicators for when a state closed k-12 schools, day cares, gyms, and movie theatres and banned nursing home visits, non-essential business, and sit-in restaurants. County and date fixed effects are included. Standard errors are double-clustered at the county and date level.

$$Social\ Distancing_{c,t} = \sum_j \beta_j (State\ Policy \times days\ to\ treatment) + \delta' * controls + \gamma_c + \gamma_t + \epsilon_{c,t}$$

Covid Economics 4, 14 April 2020: 103-123

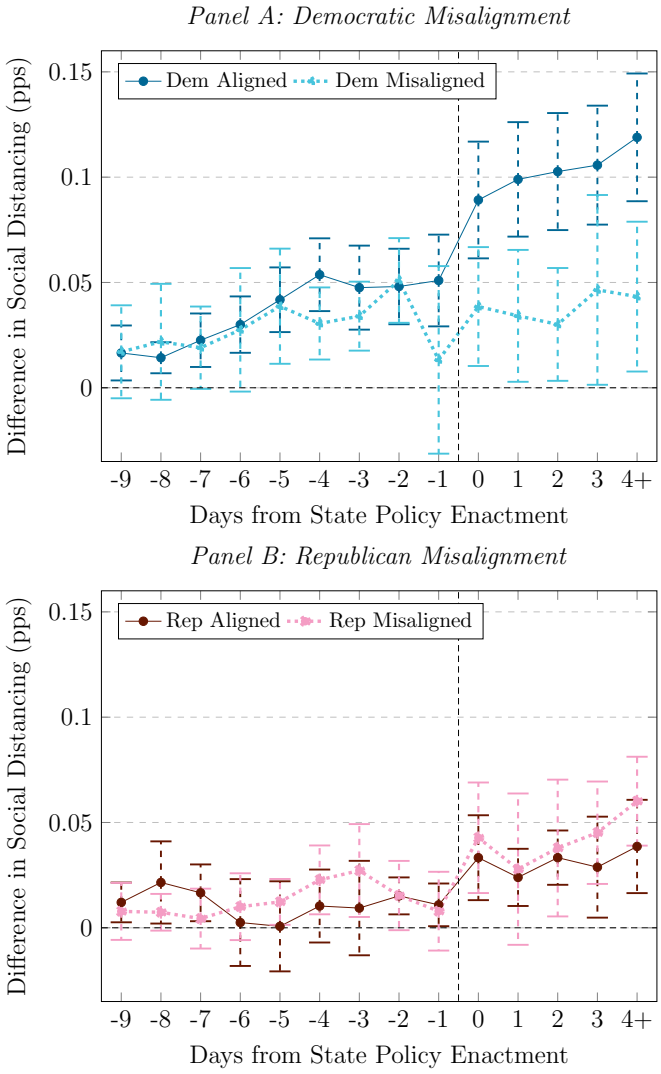

Fig. 2

Changes in Social Distancing based on Political Alignment

This figure plots coefficients of β_j from the following regression of social distancing on the interaction of state policies for shelter in place in event time, where day 0 is the first date the state order went into effect. Panel A plots subsamples for democratic counties where a democratic governor issued the order (aligned) and a Republican governor issued the order (misaligned). Panel B plots analagous subsamples for Republican counties. Controls include the lag number of cases and deaths from COVID19 at the county level as well as state level indicators if a state had closed k-12 schools, day cares, gyms, and movie theatres and banned nursing home visits, non-essential business, and sit-in restaurants. County and date fixed effects are included. Standard errors are double-clustered at the county and date level.

$$Social\ Distancing_{c,t} = \sum_j \beta_j (State\ Policy \times days\ to\ treatment) + \delta' * controls + \gamma_c + \gamma_t + \epsilon_{c,t}$$

Table 1

Summary statistics
This table reports summary statistics of our data. The unit of observation is a county-day and covers February 1st to March 29th, 2020. Panel A reports summary statistics on social distancing behavior for all observations as well as split on before and after government sanction. Panel B reports summary statistics on population and population density for all observations as well as split on political affiliation. Data source: smartphone geolocation data from SafeGraph Inc and county demographics from the 2018 American Community Survey.

Panel A: Social Distancing Behavior

	All		Before State Policy		After State Policy	
	Mean	SD	Mean	SD	Mean	SD
Social Distance	0.331	0.077	0.326	0.072	0.464	0.080
Observations	170480		163970		6510	

Panel B: County Population

	All		Dem Counties		Rep Counties	
	Mean	SD	Mean	SD	Mean	SD
Population (000s)	90.74	309.62	289.95	664.49	45.57	80.27
Population/SQMI	79.26	896.66	293.02	2054.34	30.06	69.27
Observations	170480		31511		138969	

Covid Economics 4, 14 April 2020: 103-123

Covid Economics 4, 14 April 2020: 103-123

Table 2

Resident Response to Social Distancing Orders

This table reports regression results from estimating equation (2). The unit of observation is a county-day. *State Policy* equals one if the underlying county is in a state that has a social distancing order in place on the day of observation and equals zero otherwise. Column (1) reports the baseline difference-in-differences estimation of the effect of government sanctioned social distancing orders. Column (2) includes an interaction term between *State Policy* and *Trump Vote Share* in the 2016 election from the underlying county. Column (3) repeats the same analysis as Column (2) while excluding observations that occur greater than five days before a state policy is implemented. We also exclude all observations before March 15th in our control sample in Column (3). In Columns (4) and (5) we interact *State Policy* with *Population* and *Population per Square Mile* from the underlying county, respectively. All continuous interaction variables are z-scored to a mean of zero and standard deviation of one. County and date fixed effects are included. Standard errors are double-clustered at the county and date level. *** p<0.01, ** p<0.05, * p<0.1

	Social Distancing				
	(1)	(2)	(3)	(4)	(5)
State Policy	0.051***	0.034***	0.017***	0.046***	0.050***
	(9.51)	(7.76)	(3.56)	(8.85)	(9.61)
State Policy×Trump Vote Share		-0.030***	-0.012***		
		(-11.94)	(-6.15)		
State Policy×Population				0.010**	
				(2.27)	
State Policy×Pop/SQMI					0.004*
					(1.87)
County FE	Yes	Yes	Yes	Yes	Yes
Date FE	Yes	Yes	Yes	Yes	Yes
R^2	0.654	0.658	0.772	0.655	0.690
Observations	167,479	167,479	32,423	167,479	162,170

Covid Economics 4, 14 April 2020: 103-123

Table 3

Resident Response to Social Distancing Orders: Population Splits

This table reports results of estimating equation (2) on subsamples based on county population statistics. The unit of observation is a county-day. In Panel A (Panel B), we sort the universe of observations into quintiles based on population (population density) of the county. Quintile 5 is the most populous (densest). *State Policy* equals one if the underlying county is in a state that has a social distancing order in place on the day of observation and equals zero otherwise. County and date fixed effects are included. Standard errors are double-clustered at the county and date level. *** p<0.01, ** p<0.05, * p<0.1

Panel A: Subsamples based on County Population

	Social Distancing				
	(1) Pop1	(2) Pop2	(3) Pop3	(4) Pop4	(5) Pop5
State Policy	0.021**	0.025***	0.026***	0.032***	0.031***
	(2.39)	(4.68)	(5.65)	(6.44)	(4.83)
State Policy×Trump Vote Share	-0.013**	-0.019***	-0.011**	-0.011***	-0.016***
	(-2.20)	(-3.51)	(-2.54)	(-2.72)	(-5.42)
County FE	Yes	Yes	Yes	Yes	Yes
Date FE	Yes	Yes	Yes	Yes	Yes
R^2	0.469	0.714	0.793	0.833	0.879
Observations	34,818	34,483	34,433	33,807	29,938

Panel B: Subsamples based on County Population Density

	Social Distancing				
	(1) Density1	(2) Density2	(3) Density3	(4) Density4	(5) Density5
State Policy	0.035***	0.051***	0.036***	0.027***	0.024***
	(4.46)	(9.14)	(7.90)	(5.36)	(2.75)
State Policy×Trump Vote Share	-0.004	-0.002	-0.023***	-0.024***	-0.027***
	(-0.84)	(-0.55)	(-4.92)	(-4.97)	(-6.42)
County FE	Yes	Yes	Yes	Yes	Yes
Date FE	Yes	Yes	Yes	Yes	Yes
R^2	0.546	0.741	0.783	0.800	0.826
Observations	33,561	33,179	33,431	32,783	29,216

Covid Economics 4, 14 April 2020: 103-123

Table 4

The Effect of Misaligned Political Beliefs on Adherence to Social Distancing Orders

This table reports the impact of misaligned political belief between residents and the policy announcer (the governor) on the social distancing behavior. The unit of observation is a county-day. *Misalign* equals one if the county is Democratic (Republican) and the governor is Republican (Democratic) and equals zero otherwise. *State Policy* equals one if the underlying county is in a state that has a social distancing order in place on the day of observation and equals zero otherwise. Column (1) reports result for the full sample. Column (2) and (3) report results for Republican and Democratic subsamples, respectively. County and date fixed effects are included. Standard errors are double-clustered at the county and date level. *** p<0.01, ** p<0.05, * p<0.1

	Social Distancing		
	(1)	(2)	(3)
	Full Sample	Rep	Dem
State Policy	0.066***	0.035***	0.075***
	(10.88)	(5.70)	(9.28)
State Policy×Misalign	-0.029***	-0.006	-0.015*
	(-5.69)	(-0.97)	(-1.69)
County FE	Yes	Yes	Yes
Date FE	Yes	Yes	Yes
R^2	0.655	0.639	0.733
Observations	167,479	136,523	30,956